Fluorescence Platform Development for Detection of Cystic Fibrosis Transmembrane Conductance Regulator Trafficking

by

John Holleran

B.S. Biology, Duquesne University, 2006

A Dissertation
Submitted to the
Faculty of
Carnegie Mellon University

In partial fulfillment of the requirements for the degree of
Doctor of Philosophy

Carnegie Mellon University
Department of Biological Sciences
Pittsburgh, PA
USA

September 16th, 2011
Thesis Advisor: Jonathan W. Jarvik, PhD

Table of Contents

Abstract

Cystic fibrosis is caused by mutations in the membrane chloride channel, cystic fibrosis transmembrane conductance regulator (CFTR). The most common mutation, ΔF508, disrupts protein folding resulting in premature degradation which precludes expression at the cell surface. Therapeutic strategies have been developed to rescue ΔF508 by using small molecules, called correctors, which promote folding and trafficking to the surface. Currently, the discovery and evaluation of these correctors requires indirect functional measurements or time intensive biochemical methods. In order to facilitate faster analysis of corrector compounds and provide a screening assay that directly monitors rescue of ΔF508 trafficking, we developed a rapid fluorescence detection platform using fluorogen activating proteins (FAPs) capable of labeling of CFTR at the cell surface. We created two chimeric reporter constructs by fusing the FAP to the N-terminus, or by insertion of the FAP into the fourth extracellular loop. We expressed these constructs in HEK293 cells and verified that the ion transport function, biochemical properties and cellular localization reproduced the native behavior of CFTR. Under normal conditions, CFTR ΔF508 is absent from the surface, however incubation in the presence of correctors restored trafficking to the plasma membrane that was robustly detected by FAP fluorescence. Using this approach we have characterized the efficacy of two new corrector compounds C548, C951 and the well-studied reference corrector, C4. The most potent corrector identified was C951 which performed 2 fold better than the previously described, C4 corrector. Other studies have shown that combinations of correctors exhibit an additive or synergistic effect, therefore, we tested combinations of correctors using FAP-CFTR constructs and found they had a synergistic effect on the rescue of ΔF508, improving the density of protein at the cell surface 4 fold greater than C4 alone. These results correlated closely with functional data obtained from polarized human bronchial epithelia that endogenously express ΔF508, suggesting that the FAP tagged CFTR reporters represent a physiologically faithful model of corrector rescue.

List of Figures

List of Tables

Abbreviations

AA   Amino Acid

ABC   ATP Binding Cassette

ASL   Airway Surface Liquid

ATP   Adenosine Triphosphate

BHK   Baby Hamster Kidney

C4   Corrector 4a [1]

C548   CFFT-108548 formerly EPIX compound

C951   Vertex Patent WO 2007/021982 A2

cAMP   Cyclic Adenosine Monophosphate

CF   Cystic Fibrosis

CFBE   Cysitic Fibrosis Bronchial Epithelia

CFTR   Cystic Fibrosis Transmembrane Conductance Regulator

CHIP   Carboxyl-Terminus HSC70 Interacting Protein

DMSO   Dimethyl Sulfoxide

EDEM   ER Degradation Enhancing α-Mannosidase Like-Protein

eGFP   Enhanced Green Fluorescent Protein

EL 2 or 4   Extracellular Loop 2 or 4

ELISA   Enzyme-Linked Immunosorbent Assay

ENaC   Epithelial Sodium Channel

ER   Endoplasmic Reticulum

ERAD   Endoplasmic Reticulum Associated Degradation

ERM   Ezrin, Radixin, Moesin

FACS   Fluorescence Activated Cell Sorting

FAP   Fluorogen Activating Protein

FRET	Förster Resonance Energy Transfer
Fsk	Forskolin
G_4S	Four Glycines One Serine Flexible Linker Unit
GFP	Green Fluorescent Protein
HA	Hemagglutinin
HAE	Human Airway Epithelia
HBE	Human Bronchial Ephithelia
HEK293	Human Embryonic Kidney
HTS	High Throughput Screening
ICL4	Fourth Intracellular Loop
LTR	Long Terminal Repeat
MG	Malachite Green
MMLV	Maloney Murine Lukemia Virus
mRFP	Monomeric Red Fluorescent Protein
MSD	Membrane Spanning Domain
NBD	Nucleotide Binding Domain
NHERF1	Na^+/H^+ Exchanger Regulatory Factor
ORF	Open Reading Frame
PCL	Periciliary Liquid
PDGFR	Platelet Derived Growth Factor Receptor
PDZ	Psd95, Dlg, Zo-1
PEG (p)	Polyethelene Glycol
PKA	Protein Kinase A
PM	Plasma Membrane
R domain	Regulatory Domain
scFv	Single Chain Variable Fragment

SPQ   6-Methoxy-N-(3-Sulfopropyl) Quinolinium

SRP   Signal Recognition Particle

TGN   Trans-Golgi Network

TM   Transmembrane

TMD   Transmembrane Domain

TO   Thiazole Orange

t-SNARE   Target Vesicle-Soluble *N*-Ethylmaleimide-Sensitive Factor Attachment Protein Receptors

Ub   Ubiquitin(Ation)

UGGT   UDP Glucose/Glycoprotein Glucosyltransferase

vH   Variable Heavy Domain

vL   Variable Light Domain

VSV-G   Vesicular Stomatitis Virus - G Protein

WT   Wild-Type

YFP   Yellow Fluorescent Protein

ΔF508   Deletion Of Phenylalanine At Position 508

Chapter 1 : Cystic Fibrosis and CFTR

Ch.1 – Introduction

Cystic Fibrosis

Cystic fibrosis (CF) is one of the most common lethal genetic diseases among Caucasians[2]. This disease results from mutations in the cystic fibrosis transmembrane conductance regulator (CFTR) gene[3]. The CFTR gene produces an anion channel that resides in the apical surface of epithelial cells lining the respiratory tract, intestine, pancreas and sweat glands. It's primary role is a protein kinase A (PKA) regulated ion channel responsible for secretion of chloride and bicarbonate (Cl^- and $HCO3^-$) across the apical plasma membrane (PM) of polarized epithelial cells[4]. Inherited mutations in the CFTR gene disrupt the normal function of CFTR. These mutations can cause a myriad of physiological complications including pancreatic insufficiency, malnutrition and male infertility, however, chronic lung infections are the most life-threatening manifestation[5,6]. So far there have been over 1800 CFTR mutations identified that are classified according to the type of molecular defect which lead to differently compromised protein products[7]. Class I mutants have biosynthetic defects which arise from missense or nonsense codon changes leading to truncated CFTR protein. Class II mutants have maturation and trafficking defects that prevent localization to the cell surface. This class contains the most common mutation, deletion of a phenylalanine residue at position 508 (ΔF508), which is present in 90% of patients with CF on at least one allele[2] (Figure 1-1). Class III mutants have properly localized CFTR protein at the cell surface however they do not respond to physiological stimuli; these are said to have gating defects.

Current research suggests that the impaired mutant CFTR activity leads to chronic bacterial infections in the lungs and obstructed airway passages due to inappropriate regulation of the liquid level and composition on the surface of airway epithelial cells. Airway surface liquid (ASL) sits directly above the apical surface of epithelial cells and is made of two parts, an upper viscous mucus layer and an lower

watery layer called the periciliary liquid (PCL). Ciliated epithelial cells are able to efficiently clear

bacteria and mucus through ciliary beating which is dependent on this two phase system[8,9]. Under

normal physiological conditions the PCL is maintained by the secretion of chloride into the PCL by CFTR

and to a lesser extent other chloride channels. Absorption of sodium ions by another PM protein, the

epithelial sodium channel (ENaC). When chloride secretion is impaired by the loss of CFTR activity, the

imbalance of ion transport causes a hyper-absorption of Na^+ ions and dehydration of the PCL[10]. Loss of

PCL volume collapses the mucus layer on to the surface of the epithelial cells which severely inhibits the

ability of cilia to beat and efficiently clear mucus[11] (Figure 1-2). The mucus layer soon becomes static

and creates mucin plugs which obstruct smaller airway passages. Furthermore, the protective effect of

mucus clearance is lost, and inhaled bacteria and pathogens are able to opportunistically colonize the

lung[12]. Early infections such as *H. influenza* and *Staphylococcus aureus* soon develop into more insidious

ones like *Pseudomonas aeruginosa* which are more resistant to antibiotic treatment[13]. Immediately

after birth CF patients start a vicious cycle that begins with bacterial infection in the lungs. This is

followed by an immune response involving inflammation and increased mucus production. As patients

receive treatment, they develop increasingly difficult to eradicate bacterial infections.

CF patient quality of life and lifespan have been greatly improved in the last 25 years, with the median

age of survival increasing from 25 to 36[14]. These gains in life expectancy have come largely from

symptomatic treatment of the disease. Aggressive antibiotic therapy and breathing techniques have

been successful; however, they are limited because they do not address the underlying cause of the

disease. Moreover, antibiotic treatments are rendered ineffective if the patient develops drug resistant

bacterial or fungal infections. Another angle for CF patient therapy is aimed at correcting the

homeostasis of the ASL volume. Inhaled hypertonic saline solution has been shown to have a
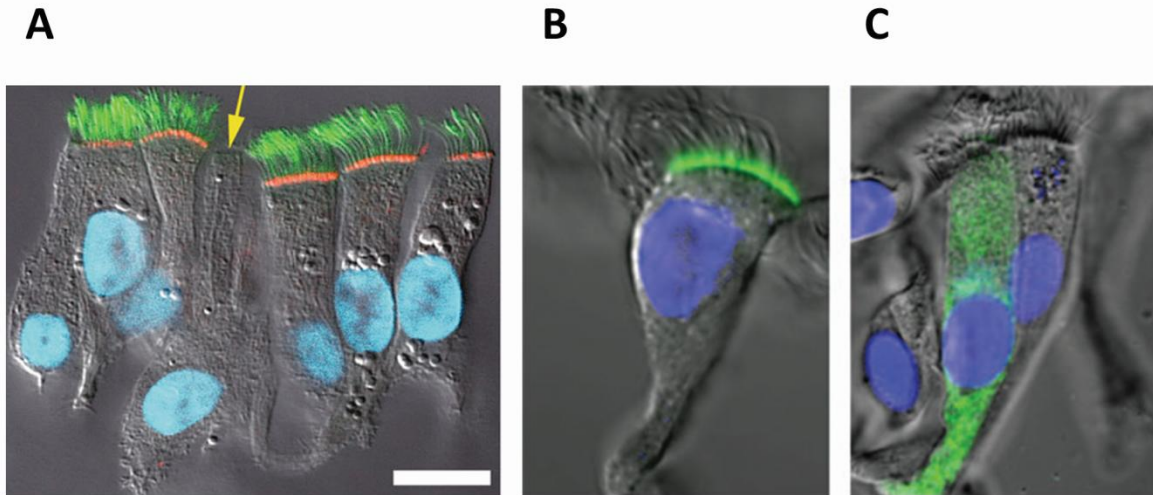
Figure 1-1: CFTR Localization in Polarized Epithelial Cells[15,16]

Immunofluorescence and DIC images of epitope tagged CFTR in ciliated, polarized airway epithelial cells. Cell nuclei are stained in blue. (A) In a culture of polarized bronchial epithelial cells, wild type CFTR is stained in red using a CFTR specific antibody and localizes to the apical PM. Tubulin (green) marks the cilia which beat to efficiently clear mucus[15]. (B) CFTR WT is stained in green and localizes to the apical PM. (C) CFTR ΔF508 (green) is blocked in trafficking and does not localize to the apical PM[16].
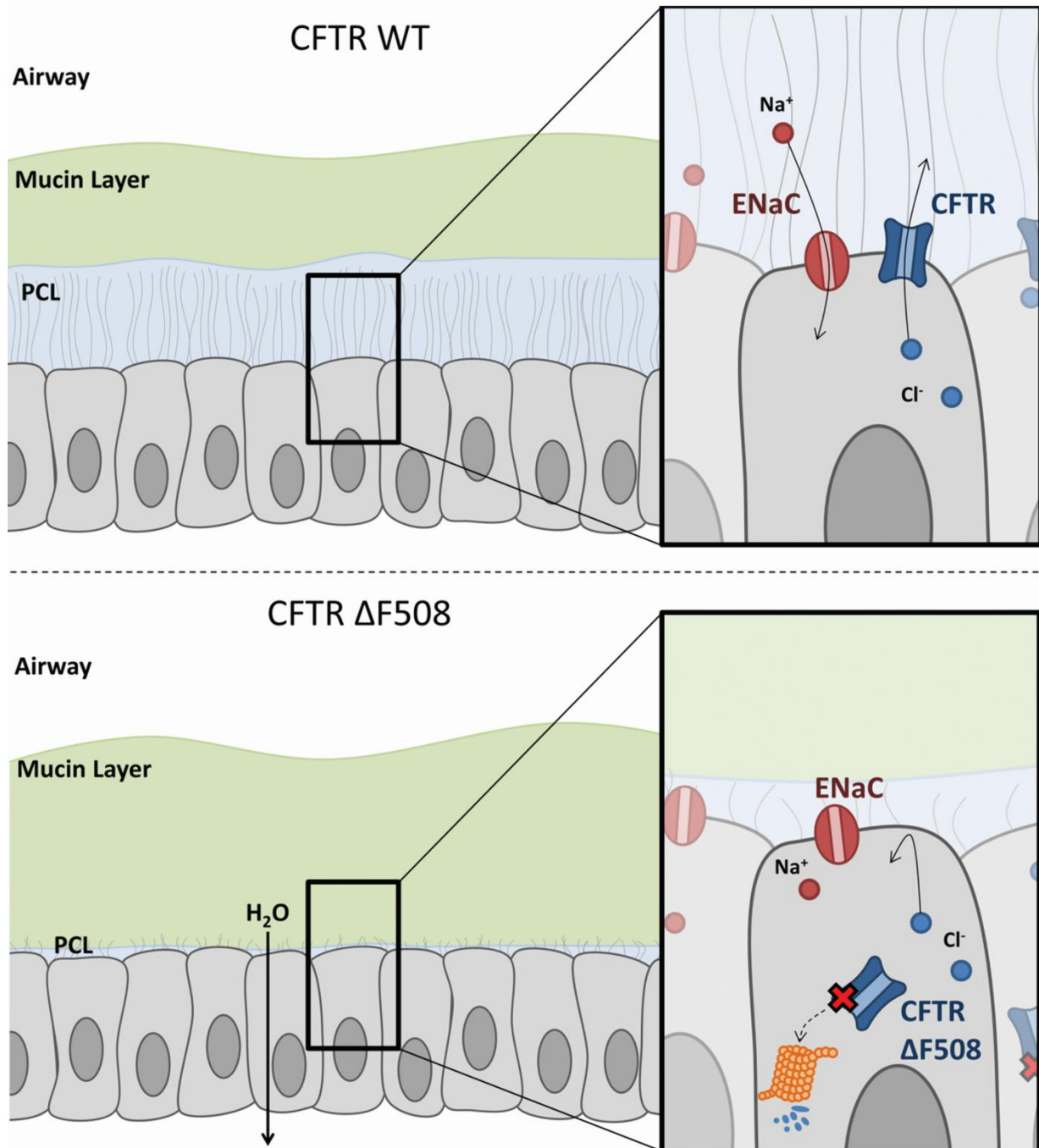
Figure 1-2: Schematic of CFTR ΔF508 Airway Fluid Depletion (adapted from [17])

Representation of ciliated, polarized epithelial cells lining human airway passages. **Top**: CFTR WT secretes chloride, while ENaC transports sodium creating an ionic balance which maintains the PCL volume. This allows the cilia to clear mucus efficiently. **Bottom**: Absence of CFTR activity due to the ΔF508 mutation results in a lack of chloride secretion and hyper-absorption of sodium. The net result is a depletion of the PCL volume and inefficient clearance of the mucus layer.

therapeutic effect. It is thought that the hypertonic saline solution changes the osmotic composition of

the ASL such that more water is retained on the surface of the airway epithelia thereby temporarily

correcting the hydration of the airway surface[18,19]. While hypertonic saline inhalation therapy does

provide some reprieve to CF patients, the effect is quite modest. Despite these strides which have

improved patient care and outcomes, there is clearly a need to directly address the cause of the disease

by targeting therapy at the defective CFTR protein, the basic defect

CFTR

In 1989, a landmark study was published describing the identification of the cystic fibrosis gene, CFTR[3,20].

Rommens and Riordan et al. were able to pinpoint the genetic location of CFTR through a combination

of genomic DNA scanning techniques such as chromosome walking/jumping and cDNA hybridization.

The CFTR gene spans a 188,700 base pair (bp) sequence on chromosome 7 and encodes a 1480 amino

acid (aa) protein. CFTR is a member of the superfamily of transporters known as the adenosine tri-

phosphate (ATP) binding cassette (ABC) proteins. The defining feature of this family of proteins is their

use of ATP hydrolysis to drive molecules across the membrane. In CFTR this task is accomplished by the

antiparallel dimerization of two intracellular nucleotide binding domains (NBD1 and NBD2). In addition

to the two NBDs, CFTR has two membrane spanning domains (MSD1, 2) each consisting of 6

transmembrane (TM) helices and a cytosolic regulatory domain (R domain). CFTR is a type II

transmembrane protein, meaning both the N and COOH (C) termini are located intracellularly (Figure

1-3).
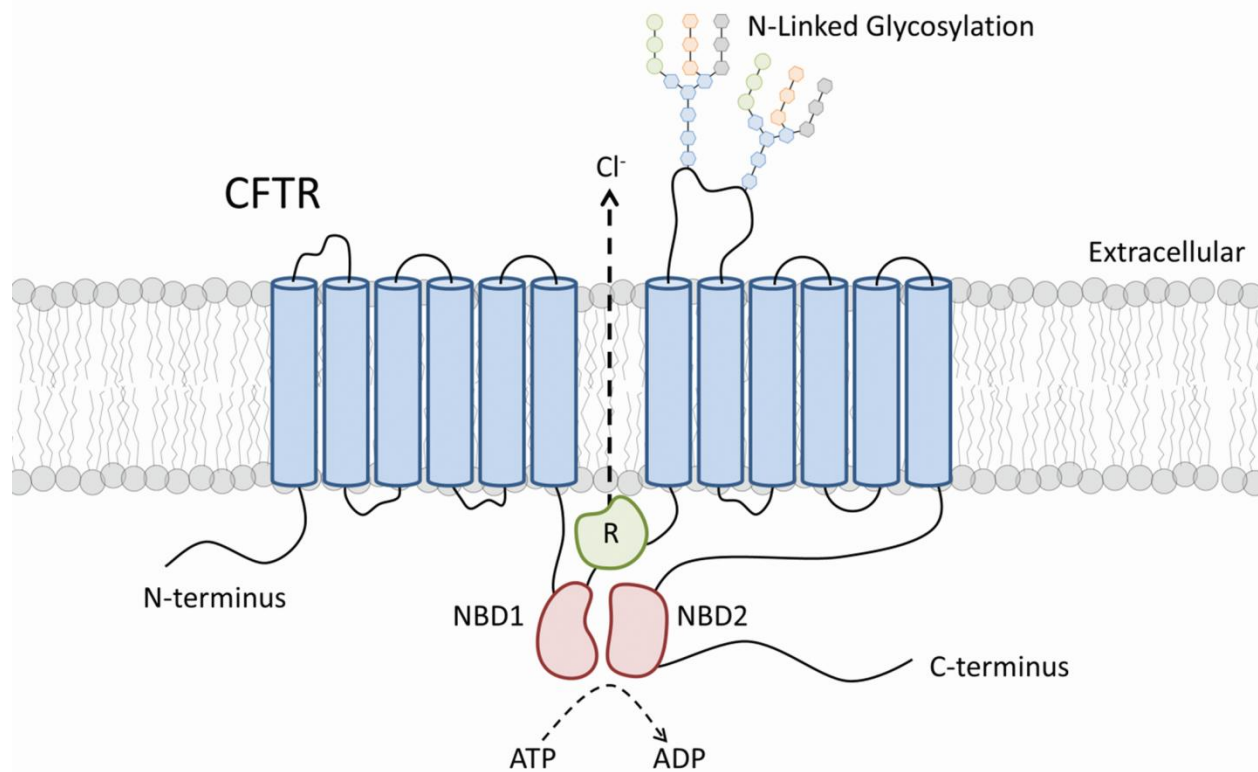
Figure 1-3: Topology of CFTR

CFTR is a type II, 12 pass transmembrane protein. Both the N and C termini are located intracellularly. Two nucleotide binding domains, NBD1 and 2 are located on the cytoplasmic face and hydrolyze ATP. The site of the most common mutation, ΔF508 resides in NBD1. A regulatory domain (R) responds to phosphorylation by PKA to modulate channel conductance. The fourth extracellular loop contains the two important asparagine residues required for N-linked glycosylation.

CFTR Quality Control at the Endoplasmic Reticulum

As CFTR is synthesized on the ribosome, it is inserted into the endoplasmic reticulum (ER) membrane co-translationally. Once inserted into the ER, there are several important quality control checkpoints that ensure CFTR is ready for export to the cell surface. An oligosaccharide modification is added to the fourth extracellular loop via N-linked glycosylation at two asparagine residues located at amino acid positions 894 and 900. The glycosylated protein produced in the ER is called the "core glycosylated" form and further glycan modifications are added in the Golgi which produces a "mature glycosylated" form. Core glycosylation is recognized by ER resident chaperones such as Calnexin and Calreticulin in order to monitor the progress of CFTR maturation. The ER chaperones verify that correct glycan modifications have been added to CFTR and if not, the ER protein UDP glucose/glycoprotein glucosyltransferase (UGGT) removes the oligosaccharide modification and starts the glycosylation process again. Correct N-linked glycosylation is important for the biogenesis of CFTR in three ways. First, incomplete glycosylation results in the premature degradation of CFTR by EDEM (ER degradation enhancing α-mannosidase-like protein). EDEM is responsible for the recognition of impaired glycosylation patterns and subsequent retrotranslocation to the cytoplasm where incorrectly glycosylated CFTR will be destroyed by the proteasome (Figure 1-4). Second, glycosylation provides direct stabilization of CFTR folding. This was demonstrated by the increased protease and glycosidase susceptibility when glycosylation was abolished either by mutating the asparagine residues or treatment with glycosidase inhibitors[21,22]. Finally, the stability of the protein at the PM is greatly affected by the loss of glycosylation. Turnover at the cell surface is increased four fold when glycosylation is removed and the amount destined for lysosomal degradation, measured by ubiquitination (Ub), is increased five fold[22,23]. These chaperone interactions, although important, are not the only determining factors in the export of CFTR. Removal of Calnexin is not sufficient to overcome the ER retention of ΔF508[21,24].
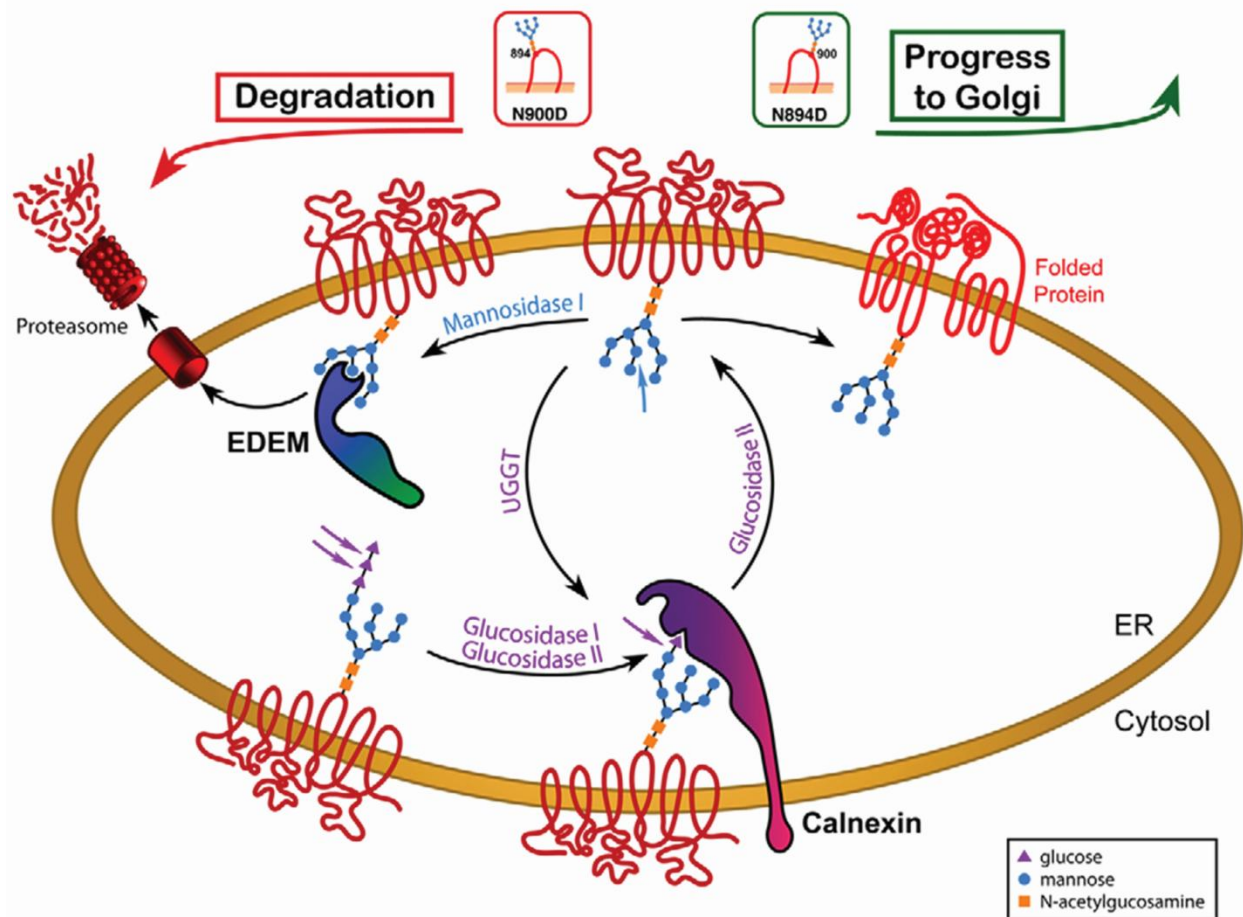
Figure 1-4: CFTR Glycosylation Quality Control Machinery[21]

Diagram illustrating ER glycosylation control for CFTR. Properly glycosylated and trimmed CFTR modifications are recognized by the lectin chaperone, calnexin. If glycosylation is complete, CFTR is exported from the ER to the Golgi. If complete glycosylation fails or folding is disturbed, the EDEM chaperone directs CFTR for degradation via the ERAD pathway.

Many studies have suggested that the folding and biosynthetic processing of CFTR is inefficient and only a small fraction of protein is properly folded (less than 25% efficiency)[25-27]. This is not surprising, given that CFTR has many domains that each requires folding stability and inter-domain interactions. Furthermore, it has been suggested that the function of CFTR (i.e. to transport anions) has necessitated the presence of certain charged amino acids that line the pore of the channel that may contribute to processing inefficiency[28].

Maturation efficiency measurements for CFTR made in heterologous overexpression systems remains the subject of some debate. Differences in the folding environment and chaperone make-up in different cell lines can certainly have an effect on the efficiency of CFTR folding and stability. One study found that in polarized epithelial cells which express CFTR endogenously (Calu-3 and T84) there was an extremely efficient processing of CFTR (nearly 100% efficiency)[29]. These conflicting reports illustrate the importance of testing many cell lines under different conditions such as polarization to verify that an observed CFTR behavior is not a cell type specific phenomena.

Stability of CFTR in the Plasma Membrane

When CFTR has acquired the correct folding conformation and glycosylation pattern in the ER and then the Golgi, it is competent for export and translocation to the PM. At the cell surface, the CFTR protein can perform its physiological function which is transporting anions across the membrane. In the apical surface of epithelial cells CFTR is responsible for secreting Cl^- and $HCO3^-$ into the lumen of the airway. Transport of these ions is controlled by the regulatory (R) domain of CFTR. The CFTR channel is opened to allow ions to flow when the R domain becomes phosphorylated. Multiple sites on the R domain are phosphorylated by PKA in response to increased levels of intracellular cyclic adenosine mono-phosphate (cAMP). Elevated levels of cAMP and PKA activity can occur naturally through a physiological signaling

cascade initiated by agonist stimulation of the β-2-adrenergic receptor or artificially by adenylate cyclase activators such as forskolin (Fsk). In order to maintain the balance of ions across the membrane of epithelial cells, the membrane must contain enough CFTR molecules to quickly respond to PKA activation. It has been shown that CFTR WT has slow metabolic turnover, a half-life ~14h, perhaps longer in polarized cells[23,30]. It has also been observed that there is an extremely fast endocytosis of CFTR from the cell surface ~5-10% per minute[31,32]. Given these two observations, CFTR must have an efficient recycling mechanism to maintain the PM density. Indeed, there is a constitutive recycling that occurs to maintain the surface pool of CFTR protein.

There has been a substantial effort to understand the mechanisms that govern endocytosis and recycling of CFTR by many groups but the story is not yet complete. CFTR trafficking is regulated by complex endosomal sorting machinery which decides the fate of this protein after it has left the cell surface. The internalization process begins with clustering of CFTR exclusively in clathrin coated pits, followed by dynamin dependent pinching into vesicles[33,34]. Once internalized, CFTR undergoes vesicular trafficking through many intracellular compartments. At the cell surface a Rab GTPase, Rab5, transports CFTR from the PM to the early endosomes. From here, CFTR can traffic to the trans-Golgi network (TGN) by Rab 9, back to the cell surface (Rab 11) or become destined for lysosomal degradation via late endosomes (Rab 7)[35]. All of this machinery works together to enable a highly efficient recycling pathway for CFTR that allows for slow protein turnover and long residency in the PM[36].

Because recycling is such a key component to maintaining the cell surface density of CFTR, even small changes in the kinetics of this pathway can have a substantial impact on the amount of protein at the cell surface. CFTR mutants with folding instabilities have altered recycling and internalization rates which profoundly reduce the amount of protein at the cell surface[37]. For this reason, a clear

understanding of these pathways would help to identify potential therapeutic targets to recover trafficking defects of these mutants.

Methods Available to Study CFTR

Thus far, the methods available to study the mechanisms that control the biogenesis, folding, trafficking and dynamics at the cell surface for CFTR turnover have been labor intensive, lacking in temporal and spatial resolution, and/or rely on indirect measurements. The cystic fibrosis research community has made enormous progress so far; however, the tools available are not well suited to examine CFTR in living cells with high temporal and spatial resolution. In the following section, the usefulness and shortcomings of currently available methods to study CFTR are discussed.

Biochemical methods such as immunochemistry and biotinylation are the backbone of CFTR localization research. CFTR exists as two forms, the ER core glycosylated form and the mature, Golgi complex glycosylated form. These two forms have different biochemical properties when visualized by immunoblotting. The core and mature glycosylated forms have different mobilities on SDS-PAGE gels, the immature form is the smaller, faster migrating band (band B) and the mature form is the slower migrating, larger band (band C). In this way, it is possible to distinguish the efficiency of CFTR maturation by immunoblot. This can be very useful for analyzing CFTR mutants before and after drug treatments or after knockdown of quality control factors for instance.

Biotinylation is a powerful technique which is used to selectively label CFTR at the cell surface. Typically, in these experiments, cells are put on ice to stop endocytosis, then exposed to an oxidizing reagent such as sodium periodate. This will permanently modify only the glycoproteins embedded in the PM at the time of exposure to the oxidizing reagent. Then the oxidized glycoproteins can be labeled with biotin-LC-hydrazide. This procedure effectively labels only proteins that are at the cell surface because the

reagents are cell impermeant. After biotin conjugation, cells are lysed and immunoprecipitated with an anti-CFTR antibody. Finally, the product is detected by HRP-avidin by immunoblot. By designing experiments carefully, a wealth of information about CFTR at the cell surface has been gleaned using this technique. For instance, measurements of CFTR cell surface stability, internalization rates and recycling to the PM have all been made with biotinylation techniques[29,38,39]. A major limitation with this process, however, is the amount of labor required and it only provides a static view.

Direct visualization of CFTR provides valuable information about the protein. Using traditional fluorescent protein tagging is a straightforward approach. Haggie et al. have successfully generated several versions of green fluorescent protein (GFP)-CFTR fusions/chimeras. They have tagged the N-terminus, the fourth extracellular loop, the C-terminus and combinations of these constructs. With this strategy they used the photobleaching properties of GFP to determine whether CFTR forms dimers or higher order multimers on the surface of mammalian cells, a question that could not be answered easily with biochemical methods. They concluded that in this system, CFTR was capable of functioning as a monomer[40]. For this purpose, GFP tagging of CFTR was sufficient to answer the question of oligomerization. A major drawback of GFP-CFTR fusions is the inability to distinguish molecules specifically at the cell surface. For studying the PM proteins, GFP-CFTR fusions are not the best choice because fluorescent signal comes from tagged protein that distributed throughout the cell. Even total internal fluorescence microscopy (TIRF), which sees only molecules very close to the microscope slide, cannot distinguish molecules that are near the surface (~100nm) from those embedded in the PM[41].

Immunofluorescence using antibodies under non-permeabilizing conditions directed to external epitopes allows for selective labeling of CFTR at the cell surface. Unfortunately, there are very few antigenic extracellular regions in this protein and therefore, raising antibodies has been difficult[42]. An alternative approach is engineering known epitopes such as hemagglutinin (HA) into an extracellular

19

facing loop. A triple HA tag inserted into the fourth extracellular loop (EL4), the largest extracellular

domain in CFTR, has been extremely successful in detection of CFTR at the cell surface[22,23,43,44]. This

construct was invaluable for following CFTR from the cell surface to intracellular compartments to

determine the fate of the protein. Using the CFTR EL4-HA construct for detection, the ubiquitin-

lysosomal pathway was found to be responsible for the removal of misfolded or damaged CFTR from the

PM. In addition, quantitative data describing internalization and recycling rates came from the use of

this system[23]. The role that N-glycans play in maintaining PM density of CFTR was also assessed using

this construct. Glycosylation of CFTR was found to be extremely important for correct localization to the

PM. The loss of CFTR from the cell surface after disruption of the glycan modifications was monitored

by immunofluorescence using the HA tag[22].

Another extracellular epitope tag was generated by modifying the second extracellular loop (EL2) of

CFTR and insertion of a HA tag. Using a complicated molecular cloning strategy, portions from the first

and fourth extracellular loop replicated in the second extracellular loop to expand this domain. A single

HA tag was placed in this expanded EL2. A distinct difference of this approach was the avoidance of the

EL4 domain for epitope tagging. Although EL4 is the largest extracellular domain, it is also the site of the

two important asparagine residues required for glycosylation. CFTR EL2-HA was instrumental in

deciphering the endocytic pathways of CFTR and identifying the key players which regulate this process,

i.e. Rab GTPases[35]. Furthermore, CFTR EL2-HA has been used in many other studies, for example to

determine cytoskeletal interacting proteins such as filamins or to look at the stability of CFTR in the

plasma membrane of polarized epithelial cells[30,45].

Fluorogen Activating Proteins

To take CFTR detection beyond what was possible with existing methods, we sought to develop a way to selectively label CFTR at the PM with the specificity of immunofluorescence, but with the high temporal and spatial resolution and convenience of fluorescent proteins. To achieve this, we chose to employ a unique fluorescence detection system developed by the Molecular Biosensor and Imaging Center (MBIC) at Carnegie Mellon University that uses fluorogen activating proteins (FAPs)[46]. FAPs enable selective labeling of proteins at the cell surface in living cells with no incubation or wash steps. FAP detection requires two parts, a genetically encodable engineered single chain antibody (scFv), the FAP, and a small organic dye, the fluorogen.

Fluorogens are derived from dye molecules that exhibit a dramatic increase in fluorescence activity when the rotation of certain bonds in the molecule are constrained. Thiazole orange and malachite green (TO and MG) are two dyes that were chosen as fluorogens because it was observed that their fluorescence was greatly increased when the molecules were intercalated into DNA, bound to an RNA aptamer or in the presence of a viscous media such as glycerol[47,48].

FAPs were isolated from a diverse yeast surface display library expressing 10^9 unique human scFvs. Human scFvs were chosen because as fragments of the antigen binding regions of IgG full length antibodies they retain antigen binding capabilities, but are much smaller than complete antibody molecules and are single polypeptides. Fluorescence activated cell sorting (FACS) was used to screen a yeast library for scFvs that were capable of not only binding the fluorogen but robustly inducing fluorescence. The fluorogens, MG and TO are not fluorescent in solution, however when bound to the cognate FAP produce a strong fluorescent signal. Therefore, each component alone is dark, but when the fluorogen is combined with the FAP there is a dramatic increase in fluorescence.

Because the fluorogen is non-fluorescent in solution, there is no need to remove the unbound excess fluorogen with wash steps. Thiazole orange (TO) and malachite green (MG) were the first fluorogens identified that were activated by FAPs. Polyethelene glycol (PEG) linkers were added to these fluorogens to make the impermeable to the cell membrane (TO1-2p and MG-11p). Since these fluorogens are chemically excluded from the cell they are only accessible to protein that is exposed to the extracellular environment. Conversely, a cell permeant fluorogen was made by replacing the 11-PEG group on MG with an ethyl-ester group (MG-ester). MG-ester passively diffuses across the PM; then cytoplasmic cellular esterases cleave the ester group preventing exit from the cell. MG-ester thus labels the total population of FAPs regardless of cellular location. TO is not amenable for intracellular applications due to its propensity to intercalate into nucleic acids and generate high background. Therefore, MG binding FAPs were best suited to tag CFTR because they provided the flexibility to visualize the total distribution of CFTR (using MG-ester) or just the surface pool (using MG-11p).

During the original screen of the yeast library expressing human scFVs to identify proteins that would bind and activate MG, clones were isolated that had different domain organization. For instance, the canonical scFV contains a heavy domain (vH), and a light domain (vL) but some of the clones were capable of binding the fluorogen with only a single domain. A single domain MG activator clone, L5 (a single vL domain) was improved by directed evolution to increase the quantum yield and binding affinity through error prone PCR. The result was a FAP capable of binding the MG fluorogen with low nanomolar affinity and significantly better brightness over the originally isolated clone. A drawback of single domain FAPs is they require homo-dimerization to activate the fluorogen (R. Stanfield and C. Szent-Gyorgyi unpublished data). To alleviate this concern, a synthetic dimer was created whereby the L5 vL domain was duplicated and covalently joined with a flexible linker comprised of four glycines followed by a serine repeated three times (G_4S 3X) linker. The resultant two domainFAP, dNP138

provided robust fluorescence activation of MG and was used for all experiments with CFTR described in this thesis.

Given the advantage of selective detection of proteins at the cell surface that FAPs provide and the lack of alternative tools for visualizing CFTR in living cells at the cell surface, we saw an opportunity to increase our understanding of CFTR trafficking at the PM using the FAP-fluorogen system. The results presented herein describe the FAP tagging strategies for CFTR, the biochemical and functional validation of CFTR FAP fusion proteins and the selective fluorescent detection of CFTR at the cell surface.

Ch. 1 – Results

In order to utilize FAP based detection for CFTR, we needed to determine the optimal tagging strategy.

Since CFTR is a type II transmembrane protein, the N and C terminus face the cytoplasm. This presented

challenges for tagging with the FAP reporter and exposing it to the extracellular environment. First, the

most straightforward approach for labeling proteins with reporter molecules is to add the tag at either

the N or C terminus; however this would result in the FAP facing the cytoplasm where it is inaccessible

to the cell impermeant fluorogen.   Therefore, we devised two separate CFTR tagging strategies which

present the FAP facing the extracellular environment where it is accessible to the cell impermeant

fluorogen.

Tagging the N-terminus of CFTR

The first tagging strategy used an unconventional approach to express the FAP extracellularly linked to

CFTR via the addition of a transmembrane linker. The inspiration for this unique design came out of a

need to express FAPs on the surface of mammalian cells. The discovery and early characterization of

FAPs was performed using a *S. cerevisiae* surface display library. In this system, the scFv is fused to the

yeast mating protein Aga2 which is covalently linked to the yeast cell surface via disulfide interactions

with the cell wall anchored protein Aga1[49-51]. This is extremely useful for many applications such as

screening a highly diverse library for scFvs that bind to new fluorogens or looking for enhanced binding

after FAP mutagenesis. There are many limitations that this system imposes however. The landscape of

the yeast cell surface is starkly different than that of mammalian cells. The cell wall and GAL induced

overexpression of scFvs can introduce artifacts such as dimers or higher order oligomers, sequestration

and concentration of dye molecules which are not representative of how the protein would behave in a

mammalian system. Although yeast has been used as a model system for some aspects of CFTR biology,

studies are best performed in a human cell background that already contains the correct complement of chaperones and trafficking pathways[52,53].

A commercially available vector, pDisplay (Invitrogen V660-20), is designed specifically to express proteins on the surface of mammalian cells. When proteins are expressed from this vector, there is an Ig-κ leader sequence fused to the N-terminus which directs the protein to the secretory pathway by binding to the signal recognition particle (SRP), docking at the ER with the SRP receptor and inserting into the ER lumen via the translocon complex. Next, the protein of interest is co-translationally inserted into the ER lumen (topologically extracellular) and the Ig-κ leader sequence is removed by the signal peptidase. Finally, the protein is anchored into the membrane by a single pass transmembrane segment, encoded by the truncated human platelet derived growth factor receptor (PDGFR)[54-57]. This system was used as the first demonstration of selective labeling at the cell surface using FAPs in mammalian cells[46]. The pDisplay vector was useful to confirm that the FAP folded and trafficked to the PM properly, but it did not represent a FAP-fusion to a true membrane protein. In order to study the properties of a membrane protein with relevance to a human disease such a CFTR, we reasoned that we could adapt the pDisplay system to fuse the FAP to the N-terminus of CFTR.

Our goal was to engineer the pDisplay vector to express the FAP at the cell surface anchored by the PDGFR transmembrane (TM) domain, then fuse the N-terminus of CFTR to the already cytoplasmically facing PDGFR domain. The FAP-CFTR fusion protein was predicted to be a 13-pass transmembrane protein with the FAP located extracellularly connected to CFTR by the PDGFR TM domain. To achieve this topology we used a new mammalian expression vector which has two modular cloning sites separated by a TM domain, called pDisplaySacLac2[58]. This vector was derived from the original pDisplay, which was modified by adding a stuffer sequence encoding the bacterial selection marker SacB. SacB was amplified with SfiI restriction sites flanked by BsmI sites for insertion in between the Ig-κ leader

sequence and the PDGFR TM domain. Next, another bacterial screening marker, LacZα complementing

fragment was inserted 3' to the PDGFR. This was accomplished by amplifying LacZα with PflmI

restriction sites, digestion and ligation into the recipient vector (See Figure 1-5 for vector map and Ch.1

Materials and Methods for detailed cloning procedure). This vector was tested for expression, cellular

localization and topology by inserting a FAP (HL1.1-TO1 or HL4-MG) into the Sac position and a

fluorescent protein, eGFP or mRFP, into the Lac position. HEK 293 cells were transfected with the

pDisplayFAP-eGFP plasmid and tested for expression by confocal fluorescence microscopy. In the

presence of impermeant fluorogen (Figure 1-6, A-H) FAP fluorescence signal is observed only at the cell

surface. The fluorescent protein signal on the other hand was distributed throughout the cell as

expected because the protein is trafficking throughout the secretory pathway to and from the cell

surface. This visual observation was confirmed by plotting the pixel intensity along a line drawn through

the middle of each cell (Figure 1-6, D, H, L). We also demonstrated the intracellular labeling capabilities

of the MG binding FAP by imaging in the presence of the cell permeant fluorogen, MG-ester. In Figure

1-6, we see direct colocalization of FAP and eGFP signal as expected because they are covalently linked

as a single fusion protein. From three observations we conclude that the pDisplaySacLac2 expression

system is working properly. First, the FAP is localized to the cell surface and exposed to the extracellular

environment, demonstrated by the ability to activate the cell impermeant fluorogen MG-11p. Second,

the FAP and fluorescent protein signal are highly colocalized, when imaged in the presence of cell

permeant dye (MG-ester), which suggests there are no significant proteolytic cleavage events or non-

specific labeling. Third, both modules of the pDisplaySacLac2 expression vector are expressed,

indicating that correct folding is possible in the extracellular and intracellular domains.

The pDisplaySacLac2 vector had proven useful for expressing separate protein domains on either side of

the PM, however, the application was limited due to the need to transiently transfect cells. This was a

major limitation because the expression was present for only 3-4 days post transfection and the levels of

expression were highly variable. Due to these limitations of transient transfection this expression

system was not amenable to studying membrane proteins in a controlled way, so we sought to create a

stable expression vector. For this purpose, we extracted the functional elements from pDisplaySacLac2,

namely the Ig-κ leader sequence, Sac domain, PDGFR TM domain and the Lac domain, and inserted this

into the mammalian retroviral vector, pBabe-puro-H-Ras-V12 (Addgene, Cambridge, MA). This was

accomplished by cutting upstream of the Ig-κ with BamHI and 3' to the Lac domain with XhoI. This insert

was ligated with the pBabe backbone prepared by digestion with BamHI and SalI (a compatible overhang

to XhoI). The resultant vector, pBabeSacLac2 is a retroviral vector that can stably integrate into the

genome of mammalian cells. A key feauture of this construct are the 5' and 3' long terminal repeats

(LTRs) which flank the SacLac unit. These serve two functions; one, they are critical for integration into

the genome of the host, two, the 5' LTR contains the promoter which drives transcription of the

transgene (Figure 1-5). The pBabeSacLac2 construct is packaged into moloney murine leukemia virus

(MMLV) particles by co-transfecting a special packaging cell line, phoenix GP, with a vector expressing

viral coat protein and vesicular stomatitis virus – G protein, (VSV-G) which pseudotypes the virus,

making it suitable for transducing human cells[59]. Once transduced into a mammalian cell line,

expression from the pBabeSacLac2 construct can be detected by fluorescence activity, or transductants

can be selected with antibiotic by culturing cells in the presence of the potent drug, puromycin.
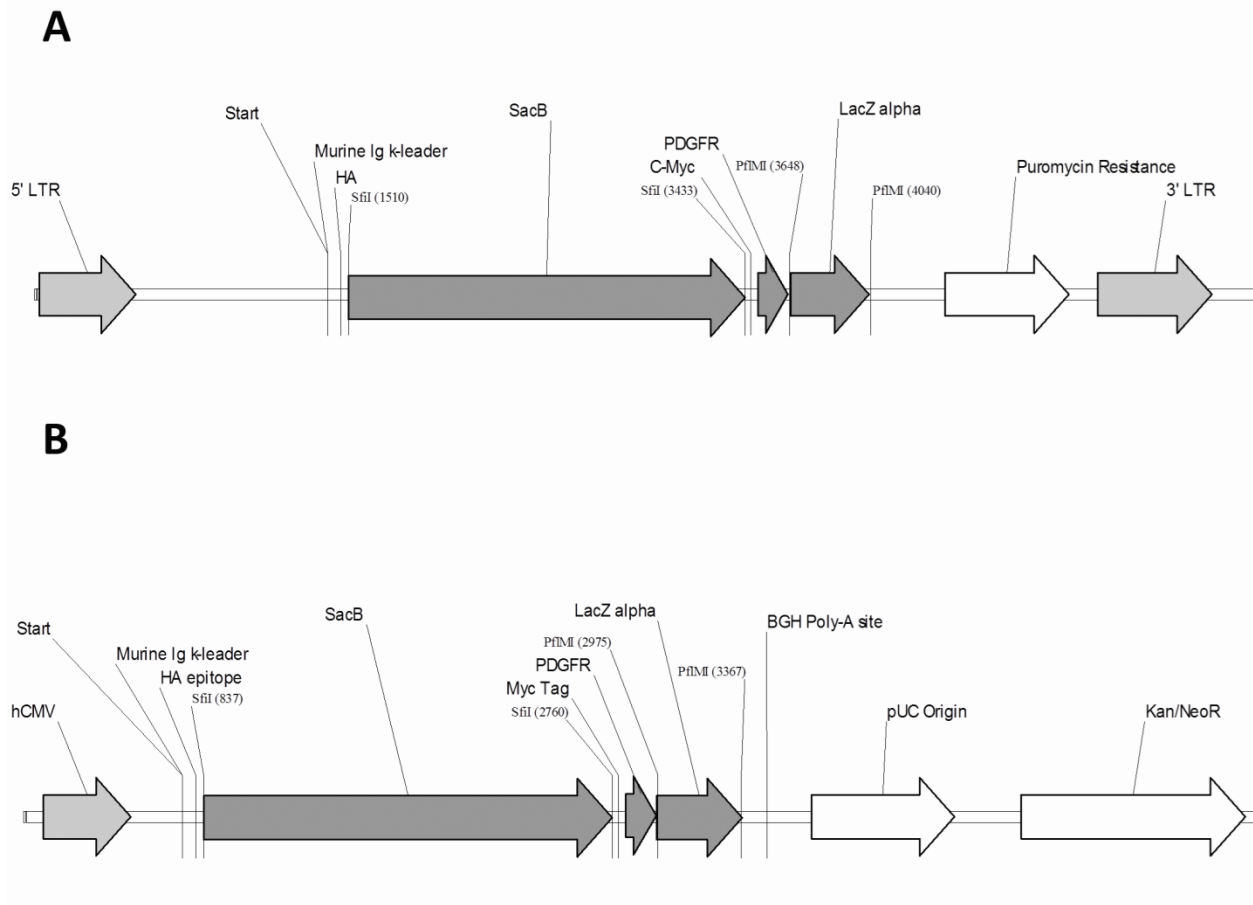
Figure 1-5: pDisplay and pBabe SacLac2 Mammalian Expression Vectors

Vector map of the expression unit in the pDisplaySacLac2 and pBabeSacLac2 vectors. From 5' to 3', the unit begins at ATG start codon followed by the murine Igκ leader sequence and an HA epitope tag. Next, is the bacterial selection marker SacB is flanked by SfiI restriction sites, followed by a c-Myc epitope. This is followed by a membrane spanning segment derived from the human PDGFR gene, and then a LacZα gene flanked by PflmI restriction sites.
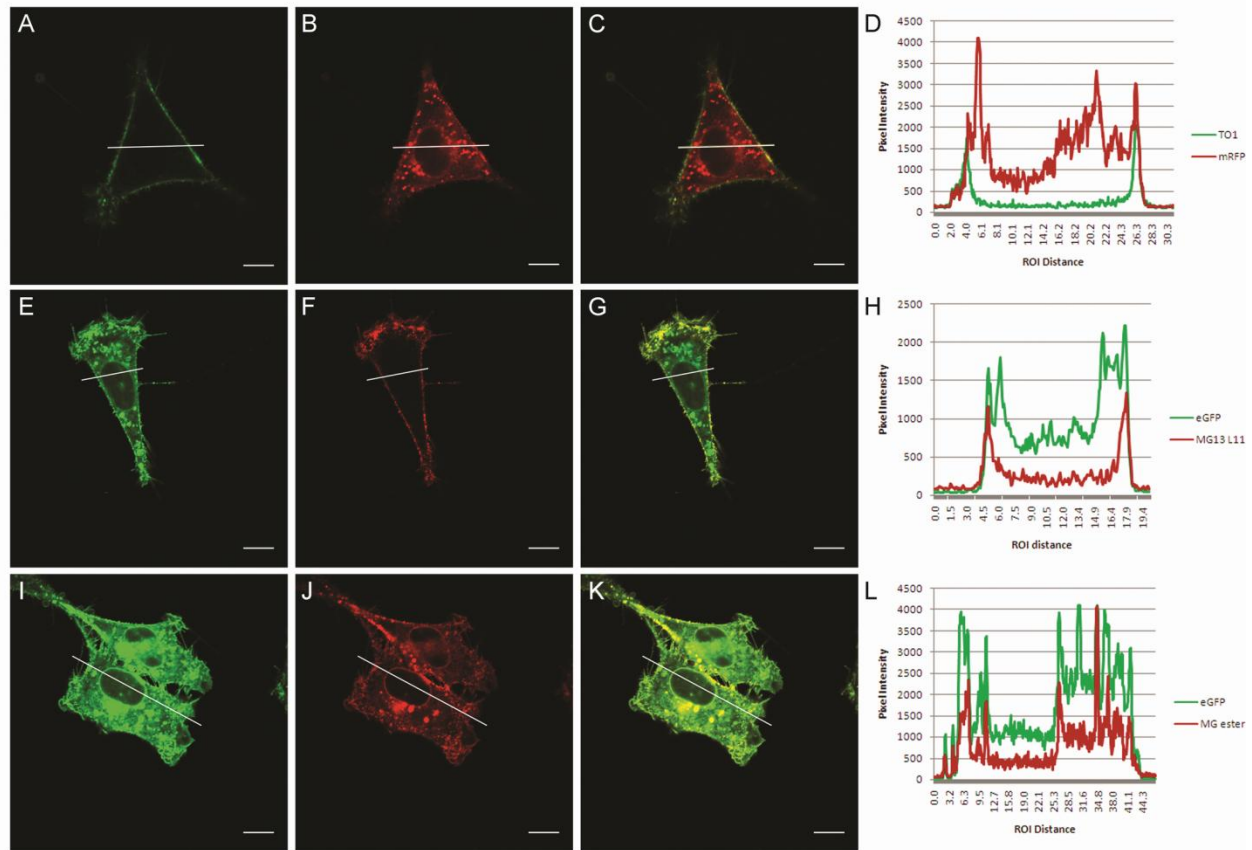
Figure 1-6: FAP and Fluorescent Protein Reporters at the PM[58]

Fluorescence images of SacLac2 constructs in mammalian cells. Cells were transfected with the following plasmids where the Sac module is listed first and Lac module second: HL1.1-TO1-mRFP (A-D), HL4-MG-eGFP (E-L). The first three columns show green, red, and merged fluorescence channels. The last column shows histograms generated from the fluorescence images by plotting the pixel intensity across a specified region (indicated by the white line). Image analysis was performed using the Image J software by specifying a linear region of interest and using the plot profile operation. Panels (A—H) are FAP-FP expressing cells in the presence of impermeable fluorogen. Cell permeable fluorogen labeling of FAP-FP cells are shown in panels I—L. Scale bars represent 10 μm.

We next generated a construct which contained a FAP (dNP138) in the Sac module and CFTR WT in the Lac module. The predicted topology of this fusion protein when expressed at the PM in mammalian cells is as follows; the FAP is exposed extracellularly and anchored in the membrane by the PDGFR TM domain which is fused to the cytosolic N-terminus of CFTR followed by the 12 transmembrane domains encoded by CFTR (Figure 1-7, A). We tested this expectation by stably expressing the pBabeFAP-CFTR in HEK 293 cells. Cells were imaged using confocal fluorescence microscopy in the presence of cell impermeant fluorogen (Figure 1-8, A). There is distinct labeling of the cell membrane, indicating that the FAP-CFTR WT fusion protein is embedded in the PM and the FAP is exposed to the extracellular environment. Furthermore, when the same cells were exposed to MG-ester, there was additional intracellular staining (Figure 1-8, B), consistent GFP-CFTR fusion construct patterns and other studies that show most of CFTR WT at the cell surface with small pools en route to or from the PM[21,29,30,35] (Figure 1-8,E).

Fourth Extracellular Loop Tagging Strategy

The second strategy that we used to tag CFTR was to insert the FAP into the fourth extracellular loop. This is the largest extracellular domain in CFTR and has been used previously to insert epitope tags and fluorescent proteins[23,40]. For these reasons, we chose this location to create a FAP and CFTR chimeric protein. To prepare the FAP for insertion into the extracellular loop, we engineered additional flexible linkers at the N and C-termini of the FAP coding sequence. This was to alleviate any folding constraints that may be imposed when inserting a large domain in the middle of a protein. For example, if the termini of the FAP sequence are not in close proximity, this might propagate undesirable changes in the native folding of CFTR. This was accomplished by amplifying the FAP (dNP138) sequence with oligos containing a $(G_4S)X3$ sequence for the forward and reverse primer as well as SfiI restriction sites and homology to the original FAP sequence.
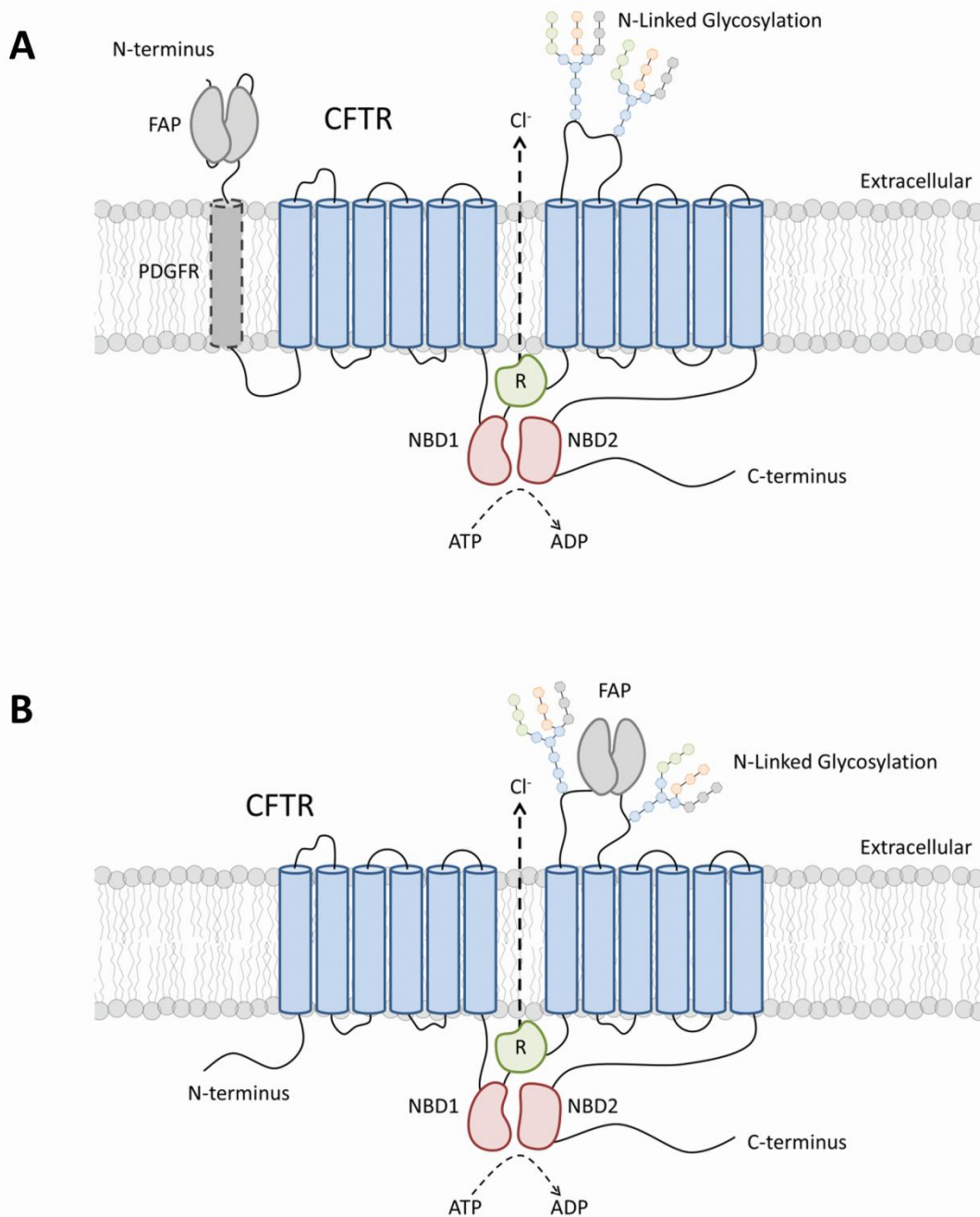
Figure 1-7: CFTR FAP Tagging Strategies

(A) CFTR tagged with a FAP reporter at the N-terminus via an extra transmembrane spanning fragment, PDGFR. This construct is referred to as FAP-CFTR. (B) Insertion of the FAP in the fourth extracellular loop of CFTR located between the two glycosylation sites. This construct is called CFTR EL4-FAP.

An additional concern in modifying the EL4 of CFTR was to preserve the consensus sequence required for N-linked glycosylation. To do this, we used a plasmid provided by Peter Haggie (University of California, San Francisco) which contained restriction sites, KpnI and EcoRV, located in between the two glycosylated asparagines. The amino acid sequence corresponding to the modification in EL4 was KG**N**STHS-(KpnI/EcoRV)-R**N**NSY, where the glycosylated asparagines N894 and N900 are indicated by underline. In order to insert the FAP in this modified fourth extracellular loop, a stuffer sequence encoding eGFP was PCR amplified with primers that added KpnI and SfiI to the 5' end and SfiI and EcoRV restriction sites to the 3' end (See Figure 1-7, B for topology diagram and Ch.1 Materials and Methods for detailed cloning procedure). This amplicon was cut with KpnI and EcoRV and ligated into the similarly digested CFTR recipient plasmid. This produced a vector with stuffer in EL4 of CFTR which when cut with SfiI, was compatible with any FAP or fluorescent protein containing our SfiI sites. This CFTR WT EL4-FAP coding sequence was shuttled into the pBabe plasmid to enable stable expression in mammalian cells. As before, pBabe CFTR WT EL4-FAP was packaged using the phoenix-GP cell line and the viral supernatant was harvested and used to transduce HEK 293 cells. Stable cells were selected by puromycin antibiotic treatment and populations were enriched by FACS. In Figure 1-8, C, selective labeling of the FAP at the cell surface is observed in the presence of MG-11p. Consistent with the FAP label at the N-terminus, when cells are imaged with MG-ester, a small pool of intracellular protein is also labeled, consistent with GFP labeling (Figure 1-8, D, F). These results demonstrate that the FAP is functional and exposed to the extracellular environment using the EL4 tagging strategy.

Functional Validation of Fluorescent CFTR Reporters

To test whether the functionality of the CFTR protein had been compromised by the addition of the FAP tag we performed iodide efflux assays. CFTR is an anion channel that is stimulated by PKA mediated
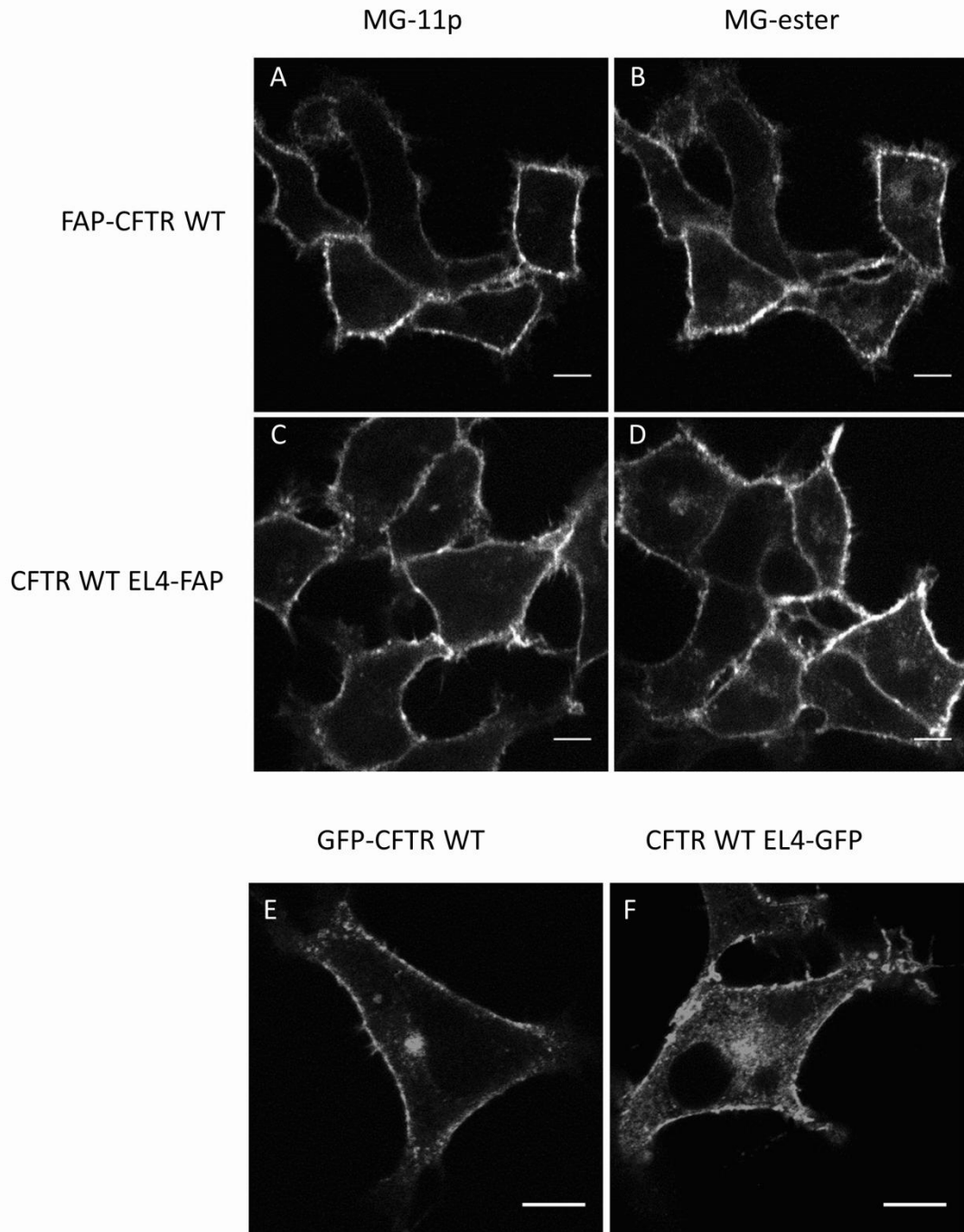
Figure 1-8: FAP Detection of CFTR

HEK293 cells imaged by confocal fluorescence microscopy. FAP-CFTR WT and CFTR WT EL4-FAP was detected exclusively at the cell surface using the cell impermeant fluorogen, MG-11p (A and C) or in intracellular compartments throughout the cell with cell permeant fluorogen, MG-ester (B and D). Intracellular staining patterns from MG-ester were consistent with constructs expressing GFP at the same tag locations (E and F).

A

Indicator fluorescence

add quencher

exchange Cl⁻ or I⁻ for NO₃⁻

add cAMP agonists

time

B

FAP-CFTR WT

Mean SPQ Fluorescence

Time (min)

C

CFTR WT EL4-FAP

Mean SPQ Fluorescence

Time (min)

Figure 1-9: Iodide Efflux of CFTR WT FAP Reporters

(A) Typical protocol for measuring CFTR iodide efflux with the fluorescent indicator, SPQ[60]. (B and C) Normalized SPQ fluorescence traces showing iodide efflux with N-terminus and EL4 CFTR WT expressing cells in response to 10µM forskolin activation.

phosphorylation of the R domain which increases the channel open probability. This can be induced

experimentally by adding an adenylate cyclase activator, Forskolin (Fsk). We investigated whether the

FAP reporter interfered with the cAMP stimulated anion transport across cells by employing a technique

which fluorescently measures the transport of ions across the cell membrane. For this purpose we used

SPQ (6-methoxy-N-(3-sulfopropyl) quinolinium), a halide sensitive fluorescent indicator dye. This dye is

quenched by halides such as iodide and chloride, but not by $NO3^-$. A typical protocol for SPQ

fluorescence based CFTR activity measurements is outlined in the Figure 1-9, A. For this method, HEK293

cells expressing FAP-CFTR WT or CFTR WT EL4-FAP are hypotonically loaded with SPQ and iodide

solution and imaged with an inverted epi-fluorescence microscope. After loading the SPQ/iodide
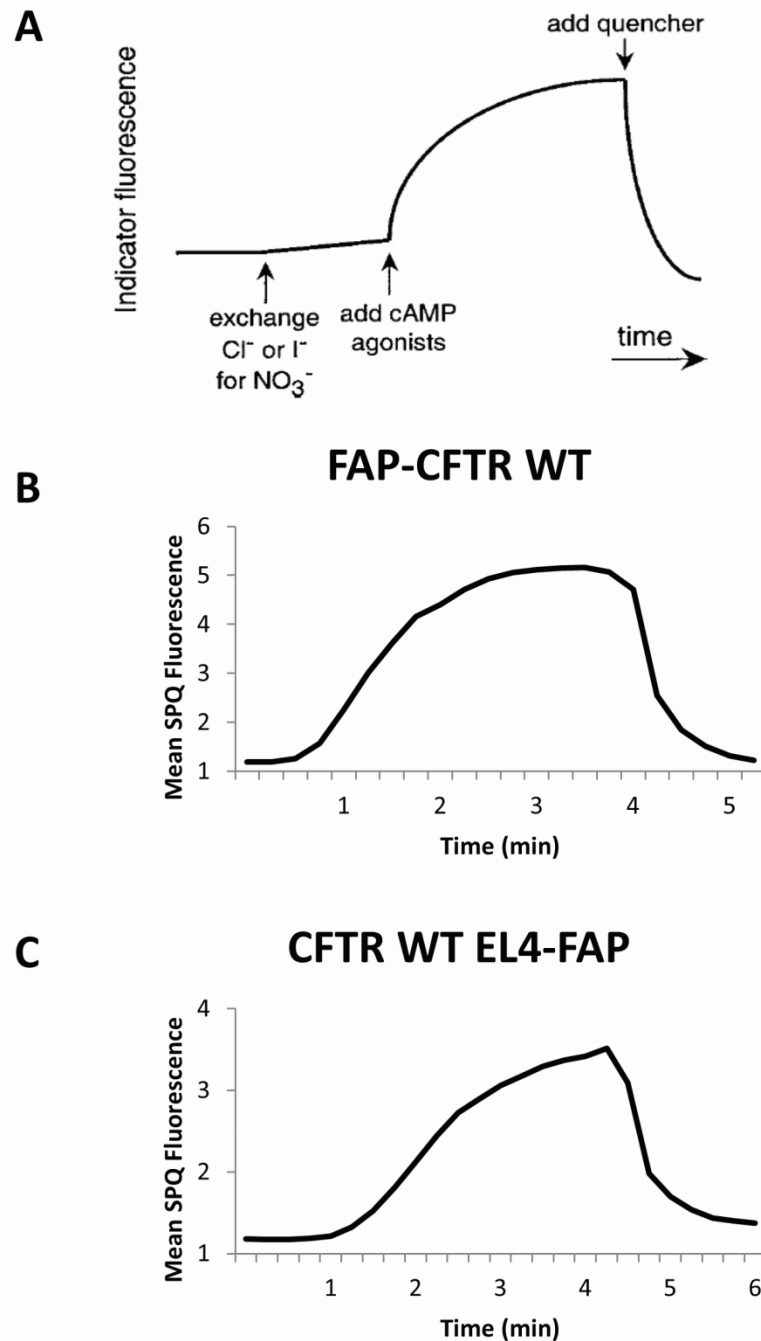
solution into the cells, the fluorescent indicator is dark because it is quenched by iodide. Iodide is

perfused over the cells to establish the baseline fluorescence and then iodide is replaced with $NO3^-$, an

anion that does not quench SPQ. Next, Fsk is added to the cells, which activates PKA and stimulates

CFTR channel opening. This results in iodide efflux from the cell in exchange for $NO3^-$ which dequenches

the SPQ dye. This process is measured by an increase in fluorescence. After the fluorescence reaches a

plateau, iodide is added back to the cells to re-establish the baseline fluorescence.

We found that both the N-terminus and EL4 FAP tagged CFTR constructs displayed a characteristic CFTR

iodide efflux in response to Fsk activation (Figure 1-9, B and C). Each of the CFTR WT FAP reporter

constructs produced a sharp iodide efflux indicating that the channel is fully functional. Therefore, the

physiological activity of CFTR had not been perturbed by the FAP reporter modifications. Moreover, the

iodide efflux was confirmed to be specific to the FAP tagged CFTR constructs because HEK293 cells do

not express CFTR endogenously which was verified by the lack of Fsk response in HEK293 control cells.

Additionally, the iodide efflux activity could be blocked in cells expressing FAP-CFTR WT by the addition

of a CFTR specific inhibitor, CFTRinh-172 (Figure S-1).

Biochemical Analysis of Fluorescent CFTR Reporters

We also examined the biochemical properties of both FAP tagged versions of CFTR WT. To do this we used immunoblotting with a CFTR specific antibody to analyze the glycosylation patterns of cell lysates from HEK cells expressing either FAP-CFTR WT or CFTR WT EL4-FAP. The FAP-CFTR WT migrated as two distinct bands which we interpret as the core and mature (B and C respectively) bands (Figure 1-10, A) with an increase in molecular weight attributed to the addition of the FAP tag. This result is qualitatively consistent with untagged CFTR, however the ratio of B:C band is higher than expected[21,22]. The CFTR WT EL4-FAP construct on the other hand did not produce distinct B and C bands (Figure 1-10, A). Although a larger migrating band was present above the core glycosylated form, it did not show the molecular weight shift expected for complete mature glycosylation.
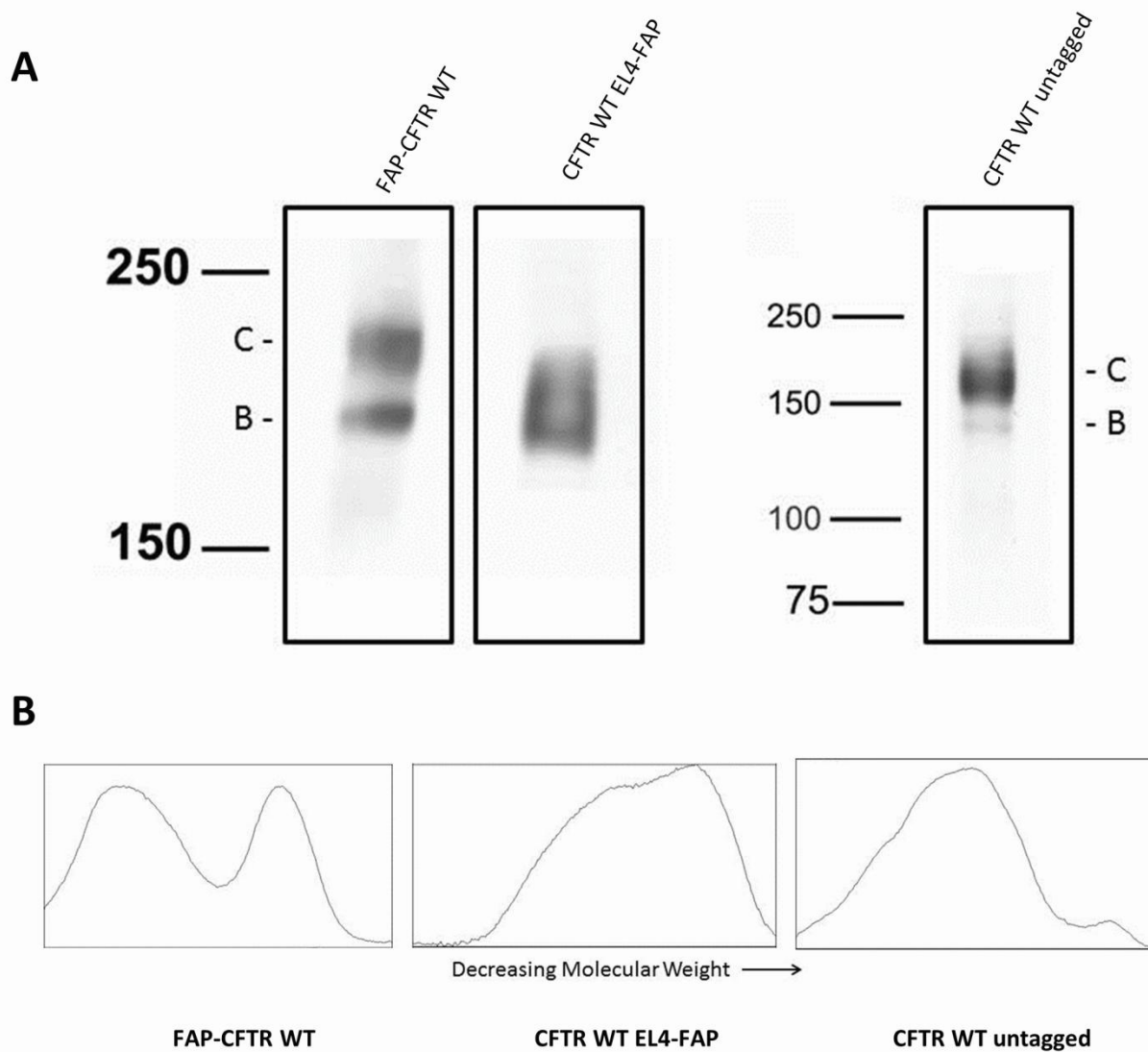
Figure 1-10: Biochemical Properties of CFTR WT FAP Constructs

Immunoblot of whole cell lysates using a CFTR specific antibody. (A) FAP-CFTR WT migrated as two distinct bands marked as B (core ER form) and C (mature Golgi acquired form). CFTR WT EL4-FAP did not have a clearly separated C band. Untagged CFTR WT from Calu-3 cells produced distinct B and C bands. (B) Densitometry analysis of immunoblot showing the distribution of signal in each lane was performed using NIH ImageJ.

Ch. 1 – Discussion

We have shown through two tagging strategies, selective detection of CFTR at the cell surface using FAP reporters. FAP fusions at the N-terminus required creation of novel modular mammalian expression vectors, pDisplaySacLac2 and pBabeSacLac2, which facilitate rapid cloning and are highly versatile for other membrane protein fusions. The CFTR WT EL4-FAP construct was engineered by modifying a CFTR vector which already contained GFP in this position. Both of these strategies produced fusion proteins that were trafficked and functional at cell surface.

The SacLac2 construct was designed to facilitate rapid cloning of ORFs into each module. This was essential for testing different FAPs and to tag different membrane proteins. SfiI and PflmI restriction sites were chosen because they are interrupted palindromic recognition sites with 3 base overhangs. For this reason, we were able to design sites that enabled the directed ligation of any amplicon with our SfiI sites into either the Sac or Lac module. This was extremely useful for generating many different combinations of fluorescent protein or various FAP-tagged versions of CFTR.

To our knowledge, this is the first use of an additional membrane spanning fragment to create a fusion protein to another full length transmembrane protein. Single pass transmembrane fusion proteins have been used extensively as tools to measure the properties of proteins at the cell surface. The prototype for the commercially available pDisplay system fused functional scFvs on the surface of mammalian cells via a PDGFR TM domain[56]. The purpose of this TM domain was to anchor the scFv to the extracellular face of mammalian cells, not to create a fusion between it and another membrane protein. As another example, peripheral protein quality control was examined by engineering a single transmembrane fusion protein between the truncated CD4 TM domain and the λ domain to determine the ubiquitination state and subcellular fate of unfolded proteins from the cell surface[61,62]. These studies have provided details on the mechanisms that recognize unfolded proteins at the cell surface by

ubiquitination and sorting after unfolding at the PM, a process that relates directly to CFTR trafficking. Although these studies provided a useful tool for dissecting the mechanisms that survey proteins that traffic to the PM, this was not an example of a fusion between an additional TM domain to a full length membrane protein. Therefore, our pBabeSacLac2 mammalian expression vector enabled the demonstration of a unique tagging approach that fuses a fluorescent reporter to an intact full length membrane protein.

A concern that arose from the N-terminal tagging of CFTR effort was whether the fusion protein would acquire the correct topology. Several strong lines of evidence show that the N-terminal FAP-CFTR fusion protein folds and expresses with the topology expected. First, the FAP-CFTR construct can be detected by cell impermeant fluorogen detection. This indicates that the FAP is exposed to the extracellular environment. Additionally, the fusion protein is capable of navigating the secretory pathway and trafficking to the cell surface where it is embedded in the PM. Further, FAP-CFTR possesses the correct glycosylation pattern with both core and mature band when visualized by immunoblotting. For this process to occur, the consensus glycosylation sequence must be accessible in the luminal side of the ER compartment. The ER resident oligosacharyltransferase which mediates N-linked glycosylation of CFTR can only glycosylate this protein if the proper topology is attained[22,63]. Finally, the most convincing piece of evidence that the FAP-CFTR fusion protein attains the expected topology is the functional studies by SPQ analysis. Anion transport in response to cAMP activation requires the correct folding of multiple protein domains and interaction between these domains. We observed a characteristic iodide efflux in response to forskolin activation. This was shown to be CFTR specific because this activity was abolished in the presence of CFinh172. The complex activity of this protein necessitates that many biosynthetic steps must occur correctly for proper CFTR activity. Taken together, these results show that the addition of the PDGFR TM domain and the FAP reporter at the N-terminus of CFTR produces a fusion protein with the expected topology that maintains native functionality.

Similarly, the chimeric fusion with the FAP in the fourth extracellular loop of CFTR was tested to confirm that normal anion transport function was not perturbed. The fourth extracellular loop was chosen as the target site for insertion of our FAP reporter for three reasons. First, EL4 is the largest extracellular domain in CFTR. Second, a triple HA tag had been inserted at this position and was used successfully to track the protein from the cell surface to intracellular compartments[23]. Third, this site was found to tolerate larger modifications such as GFP and still retain functionality[40]. As with the N-terminal fusion, trafficking and topology was verified to be consistent with expectations because upon addition of membrane impermeant fluorogen the fusion protein was detectable at the cell surface. Physiological activity was verified by SPQ iodide efflux measurements. We found that the transport activity was consistent with that of untagged CFTR as well as the N-terminal fusion construct.

Immunoblot analysis was used to reveal the glycosylation state of the FAP-CFTR WT and CFTR WT EL4-FAP fusion constructs. The N-terminal FAP-CFTR fusion migrated as two distinct bands, the core and mature bands similar to untagged CFTR WT. The presence of a mature band indicates that the protein had traversed the Golgi compartments where it underwent oligosaccharide chain elongation and modification.   Complex glycosylation (mature form) is not strictly required for the export of CFTR from the ER and Golgi to the cell surface, however it does play a major role in determining the PM stability and turnover of the protein[21]. The presence of the mature glycosylated form suggests that the protein folded correctly and is likely to have a similar turnover at the PM as untagged CFTR.

The ratio of mature to core band [C/(B+C)] is a measure of how efficiently the protein is processed. Native CFTR is predominantly detected as the mature C form with very little B band present.   In contrast, FAP-CFTR is detected with substantial B band and only slightly more C band (Figure 1-10, A and B). This difference could be attributed to a number of variables. The addition of the PDGFR and FAP domain might slow the biosynthetic processing or make the fusion protein more susceptible to

misfolding. Another possibility is that heterologous overexpression in a HEK293 cell background has overwhelmed the cellular machinery to fold FAP CFTR fusion proteins.

It has been reported that CFTR processing is very inefficient, with only 25% of synthesized protein fully processed[26]. Meanwhile, other studies have shown extremely efficient biogenesis approaching 100% in an endogenous cell line which argues that this processing is highly dependent on the cellular background[29]. Regardless of the C band to B band ratio for FAP-CFTR WT, the presence of the mature band is an important finding and directly indicates that the protein has been fully processed.

The CFTR EL4-FAP construct did not produce a distinct mature band, which suggests that its glycosylation was impaired. The fourth extracellular loop of CFTR is the site of two asparagine (N894 and N900) residues that acquire N-linked glycosylation, and therefore careful consideration was taken to preserve these residues and the consensus sequence (NXS/T) surrounding these in the FAP fusion construct. This incomplete glycosylation could be due to only a single asparagine residue receiving glycan modification or partial oligosaccharide attachment and modification on both sites. Since both asparagine and consensus sites are present in this construct, it is possible that interrupting these sites with the FAP tag has changed the amino acid context surrounding the minimal glycosylation consensus sequence and thereby impaired glycosylation enzyme recognition and/or accessibility to these sites. Steric constraints imposed by the large FAP domain may also significantly contribute to the reduced glycosylation of CFTR by blocking access to the oligosaccharyltransferase enzyme.

Selective detection of CFTR at the cell surface is a prerequisite for studying the trafficking behavior of from the PM to intracellular compartments. Traditionally this has been accomplished by time and labor intensive biochemical labeling methods such as biotinylation and immunofluorescence. By using a genetically encoded FAP reporter, we can selectively label CFTR at the cell surface instantly without the need for incubation or wash steps that may modify cellular CFTR handling. The cell impermeant

fluorogen remains dark when free in solution, however upon binding to the FAP there is a dramatic increase in fluorescence and thus eliminates the need for wash steps to remove any non-specific signal. Therefore, the FAP reporter platform for CFTR detection enables rapid and selective labeling at the cell surface compared to biochemical and immunofluorescent detection.

Ch. 1 – Materials and Methods

Reagents

Cellstripper was purchased from Mediatech (Manassas, VA). TO1-2P, MG-ester and MG-11P were provided by CMU MBIC reagent chemistry department (Dr. B. Schmidt)

Construction of Fluorescent Reporters and Plasmids

Expression vector pDisplaySacLac2 was constructed as follows. The SacB gene was PCR-amplified from the vector pDNR-1r (Clontech, Mountain View CA) using primers

SacB Fwd: TATATAGGCCCAGCCGGCCCCACATATACCTGCCGTTCAC

SacB Rev: TATATAGGCCCCTGCGGCCACGTCAATGCCAATAGGATATCG.

The amplicon was cut with SfiI and cloned into SfiI-digested pDisplayBlue to produce pDisplaySac. The Primers:

Fwd: AGAGGATCTGAATGCTGTGG

Rev: CTCGAGCTAACGCCACCTGCTGGCATCGTCCAGGCTGTGGACGTGGCTTCTTCTGCCAA

were used to generate an amplicon from a pDisplayBlue template that contained the PDGFR transmembrane-domain; the amplicon was cut with BsmI and XhoI and ligated into BsmI/XhoI-digested pDisplaySac. The resulting construct was digested with PflMI. Primers:

CCACAGCCTGGGTTAGCTCACTCATTAGGCA

CCACCTGCTGGCTAACGCCAGTTTGAGGGGACGACGA

were used to generate an amplicon from a pDisplayBlue template that contained the lacZα complementing fragment, and PflMI-digested amplicon was ligated into the construct to create pDisplaySacLac2.

Retroviral expression vector pBabeSacLac2 was constructed as follows. pBabe-puro-H-Ras-V12 (Addgene, Cambridge MA), which carries an SfiI site upstream of the puromycin resistance gene, was linearized with SfiI, treated with T4 polymerase to create blunt ends, and self-ligated to create a derivative without an SfiI site. This plasmid was digested with BamHI and SalI to produce a recipient fragment. pDisplaySacLac2 was digested with BamHI and XhoI, and a 650bp BamHII/XhoI fragment was recovered and ligated into the recipient fragment to produce pBabeSacLac2.

Generation of vector inserts

SfiI sites were added to the ends of open reading frames (ORF) by PCR. 5' primers added the 13-nt sequence:

GGCCCAGCCGGCC

to the extreme 5' end of the ORF, and 3' primers added the 13-nt sequence:

GGCCGCAGGGGCC

to the extreme 3' end of the ORF.   Amplicons were cloned into the vectors pCR2.1-TOPO or pCR-Blunt II-TOPO (Invitrogen, Carlsbad CA), sequenced to confirm that no mutations were introduced during amplification, and removed from the vector by SfiI digestion. Molecules were generated in this way for six ORFs: EGFP (template: pStealth,(12)), mRFP (template: pACT-mRFP-Mem, gift of Dr. Y. Saeki, Ohio State University), HL1.1-TO1 (template: pNL6-HL1.1-TO19 (1)), HL4-MG (template pNL6-HL4-MG,(1)), human GLUT4 (template: cDNA clone 726246, Open Biosystems, Huntsville AL), and human CFTR (template: pcDNA3.1 CFTR, gift of Dr. R.Frizzell, Children's Hospital of Pittsburgh. These two amplicons also included the template stop codon; in the other cases a stop codon was not included. A seventh fragment containing a complete ORF and stop codon from the ADRB2 gene, encoding the β2AR receptor (template: fosmid WI2-2202O9/G248P86156H5, BACPAC Resources Center, Oakland CA) was prepared in an equivalent manner, but with the sequence flanked by BsmI sites.

Synthetic Dimer FAP

The two domain synthetic dimer dNP138, FAP ORF was constructed by (C. Szent-Gyorgyi, CMU). A

derivative of the L5-MG FAP, NP138 was duplicated and genetically linked by a 3X (Gly$_4$Ser) flexible

tether. Codon optimization was carried out so each domain would encode the same amino acids,

however, have different DNA sequences in order to minimize homologous recombination and reduction

during the cloning and expression process. Cloning of the dNP138 into pBabeSacLac[2] was accomplished

by designing primers that hybridized to the original sequence but encoded SfiI restriction sites and an

additional 3X (Gly$_4$Ser) at the C-terminus (already present at the N-terminus).

NP139 Tandem Dimer Fwd: GGCCCAGCCGGCCCAGGCCGTCGTTACCCAAGA

NP 138 G4Sx3 Rev: GGCCCCTGCGGCCGGATCCTCCTCCTCCTGATCCTCCGCCTCC-

GGATCCTCCTCCGCCCAAGTCTTCTTCAGAAATAA

The resultant two domain FAP with 3X (Gly$_4$Ser) at both the N and C-termini, dNC138, was verified by

sequencing and given the name dNC138, where the NC denotes the presence of flexible linkers at the

both termini

CFTR EL4-FAP Chimera Construction

Insertion of the FAP in the fourth extracellular loop of CFTR (both WT and F508del) was generated with

an modified version of CFTR where KpnI and EcoRV sites have been introduced (a gift from Peter

Haggie)[40]. A summary of the strategy was provided by P. Haggie:

Split CFTR cloned into pcDNA3.1. The first section of CFTR cloned as NheI (gctagc) to KpnI (ggtacc). The

second section of CFTR cloned as EcoRV (gatatc –Blunt cutter) to XhoI (ctcgag). Any numbering is

relative to NM000492.3 with methionine at position 133. At junction (no CFTR residues were removed

and both Asn residues were retained for glycosylation):

AAAGGGAAT(2814)AGTACTCATAGT(2826)

GGTACCGAGCTCGGATCCACTAGTCCAGTGTGGTGGAATTCTGCA (pcDNA3.1 sequence)

GATATCTC(2827)AGAAAT(2832)AACAGCTAT

To prepare the Split CFTR construct for insertion of FAPs into the EL4, compatible restriction sites were inserted by using eGFP as a stuffer sequence. The eGFP first amplified with KpnI and EcoRV containing primers and SfiI nested restriction sites.

eGFP KpnI SfiI Fwd: GGTACCAAGGCCCAGCCGGCCAGCAAGGGCGAGG

eGFP EcorV SfiI Rev: GATATCGGCCCCTGCGGCCCTTGTACAGCTCGTC

This amplicon was then cut and inserted between the KpnI and EcoRV sites corresponding to the amino acid sequence: KG**N**(894)STHS – R**N**(900)NSY. The dNC138 FAP sequence replaced the eGFP stuffer fragment by SfiI digestion and ligation of this insert. CFTR ΔF508 EL4 constructs were made by swapping the sequence containing this mutation from a ΔF508 containing plasmid using NheI and BsgI digestion and ligation into the recipient EL4 plasmid background which was also cut with NheI and BsgI. Both WT and ΔF508 constructs were verified by sequencing. The ORF encoding the CFTR EL4-dNC138 was then transferred to a retroviral pBabeH-Ras V12-Puro plasmid via BamHI and XhoI restriction sites for stable expression in mammalian cells.

Cell lines

NIH 3T3 cells were obtained from the American Type Culture Collection (Manassas, VA). C2C12 cells were the gift of Dr. P. Campbell, Carnegie Mellon University. HEK 293 cells were the gift of Dr. R. Frizzell, Children's Hospital of Pittsburgh.

Transfection

Transfections were performed using Mirus TransIT®-LT1 Transfection Reagent (Mirus, Madison WI) and pDisplaySacLac2 vectors. For 35mm dishes: DNA (2.5µL, concentration of 1µg/mL) was added to 7.5 µL

TransIT®-LT1 in 250 μL of DMEM. Transfection complexes were allowed to form for 30 minutes and subsequently added to cells grown in antibiotic free DMEM with 10% calf serum. Transfection complexes were removed and medium changed after 24 hours.

Transduction

Transducing particles for pBabeSacLac2 constructs were generated using the Phoenix Ecotropic Packaging System (Nolan laboratory, Stanford University). Phoenix-Ecotropic cells were plated at 1.3X106 cells/ 75cm2 flask in DMEM with calf serum without antibiotics. pBabeSacLac2 DNA was transfected as described above scaled to surface area. After 24 hours, transfection complexes were removed and replaced with 8mL of DMEM with calf serum and incubated for 48 hours at 32°C/5% CO2. Medium was removed and filtered through Millex-HV 0.45μm syringe filter and flash frozen in liquid nitrogen. Recipient cells were plated at 2X105 cells/ 35mm dish 24 hours prior to transduction. Cells were infected by adding viral supernatant and 6μg/mL of hexadimethrine bromide and incubated for 24 hours at 32°C/5% CO2. Cells were replated in 75cm2 flasks and screened for expression 48 hours later.

Fluorescence microscopy

Cells were grown in DMEM plus 10% calf serum in 23 mm glass-bottom dishes (Mattek, part no p35G-1.5-14-C) and imaged with Carl Zeiss LSM 510 Meta/ UV DuoScan Inverted Spectral Confocal Microscope at 63x objective magnification or Nikon spinning disc confocal microscope with 60X magnification. For cells expressing FAP HL1.1-TO1, 40nM TO1-2P, a membrane-impermeant fluorogen, was added approximately 5 minutes prior to imaging. For cells expressing HL4-MG, 40nM MG-11P, a membrane-impermeant fluorogen or 40nM MG-ester, a membrane-permeant fluorogen, were added approximately 10 minutes prior to imaging. Times (5 minutes and 10 min) were shown in pilot experiments to be sufficient to reach saturation with regard to signal intensity and location. Excitation and emission wavelengths were 488nm and 505-550nm for EGFP, 561nm and 575-615nm for mRFP,

488nm and 505-550nm for HL1.1-TO1, and 633nm and LP 650nm for HL4-MG. Illumination intensity and detector gain settings on the microscope were held constant for all observations.

Iodide Efflux Assay

HEK293 cell lines expressing FAP-CFTR WT and CFTR WT EL4-FAP were assessed for CFTR activity by 6-methoxy-N-(3-sulfopropyl) quinolinium, SPQ, iodide sensitive fluorescent indicator. Iodide solution contained NaI 130mM, Mg(NO3)2 6H2O 1mM, Ca(NO3) 4H2O 1mM, KNO3 4mM, Glucose 10mM and HEPES Hemi-Na 20mM. Nitrate solution contained NaNO3 130mM, Mg(NO3)2 6H2O 1mM, Ca(NO3) 4H2O 1mM, KNO3 4mM, Glucose 10mM and HEPES Hemi-Na 20mM. Cells were grown in the absence of antibiotic for at least 48h before measurement and were plated on glass bottom dishes (Mattek, part no p35G-1.5-14-C) 24 hours prior to iodide efflux measurement. Samples were hypotonically loaded with Iodide and H2O 1:1 v/v and 10mM SPQ for 20min at 37°C. After loading cells with SPQ they were imaged at 40X on an inverted epi-fluorescence microscope capturing images every 15s. Fluorescent filter set up used to excite SPQ was 350nm and capture emission at 455nm. Cells were perfused with buffers warmed to 37°C. For each experiment the following protocol was used: Iodide buffer was perfused for 3 min, exchanged with Nitrate buffer for 3 min, then Nitrate buffer with 10µM Forskolin and finally switched back to Iodide buffer for 3 min. Images were analyzed using NIH ImageJ by measuring the mean fluorescence intensity of 5-10 cells.

Chapter 2 : Detection of CFTR ΔF508

Ch. 2 - Introduction

CFTR ΔF508

The most common cause of cystic fibrosis is the ΔF508 mutation in the CFTR gene, present on at least one allele in 90% CF patients[2]. The CFTR ΔF508 gene product is translated and co-translationally inserted into the ER. The missing phenylalanine residue mutation causes a folding defect and misfolded protein is recognized by the endoplasmic reticulum associated degradation (ERAD) pathway and targeted for premature destruction. Misfolded CFTR ΔF508 is marked as such by ubiquitin conjugating enzymes which signal for the protein to be retrotranslocated from the ER to the cytosol. From here, the misfolded and ubiquitinated protein is degraded by the proteasome[27]. ERAD recognition and proteasomal degradation is a highly efficient process and virtually all of the CFTR ΔF508 protein is removed in this way. As a consequence, CFTR ΔF508 does not traffic to the cell surface which results in a lack of chloride transport across the membrane.

The ΔF508 mutation maps to the first nucleotide binding domain (NBD1) of CFTR[64]. Protease susceptibility experiments indicate that it directly causes folding instability within this domain. *In vitro,* NBD1 folding is disrupted by the ΔF508 mutation; however, this can be overcome by replacing the missing residue with any amino acid except tryptophan and other hydrophobic residues[65]. This suggests that the particular side chain of the residue at position 508 is not as important as the overall backbone structure. Suppressor mutations within the NBD1 have been identified which are capable of alleviating the folding defect within NBD1. Several compensatory mutations have been identified by genetic analysis of patients with a mild CF phenotype. These include the R553Q, I539T, G550E and R555K mutations[66,67]. Interestingly, the I539T suppressor mutation robustly rescues the folding and trafficking

defect both *in vitro* and in mammalian cells. The threonine at position 539 is present among many species such as mouse, rat and rabbit, suggesting that either isoleucine or threonine at this position are important residues for the structural integrity of NBD1[68]. Mapping the locations of these mutations and understanding the structural changes that they impart will provide insight into how the ΔF508 mutation affects NBD1 folding.

Inter-domain interactions are also critical for the proper folding of CFTR. Several studies have shown that the interface between NBD1 and MSD2 is perturbed as a result of the ΔF508 mutation. Specifically, structural models and have identified the fourth intracellular loop (ICL4) as an interface which interacts with NBD1[69-71]. The contacts between NBD1 and ICL4 are predicted based on homology models from the bacterial proteins Sav1866 and MsbA so caution should be taken when inferring specific physical contacts from these models. Nevertheless, support for the ICL4-NBD1 interface has also come from biochemical experiments, where mutant forms of CFTR were analyzed from a heterologously expressing mammalian cell line. It was found that a particular residue, R1070, when substituted for tryptophan can promote the maturation of CFTR ΔF508. Smaller amino acid side groups such as lysine and alanine failed to rescue trafficking and therefore it is thought that the bulkiness of the tryptophan side group stabilizes interactions between the ICL4 and NBD1 domains[66]. Due to the number of domains present in CFTR and the fact that biosynthesis takes ~30min, folding of CFTR likely involves a complex set of inter-domain interactions, many of which have yet to be identified[26]. One should therefore keep in mind that the interactions disrupted by the ΔF508 mutation may not be confined to NBD1 and ICL4.

Temperature Sensitivity and Gating Defect of the ΔF508 mutation

The ΔF508 protein has a temperature sensitive defect that can be overcome by incubation at low temperature (27-32°C)[72]. At this permissive temperature CFTR ΔF508 can exit the ER, navigate through the Golgi and translocate to the cell surface. Not only can CFTR ΔF508 trafficking be rescued to the PM by low temperature, but a small amount of anion transport activity is retained. The mechanism by which low temperature rescues the trafficking of CFTR ΔF508 is not completely understood. One factor may be that by reducing the temperature, the kinetic properties of the protein are altered which may alleviate kinetic folding traps. Thermodynamic stabilization of the CFTR ΔF508 by reduced temperature cannot completely account for the rescue of the protein, as the degree of rescue is highly variable depending on the cell type examined[73]. This implies other factors are involved that may promote protein maturation. In addition to thermodynamic stabilization, the local folding environment of different cell types has a significant impact on the potential for temperature rescue.

Chaperone Quality Control Checkpoints

Cyotoplasmic stress inducible factors such as the Hsp70 and Hsp90 chaperones and associated proteins are associated with CFTR during biogenesis. Hsp70 increased during incubation at low temperature whereas Hsp90 had the opposite behavior in a HEK293 cell background[73]. The balance of these and other chaperones exhibit a dynamic expression and association with CFTR and may reflect the binding to different folding intermediates. On the luminal side of the ER there are also lectin- like chaperones that sense the folding state of CFTR and determine if the protein is competent for ER export. Calnexin, calreticulin and EDEM are ER chaperones that bind to the N-glycans that are added to the fourth extracellular loop of CFTR[74,75]. By binding to the N-linked oligosaccharide modifications, calnexin and EDEM ensure that the glycosylation state is correct and if not, initiate the removal and reattachment of

N-glycans. The improperly folded and incompletely glycosylated forms are detected by EDEM and targeted for degradation by the 26S proteasome[21]. Although calnexin and calreticulin appear to ensure that the N-glycosylation is complete, inhibition of these proteins does not necessarily rescue the export of CFTR ΔF508 from the ER. For example, there have been conflicting reports about whether removing calnexin or calreticulin is sufficient to facilitate trafficking of CFTR ΔF508 to the cell surface. Depending on the study, these chaperone interactions were perturbed either by siRNA knockdown or by pharmacological interruption using thasparigin, 1-deoxymannojirimycin, kifunensine or castanospermine; however export of CFTR ΔF508 after these treatments was inconsistent and in some cases, unable to be reproduced[21,76-78]. This indicates that the ER export block of CFTR ΔF508 is not completely controlled by ER lectin chaperones. Therefore, there must be other quality control checkpoints at the ER level that restrict CFTR ΔF508 from trafficking that are more important.

Since the ER lectin chaperones are not the only molecules that control the retention of CFTR ΔF508 there must be other mechanisms involved. In fact, studies have shown that the ubiquitin pathway is primarily involved in the targeting of improperly folded CFTR for degradation. More specifically, ubiquitylation of misfolded CFTR ΔF508 by E3 ubiquitin ligating enzymes, Hsc70 and CHIP (carboxyl-terminus HSC70 interacting protein), direct this protein to the proteasome for degradation[79]. Other quality control mechanisms are in place to monitor the proper folding of CFTR. For example, another ubiquitin ligation factor that recognizes misfolded CFTR is the RMA1 and Ubc6e complex. This complex is recruited to inappropriately folded CFTR by the Derlin-1 protein. Derlin-1 brings RMA1 and Ubc6e in close enough proximity to ubiquitylate CFTR ΔF508 thereby signaling this protein for premature proteasomal degradation[80,81]. Both of these ubiquitylation pathways serve as quality control checkpoints that prevent misfolded CFTR from exiting the ER. Whether these pathways are redundant or complementary, the net result is very efficient destruction of CFTR ΔF508 and consequently virtually no CFTR ΔF508 escapes the ER compartment.

Repairing the Gating Defect

When CFTR ΔF508 trafficking to the PM is restored by low temperature, it still retains some functionality as a chloride channel. Relative to wild type CFTR however, temperature rescued CFTR ΔF508 has a severe gating defect[82]. The gating defect drastically reduces the open probability of the channel, even after cAMP activation thereby limiting its activity despite proper membrane localization. Because the channel activity is not restored despite PM localization, there have been efforts to identify compounds that would alleviate the gating defect to maximize channel activity after rescue.

High throughput drug screening efforts have successfully identified many compounds that ameliorate the gating defect of CFTR mutants[83-86]. Compounds that improve the CFTR channel conductance are coined "potentiators". These small molecule potentiators are potent activators of CFTR with low nanomolar affinity. Many act directly on the channel by binding to the NBDs which hydrolyze ATP, the process which controls the flow of ions through the CFTR pore. There has been significant progress made in the optimization of potentiator compounds. The flavone compound, genistein, has been used for many studies but the therapeutic potential for this molecule is limited as it must be applied at relatively high concentrations (50µM) and the effects are not specific to CFTR as it produces off target effects[87]. More recently, new classes of potentiators such as the phenylglycine derivative (P2) or VX-770 compounds have been used because they require lower concentrations and are highly specific to CFTR. The latter compound is currently through phase 3 of clinic trials to treat the G551D, class III mutation, and will soon be on the market[84,85].

One approach that has been taken to discover potentiator small molecules by HTS was through the use of a fluorescent protein that is sensitive to selective anions. The yellow fluorescent protein (YFP) mutant, YFP-H148Q, has an amino acid substitution near the chromophore that makes its fluorescence
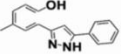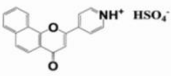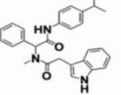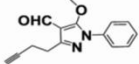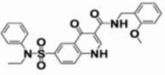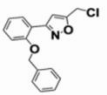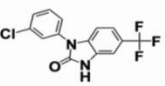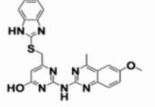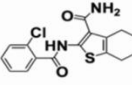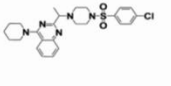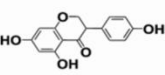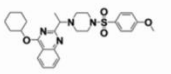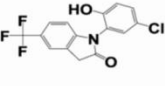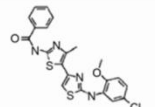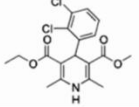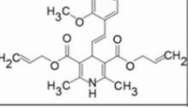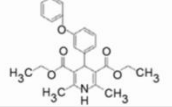
sensitive to increasing Cl⁻ or I⁻ concentrations[88]. Initially YFP-H148Q had relatively poor sensitivity, but was later mutated further and variants were selected with a greater Cl⁻ and I⁻ sensitivity (YFP-H148Q/I152L)[89]. This halide sensitive YFP was co-expressed with CFTR ΔF508 in human bronchial epithelial cells and used to screen a library of small molecules. This assay depended upon the low temperature trafficking rescue of CFTR ΔF508 to the cell surface, stimulation of CFTR by a cAMP activator and addition of the test compound, then measurement of YFP fluorescence. If the YFP fluorescence was reduced, this indicated an influx of I⁻ from the extracellular environment into the cells via CFTR ΔF508. Compounds that produced the most robust YFP quenching were chosen for further validation. This approach has been extremely productive, identifying multiple classes of diverse potentiators[83,84,86] (See Figure 2-1, A for a list of potentiator compounds).

An alternative to the YFP based screening technology taken by another group, used a förster resonance energy transfer (FRET) based voltage-sensitive dye to measure membrane potential[90]. In this assay, NIH3T3 cells were loaded with a voltage sensitive dye, DiSBAC2, and a coumarin fluorescent dye was attached to the cell membrane. The principal of this assay is essentially the same that was used for the YFP compound screening scheme. Cells expressing CFTR ΔF508 are incubated at low temperature for 24 hours to deliver CFTR ΔF508 to the cell surface, then CFTR is stimulated with Fsk and the test compound and then any fluorescence change is measured by high throughput fluorimetry. As with the YFP based approach, the membrane potential probes have proven very successful in identifying compounds that are capable of ameliorating the gating defect. Furthermore, combinatorial chemistry was used to diversify a potentiator scaffold to generate VX-770, the most promising clinically relevant compound to date[85].

Correctors

Just as high throughput screening can be used to identify potentiators of CFTR, this approach can also be

used to search for compounds that rescue the trafficking defect of CFTR ΔF508. These molecules are

termed "correctors". By changing the protocol for screening with the halide sensitive YFP-H148Q/I152L

indicator, several small molecules were found that promote trafficking to the cell surface. Instead of

adding the compounds after low temperature rescue, the compounds were added to cells co-expressing

CFTR ΔF508 and YFP-H148Q/I152L and incubated for 24 hours. This step allowed the compounds to

exert their effect on the folding of the protein and permit the protein to traffic and accumulate at the

cell surface. If the test compound successfully rescued the protein to the cell surface this could be

detected by the cAMP responsive I⁻ transport in the presence of a known potentiator, as measured by

quenching of YFP fluorescence in a microwell format. Indeed, the first attempt to fish out correctors

from a library containing over 150,000 compounds produced four candidates[1] (See Figure 2-1 for a list of

correctors and screening strategy). Corrector 4a (C4) was the most potent compound identified in this

study. A near linear dose dependent response for this C4 up to 10µM concentration improved the

surface density and Cl⁻ conductance. Within 12 hours C4 was shown to increase the amount of mutant

CFTR at the cell surface. Biochemical indicators of folding rescue were also detected in the presence of

this corrector. Using immunoblot analysis, the maturation of CFTR ΔF508 was visualized by the

accumulation of a complex glycosylated C band in the presence of C4 corrector that was absent in the

vehicle treated control. The amount of rescue that C4 provides is comparable to low temperature

treatment, about 8% in human airway epithelia. This effect was modest, but was the first

demonstration that this type of screen was capable of identifying small molecules that could correct the

complex folding defect of CFTR ΔF508.

CFTR Modulator	Structure	Activity	Name		Structure	Activity	Name
				P8		potentiator	UCCF-029
P1		potentiator	VRT-532	P9		potentiator	UCCF-180
P2		potentiator	PG-01	P10		potentiator	UCCF-152
P3		potentiator	SF-03	C1		corrector	corr-3a
P4		potentiator	UCCF-853	C2		corrector	VRT-640
P5		potentiator	ΔF508act-02	C3		corrector	VRT-325
P6		potentiator	Genistein	C4		corrector	corr-4a
P7		potentiator	NS004			potentiator	felodipine
						potentiator	DHP-229
						potentiator	DHP-256
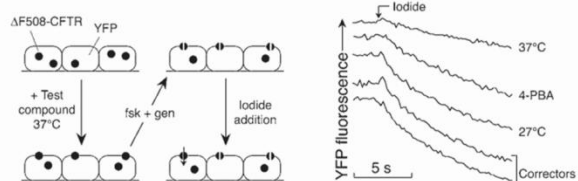
Figure 2-1: CFTR Correctors and Potentiators[1,53]

(A) List of currently available correctors and potentiators for CFTR mutants identified by high throughput drug screening[53]. (B) Halide sensitive YFP corrector screening strategy and representative output[1].

By modifying the protocol to incubate cells with the test compounds for 24 hours before fluorescence measurements, in the same membrane potential FRET based screening effort to obtain potentiators, Van Goor et al. also described two new corrector compounds that modulate the folding of CFTR ΔF508 and promote trafficking to the PM[90]. Correctors VRT-422 and VRT-325 increased the PM density and mature glycosylated form without altering the transcriptional levels of CFTR ΔF508. These molecules apparently improved the folding of this protein to a state that passed the cellular quality control checkpoints. Correction achieved 47% and 75% the level of low temperature incubation for VRT-422 and VRT-325 respectively. As with the C4 corrector, the amount of rescued activity was very modest (~10%) compared to wild type after treatment with VRT-422 or VRT-325.

The relatively poor efficiency that all of these correctors exert on the ΔF508 mutant suggests that these small molecules are not completely addressing the underlying molecular defect. Furthermore, even though trafficking is restored by these correctors, potentiators are still needed to overcome the gating defect, highlighting the fact that the protein is still functionally impaired by this mutation. But how much CFTR activity is really needed to provide a therapeutic benefit. If this estimate is accurate, the C4, VRT-422 and VRT-325 correctors should be sufficient to overcome the pathology of cystic fibrosis. Unfortunately, due to toxicity, off-target and inconsistent efficacy among different cell lines, none of these correctors in their current form are suitable candidates for clinical therapeutic agents.

Both the YFP and the membrane voltage potential fluorescence strategies for drug screening rely on the indirect functional measure of CFTR ΔF508 rescue. Some of the pitfalls of these methods are: (1) small molecules do not necessarily act directly on the CFTR protein but rather may interact with a chaperone or modulate a quality control checkpoint leading to off-target effects (2) Compounds may be specific to the cell type in which they were screened and may not translate to a polarized epithelial cell background.

A more direct approach to develop small molecules that stabilize the molecular defect (i.e. folding

instability from NBD1) uses differential scanning fluorimetry (DSF) to assess the folding state of NBD1 *in*

vitro. Potential compounds (224) were isolated from a previous HTS effort[91] to test on purified murine

NBD1 protein. Only one of the selected compounds stabilized the thermal unfolding of NBD1-ΔF508.

This small molecule, RDR-1, was further validated by biochemical and functional assays to determine if it

was capable of rescuing full length CFTR ΔF508 *in vivo*[92]. In the presence of RDR-1, CFTR ΔF508 acquired

complex glycosylation and the ion conductance was increased over the vehicle treated control. The

effect was quite modest, producing only 25-30% the functional rescue of VRT-325 and less than 3% that

of low temperature in a polarized CFBE41o- cell line. Even after testing structurally related molecules to

RDR-1, no compounds were found to have a greater impact on stabilization of ΔF508. The low efficacy

of the RDR-1 corrector may be attributed to several factors. Starting with a small number of potential

leads (224) could have limited the chemical diversity and hampered the potential for more potent

compounds. Using only the NBD1 domain of CFTR in purified protein form might not reflect the overall

folding defect that ΔF508 imposes. Additionally, the purified NBD1 was from murine origin which may

not reflect the same folding properties as human CFTR ΔF508.

Another small molecule screening effort used immunofluorescence detection of an epitope tagged CFTR

ΔF508 – 3X HA in baby hamster kidney (BHK) cells to detect trafficking rescue at the cell surface[91]. In

this assay, cells were grown in the presence of compounds from a drug library, then fixed and stained

with fluorescently conjugated antibodies. The protocol for fixation was tailored to minimize

permeabilization in order to only detect CFTR ΔF508 that was at the cell surface, however substantial

intracellular labeling was present after labeling. Even with this limitation, many classes of compounds

(16 strong hits out of 2000 possible compounds) that functionally and biochemically rescued CFTR ΔF508

were discovered by this screen.

High Content Screening

Screening a protein expression library offers a unique perspective over small molecule libraries because it can provide direct evidence for proteins that participate in controlling CFTR ΔF508 trafficking. In order to discover proteins and/or pathways that modulate the folding and export of this CFTR ΔF508, high content screening was employed. Instead of screening a vast library of chemically diverse small molecules, fusion proteins were created between the YFP-H148Q/I152L and cDNA clones from the human ORFeome library[93]. These fusion proteins were then co-expressed with CFTR ΔF508 in a modified HEK293 cell background. YFP fluorescence quenching was indicative of correction and was monitored by a Cellomics KSR detection system. The Cellomics system utilizes an automated camera-based screening approach and is amenable to multiplex fluorescence imaging with capabilities of time lapse data collection and providing visual information which is not possible with traditional multi-well fluorimetry. This particular study did not exploit these advantages however; their screening strategy only measured the amount of YFP fluorescence quenching dependent on the protein from the fusion protein from the ORFeome library, a process that could have been detected easily by traditional fluorimetry. For this reason, this study is not an example of a true high content screening effort. Nevertheless, several proteins were identified which conferred robust rescue of CFTR ΔF508. Chaperones such as HspA4 and HspBP1 were top hits in this screen. These chaperones are known to be associated with the Hsp70 and Hsp90 complexes, key factors involved in CFTR biogenesis. Other proteins that rescued CFTR ΔF508 function came from classes such as trafficking regulators, Golgi proteins, transcription factors and ubiquitin pathway proteins. The proteins identified in this screen are from pathways expected to be involved in the biosynthesis of CFTR ΔF508. Future studies should expand upon this approach to truly implement a high content screen with RNAi and/or small molecules in a multiplex imaging format to provide a more detailed readout of how CFTR ΔF508 trafficking is controlled.

Corrector Additivity and Synergy

Combinations of treatments such as low temperature and correctors have been shown to enhance the

amount of rescue in several studies[30,94,95]. If the low temperature and corrector treatments act through

different pathways or during different stages of CFTR ΔF508 folding and biosynthesis, then the

combination of these interventions may complement each other. This observation led to the hypothesis

that multiple correctors, in combination, could also complement the rescue effect if they acted through

distinct mechanisms. Indeed, VRT-325, Corr2a and C4 were examined in various combinations and an

additive effect on the rescue of CFTR ΔF508 was observed[95]. VRT-325 plus Corr2a or C4 increased CFTR

ΔF508 maturation by up to 4 fold over single corrector treatment. A possible explanation for this result

proposed by the authors of this study is that the correctors bind to different parts of the CFTR protein

and serve as chemical linkages to stabilize the folding of the protein. Unfortunately, VRT-325 was found

to have promiscuous rescue activity when other folding and trafficking defective proteins were

examined. The structurally related P-glycoprotein trafficking was also improved by VRT-325 treatment

suggesting that the molecule indirectly enhances folding through other proteins or binds to a protein

motif that is common to both CFTR ΔF508 and P-glycoprotein. In either case, this molecule is not

specific for the ΔF508 mutation and therefore has limited therapeutic potential. Corr2a and C4

exhibited more specificity to the CFTR ΔF508 mutation as they did not improve the trafficking of P-

glycoprotein. It is still unclear whether any of these correctors bind directly to CFTR ΔF508. This study

demonstrated that combinations of correctors can co-operatively and more effectively rescue CFTR

ΔF508 over single compounds alone. Going forward, a combinatorial pharmacology may be the best

approach for correcting the CFTR ΔF508 folding defect.

Building on the idea that combinations of correctors can improve rescue over a single compound, a

screening effort focusing on combinatorial pharmacology was undertaken[94]. The halide sensitive YFP

assay was modified and improved to reduce the amount of time between solution exchanges and fluorescence measurements were taken. Over 3,000 compounds from a library of approved drugs and research tools as well as 5,000 combinations were tested to look for functional rescue of CFTR ΔF508 in Fischer rat thyroid (FRT) cells. Each of these compounds were tested alone and in various combinations across a range of concentrations to establish dose dependent responses for all conditions. These improvements to the assay design allowed the authors to pull out over 100 hits from a library that was expected to produce only a few active compounds. A dose dependent response with combinations of correctors was carried out and revealed that the most effective pair of compounds is VRT-325 (also referred to as C3) and C4. Careful analysis of the dose dependent co-operativity between C3 and C4 demonstrates a synergistic effect that is greater than expected from a simple additive model.

In the study described below, we examined the recue potential of three CFTR ΔF508 corrector compounds, C4, C548 and C951 (See Table 2-1 for a list of compounds and combinations tested in this study). The C4 corrector had already been described and studied in detail in the literature; however, C548 and C951 are new compounds that had not yet been characterized. Our goal was to test if the trafficking rescue of CFTR ΔF508 to the cell surface by correctors could be detected using the FAP reporter platform and to quantify the effects of single corrector compounds and combinations of corrector treatments.

Ch. 2 – Results

In order to study the trafficking defects of CFTR ΔF508, we generated FAP fusions to this mutant protein to study its localization at the cell surface. The same tagging strategies used for CFTR WT were implemented for the CFTR ΔF508 protein. N-terminal FAP fusions were engineered by expressing the FAP and CFTR ΔF508 from the mammalian expression vector pBabeSacLac2. The MG binding FAP, dNP138, was cloned into the Sac module while the ORF encoding CFTR ΔF508 which was amplified with SfiI restriction sites was inserted into the Lac position. The CFTR ΔF508 EL4-FAP chimera was constructed by exchanging the sequence containing the ΔF508 mutation into the CFTR WT EL4-FAP sequence (for a detailed cloning procedure see Ch.2 Materials and Methods). The products were verified by sequencing to ensure that the constructs contained the ΔF508 mutation.

Stable cell lines expressing the FAP-CFTR ΔF508 and CFTR ΔF508 EL4-FAP constructs in HEK293 cells were created in the same way as the CFTR WT FAP. pBabe retroviral plasmids containing either the N-terminal FAP fusion or the EL4-FAP chimera were packaged into pseudotyped viral particles by co-transfecting the phoenix-gp packaging cell line with the FAP containing plasmids and a VSV-G coat protein containing plasmid. Viral supernatants were harvested and filtered to remove any detatched phoenix cells. Naïve HEK293 cells were transduced with the viral particles containing the FAP tagged CFTR ΔF508 constructs. Transduced populations were subjected to puromycin selection for 4 days to eliminate any cells that had not received the retroviral vector and retain cells that underwent stable incorporation of the transgene into the genome. Puromycin selected populations of cells next underwent several rounds of flow cytometry enrichment to increase the level of transgene expression. Due to the random nature of the retroviral insertion process, transgene expression can vary widely within a population of cells. This is caused by genomic position effects that influence the amount of transcription depending on the surrounding genetic sequences. Additionally, mammalian cells have

silencing mechanisms that can reduce the amount of transgene expression. To ensure that we had populations of cells that were expressing sufficient levels of FAP tagged CFTR ΔF508, we used flow cytometry to isolate cells based on MG fluorogen activation. The first round of FACS population enrichment was performed with the cell permeant fluorogen MG-ester. Under normal conditions, CFTR ΔF508 is not expected to be present at the cell surface and therefore would not be accessible to activate the cell impermeant fluorogen, MG-11p. The next round of enrichment was carried out after the populations of cells had been incubated in the presence of 2 known correctors of CFTR ΔF508 trafficking, C4 and C951, for 24 hours[1] (corrector C951 reagent and information pertaining to rescue provided by Frizzell lab). For each population, FAP-CFTR ΔF508 and CFTR ΔF508 EL4-FAP, a control group which had been treated with the vehicle (DMSO) and a group that had been treated with a combination of corrector compounds (C4 10uM and C951 5uM) were sorted in the presence of the fluorogen MG-11p. CFTR ΔF508 expression and rescue was determined by the activation of fluorescence (630nm excitation and 685/35nm emission) and cells that were above a threshold determined by the control groups were collected and expanded. Several rounds (4-5) of this enrichment process were performed to acquire stable populations of cells that responded to corrector treatment. Clonal isolation of cells was also performed in parallel which provided cell lines that had satisfactory levels of expression. Interestingly, the uniformity of rescue in cloned cell lines was unexpectedly not better than sorted populations of cells. Furthermore, many of the clonal cell lines exhibited slow growth and sometimes unusual cell morphology. For these reasons, enriched populations of cells were chosen to continue with later experiments.

Visualization of CFTR ΔF508 Rescue

Once stable cell lines with adequate levels of transgene expression were obtained, we examined whether the MG-11p activation after corrector treatment was detectable by fluorescence microscopy.

HEK293 cells expressing either the N-terminal or EL4 FAP ΔF508 were incubated in the presence of the vehicle (DMSO) for 24 hours and imaged with MG-11p by confocal fluorescence microscopy. As expected there was no activation of the fluorogen because the CFTR ΔF508 mutation prevented the trafficking to the cell surface and embedding in the PM (Figure 2-3, A and D). Consequently the FAP is not exposed to the extracellular environment and is unable to bind and activate the chemically excluded MG-11p fluorogen. To test for fusion protein expression, cells were incubated with the cell permeant MG-ester fluorogen and an intracellular pattern was observed (Figure 2-3, B and E). This observation is consistent with the trafficking route of untagged CFTR ΔF508 as the protein is translated and inserted into the ER but export to the Golgi is blocked. MG-ester staining reveals that both of the CFTR ΔF508 FAP fusion constructs are present in a reticulated network like pattern that is consistent with ER structures.

Since the CFTR ΔF508 mutation is temperature sensitive, low temperature incubation (<30°C for 24h) can rescue the trafficking defect and allow some CFTR ΔF508 to accumulate at the cell surface. HEK293 cells expressing the CFTR ΔF508 FAP reporter constructs were incubated at low temperature and then exposed to cell impermeant fluorogen. Cell surface labeling of the FAP with MG-11p was observed for cells incubated at the permissive temperature (30°C), but not at the restrictive temperature (37°C) (Figure 2-2). This verifies that both FAP-CFTR ΔF508 and CFTR ΔF508 EL4-FAP fusion proteins are able to overcome the folding defect with low temperature.

Next, we tested whether the FAP fusions to CFTR ΔF508 were sensitive to pharmacological rescue by corrector compounds. Cells were treated with a combination of correctors (C4 and C951) for 24 hours, then imaged with MG-11p fluorogen (Figure 2-3, C and F). In stark contrast to the vehicle treated control, both the N-terminal and the EL4 CFTR ΔF508 expressing cell lines had strong positive

64
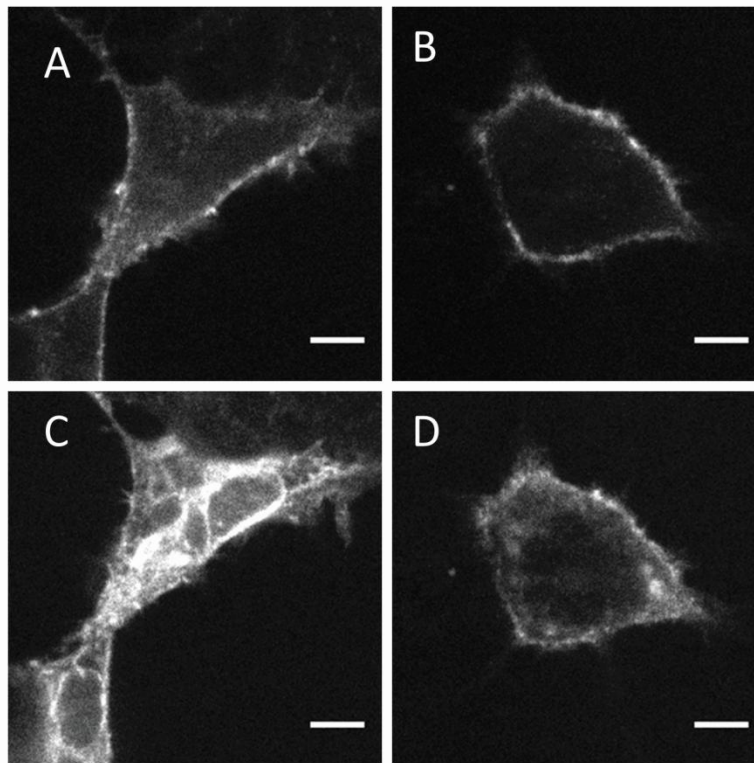
Figure 2-2: Temperature Rescue of FAP CFTR ΔF508

Trafficking rescue of FAP CFTR ΔF508 reporters by low temperature visualized by confocal fluorescence microscopy. HEK293 cells expressing FAP CFTR ΔF508 reporter constructs were incubated at the permissive temperature, 30°C, for 24 hours. Surface expression was confirmed by activation of the impermeant fluorogen, 50nM MG-11p, for both FAP-CFTR ΔF508 (A) and CFTR ΔF508 EL4-FAP (B). Cell permeant staining with 50nM MG-ester revealed that there were intracellular pools of signal for FAP-CFTR ΔF508 (C) and to a lesser extent for CFTR ΔF508 EL4-FAP (D). Scale bars indicate 10µm.
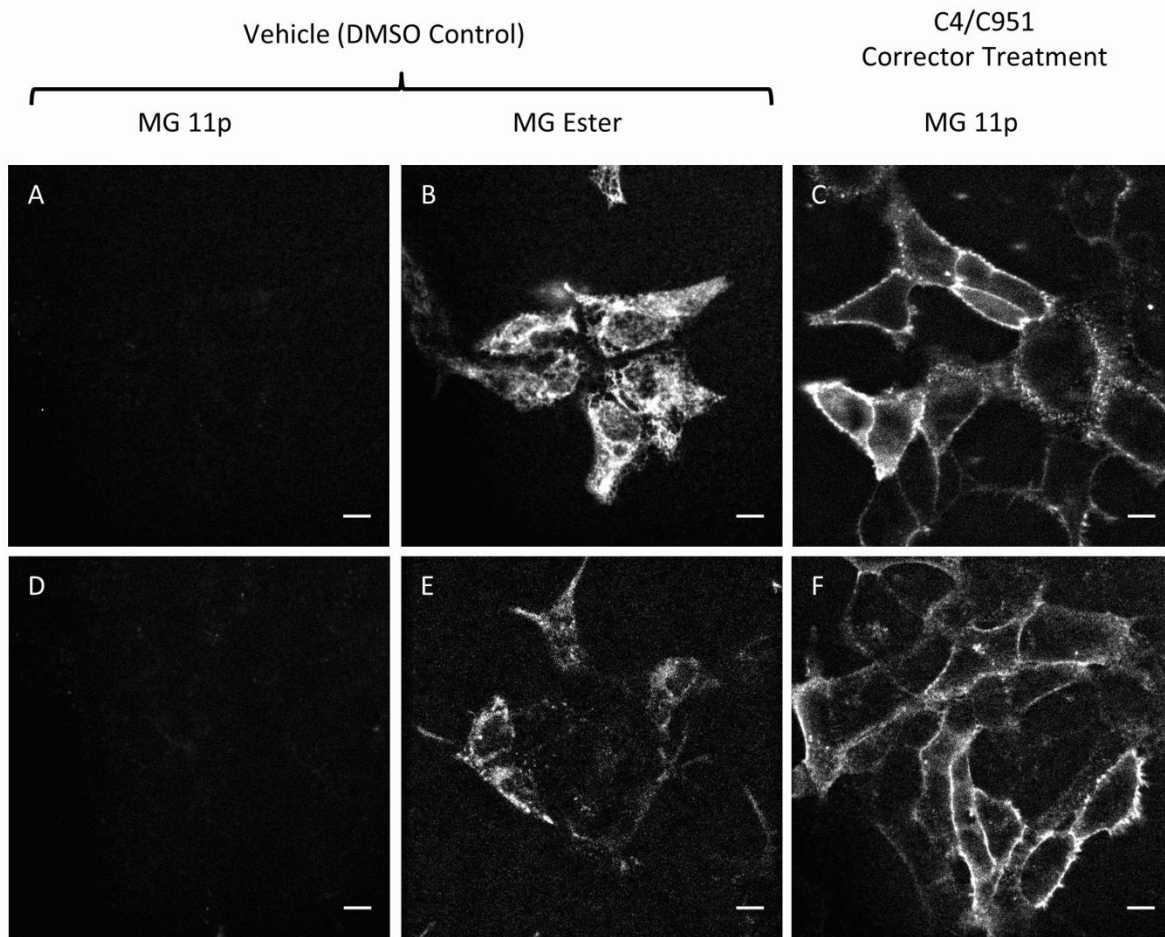
Figure 2-3: Correctors Rescue the Trafficking Defect of FAP CFTR ΔF508 Reporters

HEK293 cells stably expressing FAP-CFTR ΔF508 (A-C) or CFTR ΔF508 EL4-FAP (D-F) imaged using confocal fluorescence microscopy. After treatment with the vehicle control (DMSO) for 24 hours, there was no staining observed in the presence of cell impermeant fluorogen, 50nM MG-11p (A and D), however, strong intracellular signal that was not localized to the PM was revealed upon addition of the cell permeant fluorogen, MG-ester (B and E). After treatment with a combination of correctors, C4 and C951 for 24 hours, CFTR ΔF508 was detected at the cell surface using cell impermeant fluorogen, 50nM MG-11p (C and F). Scale bars indicate 10μm.

fluorescent signal from the cell impermeant fluorogen. This result demonstrated that the trafficking

defect of CFTR ΔF508 had been rescued and the protein was present at the cell surface. It should be

noted that corrector treatment was expected to rescue these fusion proteins to the PM as this was the

method for population enrichment. Microscopy provided confirmation that trafficking was rescued and

fluorescence signal was localized to the cell surface. This result was important because it ruled out the

possibility of non-specific fluorogen labeling. The MG fluorogen does label dead or dying cells (data not

shown), although the mechanism is not completely clear, which can give misleading results in non-

imaging based detection methods such as FACS.

Functional Rescue of CFTR ΔF508

Next, we tested whether the rescued CFTR ΔF508 FAP fusion proteins were capable of transporting ions

across the membrane. SPQ fluorescence was used to measure the iodide efflux capabilities of each of

the heterologous FAP CFTR ΔF508 cell lines. In the vehicle treated control, neither the N-terminal nor

the EL4 FAP CFTR ΔF508 constructs were able to transport iodide across the cell membrane (Figure 2-4,

B and C). This result was expected because flow cytometry and fluorescence microscopy had

demonstrated that the fusion protein was absent from the cell surface. In order to test whether the

trafficking rescue of CFTR ΔF508 FAP fusions results in the production of functional channels we

performed SPQ fluorescence measurements. Addressing this question, we treated both cell lines with

C4 and C951 correctors for 24 hours. After corrector treatment, cells were loaded with SPQ dye and

stimulated with Fsk. Weak iodide efflux which was greater than that of the vehicle treated control was

detected (data not shown). Since even rescued CFTR ΔF508 has a gating defect, activation was

performed in the presence of Fsk and a potentiator, P2. The corrector treated cells generated

substantial iodide efflux response that was completely absent in the vehicle treated control groups

(Figure 2-4, B and C). The magnitude of the iodide response as measured by a dequenching of the SPQ

dye is an indicator of the number of channels in the PM and the open probability of these channels. SPQ

fluorescence can easily saturate the image capture system however, and can confound interpretation of

CFTR activity. To eliminate this possibility, the slope of the iodide efflux was taken for each condition.

Rescued FAP-CFTR ΔF508 produced a slope that was less than its WT counterpart, 1.17 compared to

1.44 respectively but was substantially greater than the vehicle treated control (0.01) (See Figure 2-4

and Figure 2-5). Less robust functional rescue was seen for the CFTR ΔF508 EL4-FAP construct with a

slope of 0.24 versus 1.12 for the WT construct in the same experiments. This modest response was still

six times greater than the same cell line that received a vehicle control treatment (0.04).   These data

indicates that functional rescue of CFTR activity by corrector treatment, i.e. anion transport across the

membrane, occurs with both of the FAP tagged CFTR ΔF508 constructs.

Biochemical Rescue of CFTR ΔF508

An established method of assessing the folding of CFTR is by immunoblot analysis. Presence of a mature

glycosylated C band indicates proper folding and processing of CFTR that has exited the ER and is

competent to traffic to the cell surface. Native CFTR ΔF508 does not produce a mature glycosylated

band because it is degraded before export to the Golgi. Previous studies have shown that correctors

promote the maturation of CFTR ΔF508 which is visualized by the appearance of a C band[1,90]. To test

whether the CFTR ΔF508 FAP reporter proteins also retain this behavior, we performed immunoblots

using a CFTR specific antibody. Whole cell lysates from stable HEK293 cell lines expressing either the

FAP-CFTR ΔF508 or the CFTR ΔF508 EL4-FAP were extracted from cells grown in three different

conditions for 24 hours; (1) Corrector combination C548 and C951, (2) Corrector combination C4 and

C951, and (3) vehicle (DMSO). Densitometry plots of each of the lanes from this immunoblot were

generated to facilitate detection and interpretation of the bands (Figure 2-6, B).   FAP-CFTR ΔF508

acquired a band that migrated at the same position as the C band for the FAP-CFTR WT construct after
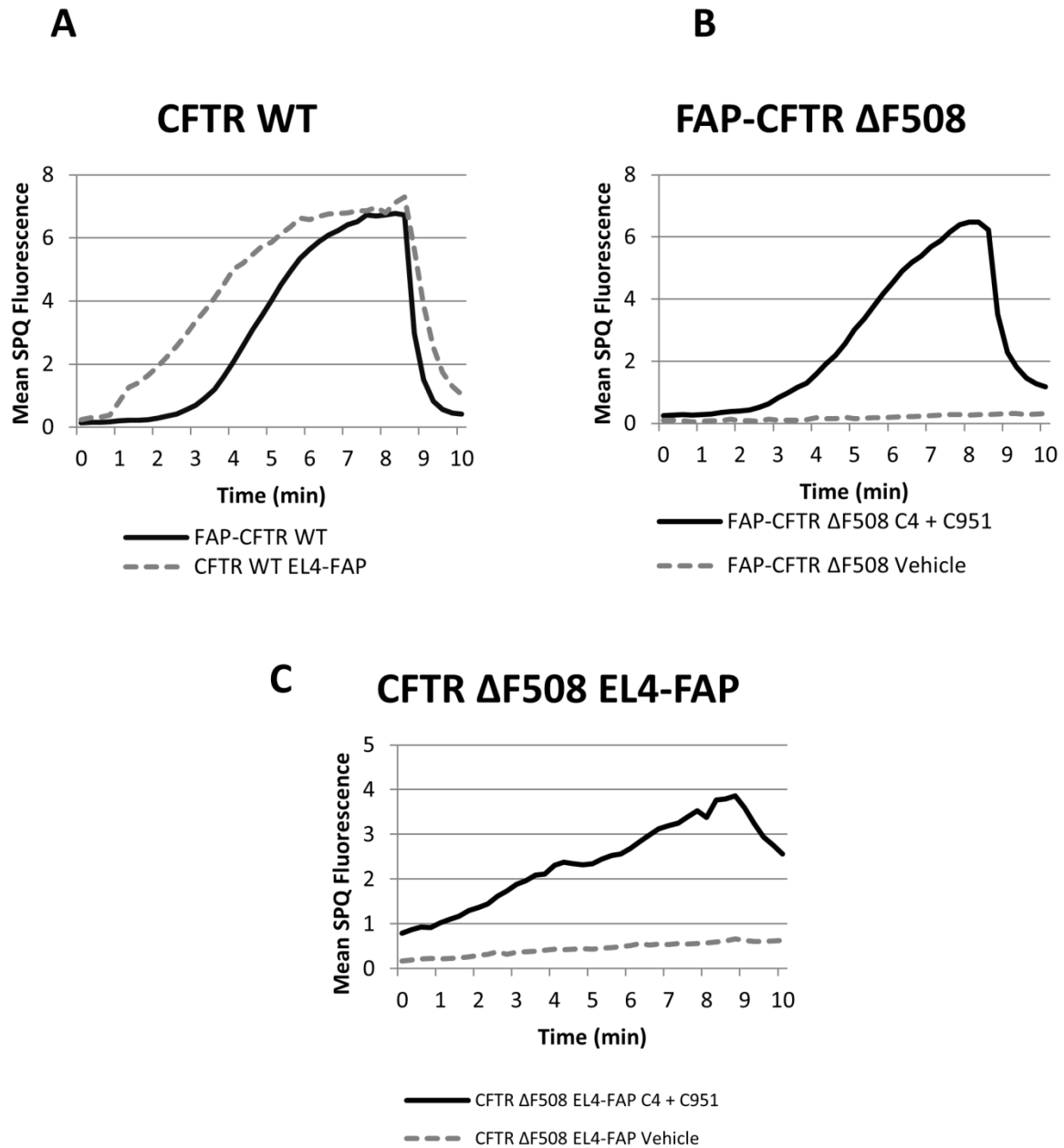
Figure 2-4: Correctors Functionally Rescue CFTR ΔF508 FAP Constructs

Normalized SPQ fluorescence showing iodide efflux in response to 10µM Fsk stimulation. (A) CFTR WT FAP reporters show normal channel function. (B and C) Stably expressing FAP tagged CFTR ΔF508 cells were treated with either Vehicle (DMSO) or a combination of correctors, C4 and C951 for 24 hours. Iodide efflux was stimulated with Fsk and a potentiator, 300nM P2.
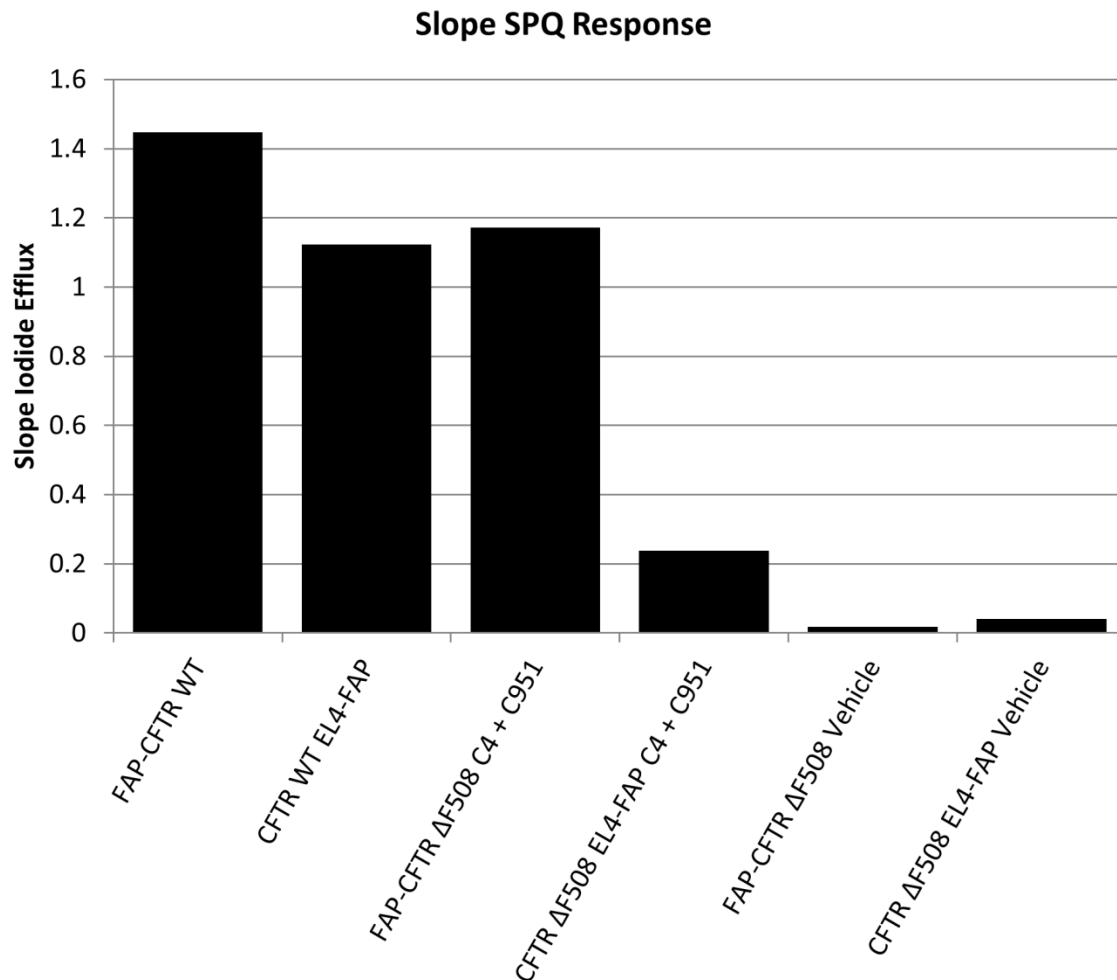
Figure 2-5: Slope of CFTR Iodide Efflux

The slope of the iodide efflux was taken from Figure 2-4 to measure CFTR channel activity. The slope was calculated from normalized SPQ fluorescence traces at the steepest point of iodide efflux. Neither of the CFTR ΔF508 constructs treated with the vehicle alone showed ion transport, however, treatment with C4 and C951 correctors rescued FAP-CFTR ΔF508 function nearly to WT levels, and CFTR ΔF508 EL4-FAP showed imporovement over the vehicle control.
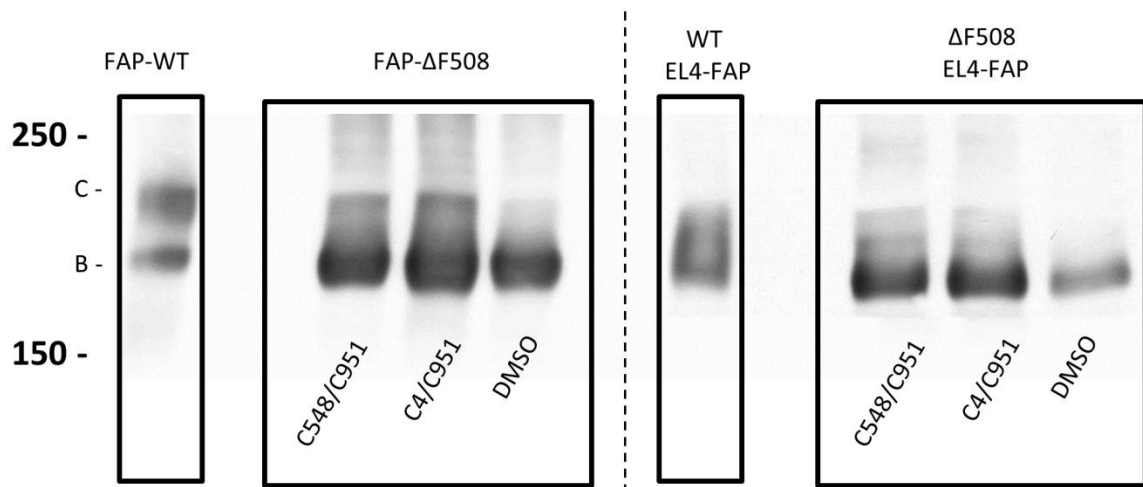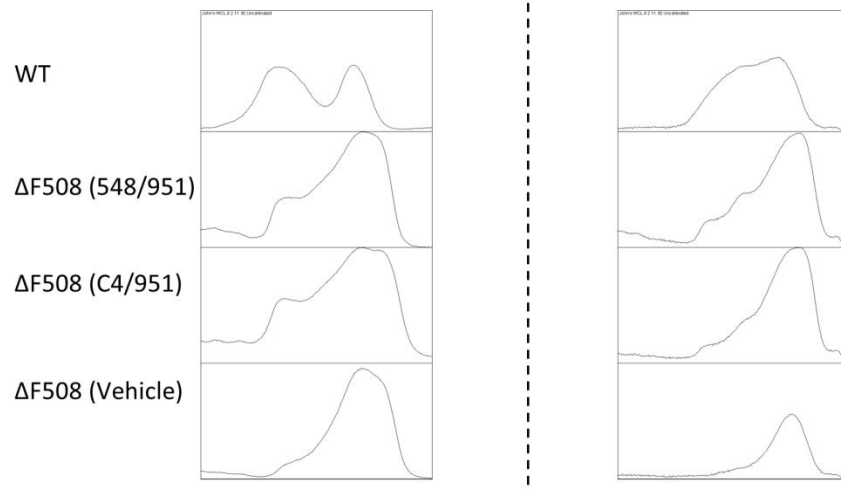
Figure 2-6: Biochemical Evidence of Corrector Rescue

Immunoblotting was performed on whole cell lysates from cells stably expressing FAP CFTR reporters. (A) Treatments with correctors C548/C951 or C4/C951 for 24 hours showed an accumulation of higher molecular weight bands that were not present in the vehicle treated control. FAP-CFTR ΔF508 corrected lanes have acquired a fully glycosylated C band, but corrected CFTR ΔF508 EL4-FAP shows incomplete glycosylation. (B) Densitometry analysis of this immunoblot shows the signal distribution for each lane with decreasing molecular weight from left to right. Clear differences are observed between the corrector treatment and vehicle for both cell lines.

corrector treatment with either C548/C951 or C4/C951 combinations which was not present in the vehicle treated control lysates (Figure 2-6, A). CFTR ΔF508 EL4-FAP also acquired higher molecular weight bands after both corrector treatments, C548/C951, that were absent under control conditions (Figure 2-6, A). Complete glycosylation was not achieved for the CFTR ΔF508 EL4-FAP relative to the N-terminal constructs even after corrector treatment, an observation that is consistent even with CFTR WT EL4-FAP. Despite this impaired glycosylation, CFTR ΔF508 EL4-FAP did have multiple larger bands in the presence of correctors and not under control conditions which indicates that some maturation has occurred. The ratio of C:B bands for both the N-terminal and EL4 FAP CFTR ΔF508 constructs even after corrector treatment was quite low compared to untagged CFTR WT indicating that biochemical rescue by these correctors is inefficient.

Quantification of Corrector Efficacy

Thus far, correctors have been used in combination to provide the most robust rescue of FAP based CFTR ΔF508 reporters. To gain insight on the individual properties and to comprehensively characterize all of the correctors and combinations available, we used flow cytometry to accurately quantify the effects of each corrector condition. Flow cytometry offers a quantitative output of the fluorescence for each cell. We analyzed populations of cells (10,000 per condition) and took the average fluorescence intensity from activation of MG-11p which reduced the effects of heterogeneity between cells due to subtle expression differences and other factors such as cell cycle. HEK293 cell lines expressing either the FAP-CFTR ΔF508 or the CFTR ΔF508 EL4-FAP were incubated in either single correctors or combinations of correctors for 24 hours. A summary of the correctors and combinations analyzed is provided in Table 2-2. After corrector treatments the cells are removed by a non-enzymatic reagent to ensure that proteins at the cell surface remain intact, unlike enzymatic procedures like trypsinization. Next, the cells are resuspended in phosphate buffered saline (PBS) with cell impermeant fluorogen MG-11p. Each

condition is measured as the average MG fluorescence activation for the across the population over three independent trials and normalized to the signal obtained for C951 (See Table 2-2 for a summary of corrector efficacy data).

For both the N-terminus and EL4 CFTR ΔF508 constructs the reference corrector, C4, only produced a small improvement in PM density compared to the vehicle treated control, 0.53 vs. 0.34 and 0.51 vs. 0.37 respectively (Figure 2-7and Figure 2-8). Based on microscopy data, the populations treated with DMSO as a control have virtually no activation of the MG-11p fluorogen, therefore values for the control groups reflect the autofluorescence or noise from the data acquisition. A statistically significant difference was found for FAP-CFTR ΔF508 when treated with C4 but not for CFTR ΔF508 EL4-FAP. Another corrector, C548 performed similarly to C4, increasing the density of the N-terminus and EL4 fusion at the cell surface to 0.55 and 0.47 respectively (Figure 2-7and Figure 2-8). The most potent single agent corrector tested was C951. Levels of trafficking correction reached 2 fold better than the reference corrector, C4, for both the N-terminus and EL4 FAP tagged CFTR ΔF508 constructs.

Combinations of correctors were tested to look for additive or synergistic effects from these corrector compounds. In the FAP-CFTR ΔF508 expressing cells, a combination of C4 and C548 did not statistically improve the efficacy over either compound alone (Figure 2-7). A combination of C548 and C951 however, did significantly rescue the surface expression resulting in a 3.7 fold increase over the rescue achieved by C4 alone (Figure 2-7). This is clearly illustrated by the histogram showing a dramatic shift in MG-11p fluorescence activation after C548 and C951 corrector treatment over the vehicle treated control (Figure 2-10, A). Similarly, C4 and C951 treatment achieved 4 fold improvement compared to C4 correction. There was no statistically significant difference found for the C548/C951 versus C4/C951 corrector conditions. The FAP-CFTR ΔF508 construct in a HEK293 cell background showed a synergistic

Compounds	Source
C4	Pedemonte et al. 2005
C548	CFFT-108548 (Formerly EPIX compound)
C951	Vertex Patent WO 2007/021982 A2
DMSO	

Combinations of Correctors
C4 + C548
C4 + C951
C548 + C951

Table 2-1: List of Correctors Characterized

Correctors from the sources listed were used at the following concentrations based on previous studies and EC50 values: C4 ($10\mu M$), C548 ($5\mu M$) and C951 ($5\mu M$).

	FAP-CFTR ΔF508	CFTR ΔF508 EL4-FAP	HBE CF172P1
C4	0.53*	0.51	0.25
C548	0.55*	0.48	0.5
C951	1*	1*	1*
DMSO	0.34	0.37	0.18
C4/C548	0.68*	0.52	0.58
C4/C951	2.11*	1.29*	0.96*
C548/C951	1.97*	1.37*	1.30*

Table 2-2: Summary of Corrector Efficacy

The corrector efficacy for single compounds and combinations summarized from Figure 2-7, Figure 2-8 and Figure 2-9. Results are presented as the mean value normalized to C951. * indicates a statistically significant difference compared to DMSO control. See Ch. 2 Materials and Methods for statistical analysis.
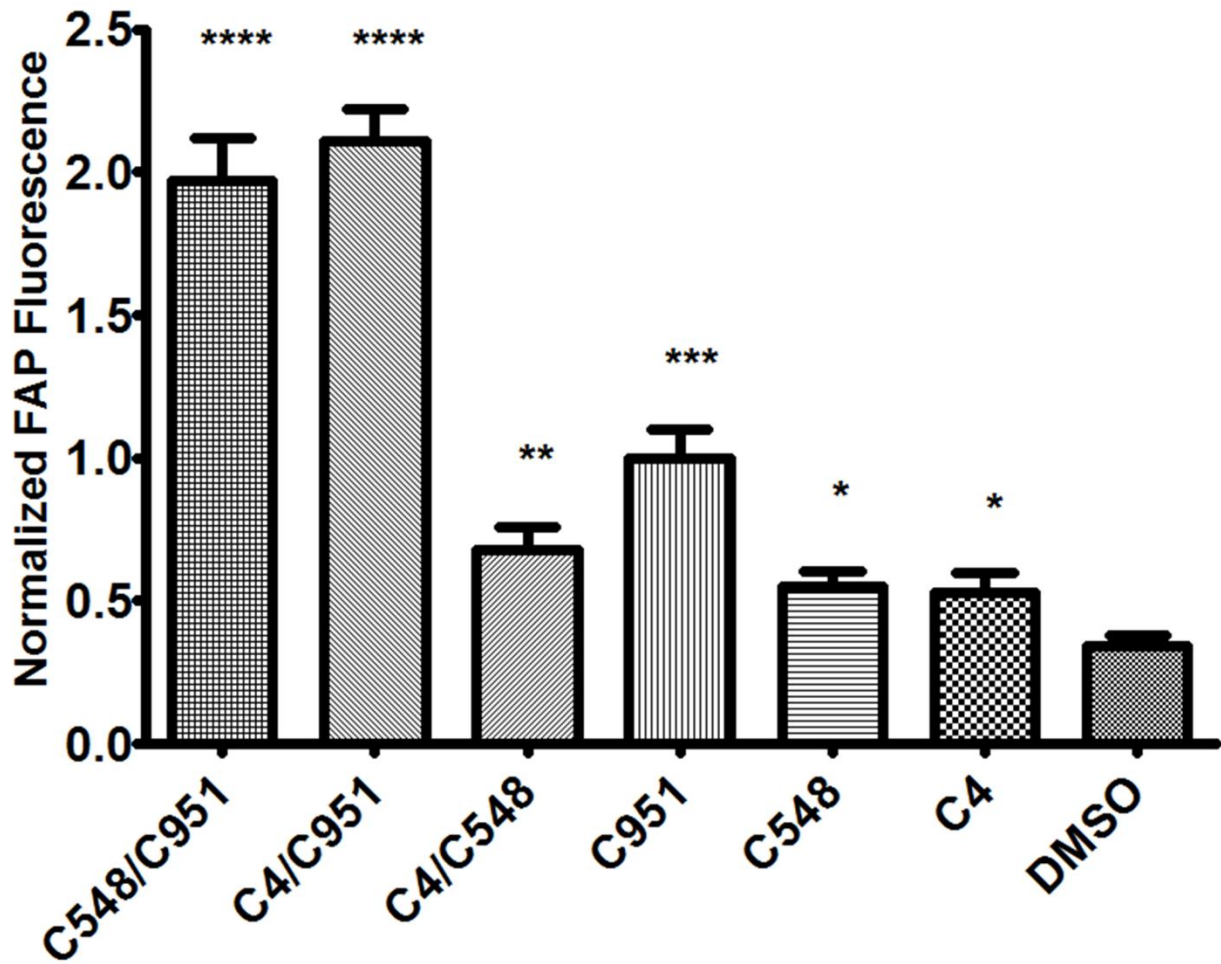
Figure 2-7: Corrector Efficacy for FAP-CFTR ΔF508

Corrector efficacies of single compounds or combinations were determined by flow cytometry. C4 was used at 10μM, C548 and C951 were used at 5μM. HEK293 cells stably expressing FAP-CFTR ΔF508 were treated with each condition for 24 hours prior to measurement. After treatments, cells were exposed to 50nM MG-11p and fluorescence activation was measured by flow cytometry for 10,000 cells per condition. The mean fluorescence intensity for each condition was normalized to C951. Data are presented as the mean ±SEM, n=3.
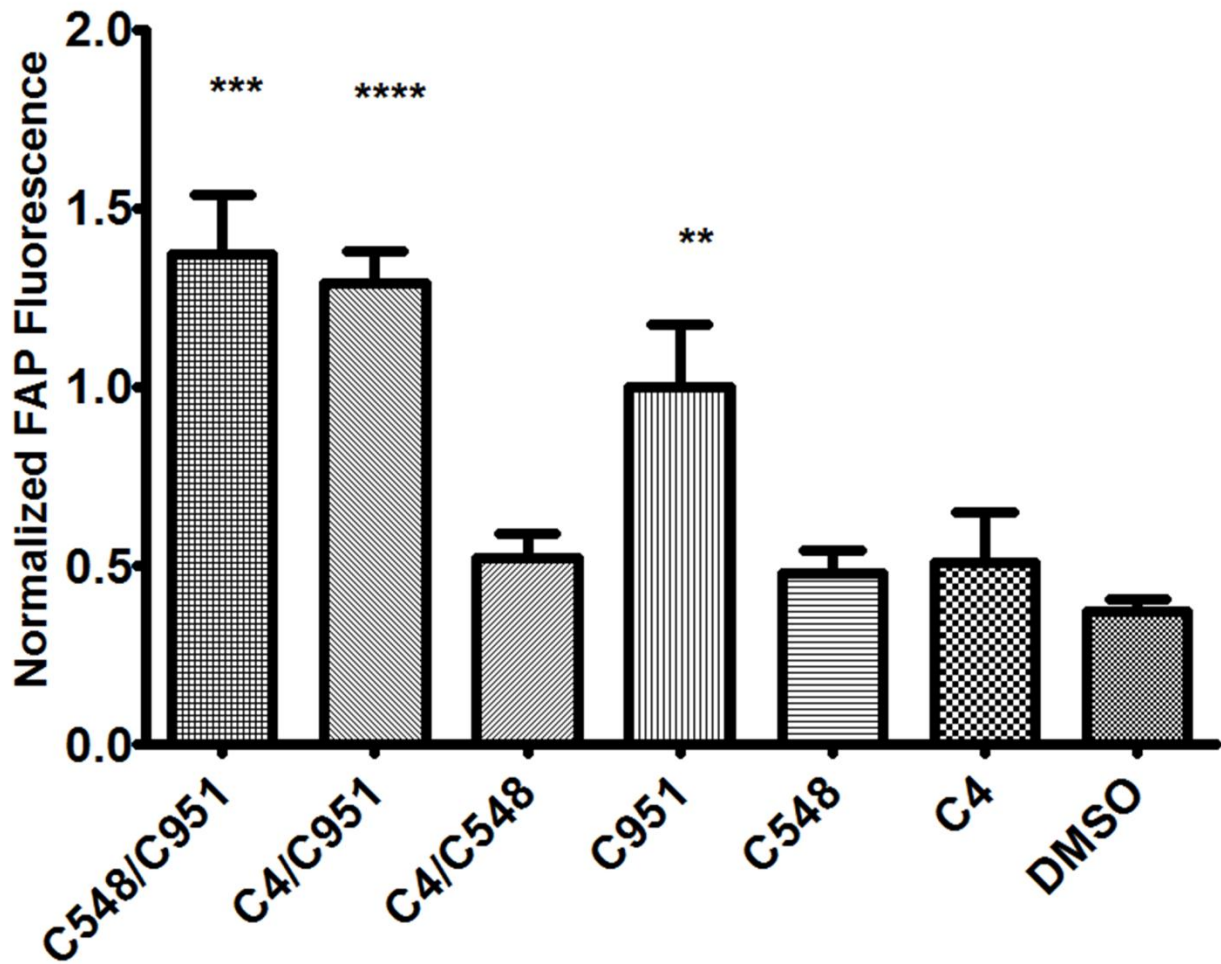
Figure 2-8: Corrector Efficacy for CFTR ΔF508 EL4-FAP

Correctors were tested in the same way as in Figure 2-7. C4 was used at 10µM, C548 and C951 were used at 5µM. HEK293 cells stably expressing CFTR ΔF508 EL4-FAP were treated with each condition for 24 hours prior to measurement. After treatments, cells were exposed to 50nM MG-11p and fluorescence activation was measured by flow cytometry for 10,000 cells per condition. The mean fluorescence intensity for each condition was normalized to C951. Data are presented as the mean ±SEM, n=3.
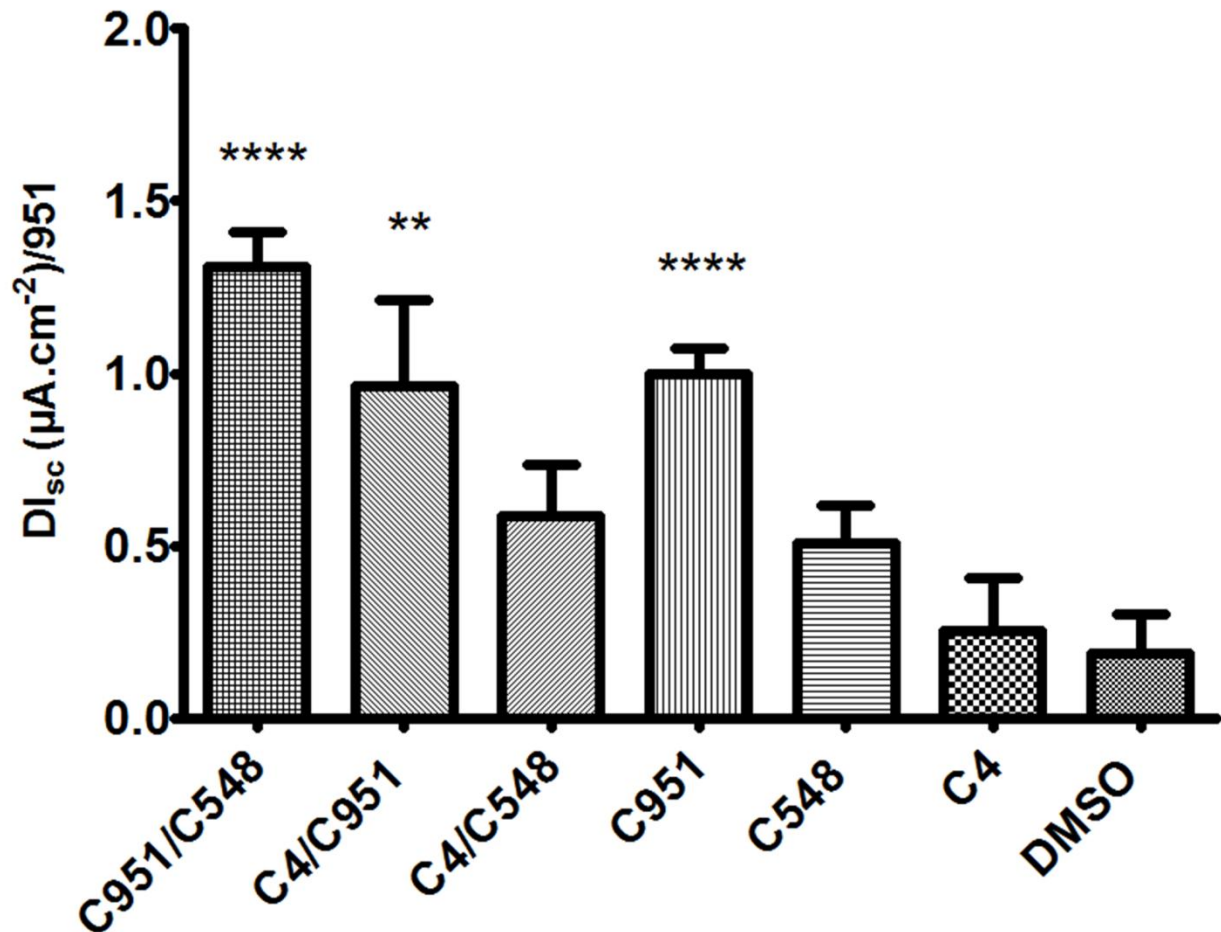
Figure 2-9: Corrector Efficacy for Untagged CFTR ΔF508 in HBE Cells

Short circuit currents performed by M. Glover (Frizzell laboratory) were measured in Ussing chambers using polarized HBE cells which express untagged CFTR ΔF508. Correctors C4 (10µM), C548 (5µM), C951 (5µM) were added alone or in the combinations indicated 24 hours prior to measurement. Corrector efficacy was determined by functional rescue of CFTR activity and normalized to C951. Data are presented as the mean ±SEM, n>6.
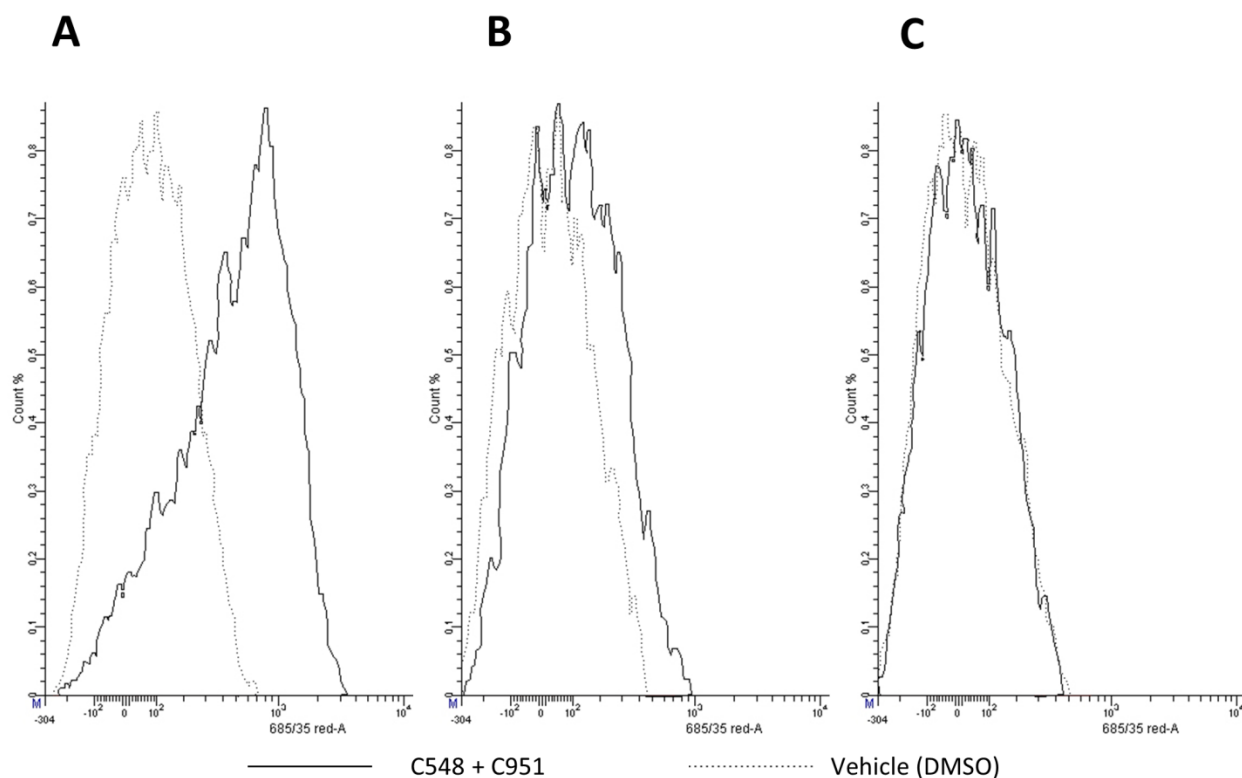
Figure 2-10: Relative Cell Surface Density of CFTR ΔF508 Measured by Flow Cytometry

Flow cytometry was used to examine the trafficking rescue capabilities of correctors by measuring increases in activation of the cell impermeant fluorogen. A representative histogram for each cell line shows the distribution of fluorescence signal for the vehicle control (dashed line) and C548/C951 (solid line) corrector conditions. Fluorescence activity is plotted along the horizontal axis using a logarithmic scale. (A) FAP-CFTR ΔF508 (B) CFTR ΔF508 EL4-FAP (C) Naïve HEK293 control cells

effect with the corrector combinations C4/C951 or C548/C951 on trafficking rescue which was greater than the expected additive effect (Table 2-2 and Figure 2-7).

CFTR ΔF508 EL4-FAP engineered cell line similarly did not show an increase of surface expression for the C4 and C548 corrector combination compared to either compound alone. C548 and C951 increased the PM density 2.7 fold, and C4 with C951 rescue was 2.5 fold greater than C4 treatment alone (Table 2-2 and Figure 2-8). This effect is shown by the histogram where a detectable shift in MG-11p fluorescence activation is observed after C548 and C951 corrector treatment compared to the vehicle treated control (Figure 2-10). No statistical difference was shown between these corrector combinations, C548/C951 and C4/C951. Both corrector combinations increased the PM density of CFTR ΔF508 EL4-FAP over the single corrector treatments alone; however, the level of improvement was additive and not synergistic like the effect seen from the FAP-CFTR ΔF508 cell line (Table 2-2, Figure 2-8).

Corrector Efficacy for Untagged CFTR ΔF508 in HBE Cells

Human bronchial epithelial (HBE) cells obtained from CF patients homozygous for the ΔF508 mutation (CF172p1) were used as an alternative cellular model to test the efficacy of the correctors used to test the HEK293 FAP tagged CFTR ΔF508 cell lines. HEK293 cells are commonly used for studying CFTR, but they are derived from a fibroblast cell type and do not necessarily recapitulate the native environment for CFTR expression. In order to determine if the corrector efficacy seen in the HEK293 cell background with the FAP-tagged CFTR ΔF508 is representative of the endogenous system, we compared rescue in HBE cells with the same panel of correctors. Research on HBE CFTR ΔF508 cells was carried out by the Frizzell lab, primarily the work of Matthew Glover. The experimental protocol to measure corrector efficacy in HBE cells is as follows: (1) HBE cells are grown under conditions that induce polarization (2) Polarized HBE sheets are treated with various corrector conditions (Table 2-1) for 24 hours (3) Cells

were stimulated to activate CFTR ΔF508 in the presence of a potentiator, P2, and Fsk (4) Rescue is determined by short circuit values that correspond to the amount of cellular conductance, a measure of how many CFTR channels are in the membrane and the open probability of these channels. Consistent with data obtained in HEK cells, for untagged CFTR ΔF508 in the native HBE cell background it was found that the most potent single agent compound was C951. In this particular genetic background, C951 outperformed the reference corrector, C4 by 4 fold (Table 2-2 and Figure 2-9). In the HBE cell background, neither C4 nor C548 showed statistically significant rescue of CFTR ΔF508 over the vehicle treated control. The combination of C548 and C951, but not C4 and C951 increased the amount of functional rescue compared to these compounds when used individually. This co-operative effect was an additive correction which was 5.2 fold better than C4 treatment (Table 2-2 and Figure 2-9).

The pattern of correction was consistent across all of the disparate methods of measurement. Very similar rescue of CFTR ΔF508 was observed in both the HEK cell background as well as the native HBE cell line. These results highlight the fidelity of the FAP reporter system and its ability to recapitulate the behavior of untagged CFTR ΔF508 in an endogenous system.

Ch. 2 – Discussion

We successfully generated stable cell lines that express CFTR ΔF508 with FAP reporters located at either the N-terminus or in the fourth extracellular loop. Using these cell lines, we showed that under normal conditions CFTR ΔF508 is not present at the cell surface yet is detectable in intracellular compartments in a reticulated, ER like pattern, a behavior that is consistent with the untagged protein. Importantly, CFTR ΔF508 was detected at the PM using MG-11p after corrector treatment. Since both tagging strategies displayed rescue by correctors, which closely mirrored the behavior of untagged CFTR ΔF508 in a native cell background, we conclude that HEK293 cell lines expressing CFTR ΔF508 FAP reporter constructs are useful models for studying the rescue of trafficking to the cell surface by corrector treatment.

Immunoblot analysis revealed that the correctors are capable of rescuing the maturation of CFTR ΔF508, albeit quite modestly. The amount of C band that was recovered in FAP-CFTR ΔF508 expressing HEK293 cells after C548/C951 or C4/C951 treatment was small compared to FAP-CFTR WT. The CFTR ΔF508 EL4-FAP constructs also showed the presence of larger molecular weight bands after corrector treatment but had similarly low efficiency. These results highlight the poor efficiency of corrector treatments. Accumulation of the C band after corrector treatment is even quite low with untagged CFTR ΔF508 and can depend highly on the cell type examined[1,53] (Figure 2-6).

Functional rescue of CFTR ΔF508 FAP constructs was demonstrated by iodide efflux assays. As predicted, because CFTR ΔF508 is lacking from the cell surface under basal conditions, cells were not able to transport iodide across the cell membrane is response to cAMP activation even in the presence of a CFTR specific potentiator, P2. After treatment with correctors however, both the N-terminus and EL4 FAP CFTR ΔF508 expressing cell lines regained the ability to transport iodide (Figure 2-4). The slope and magnitude of the FAP-CFTR ΔF508 iodide efflux was much greater than the CFTR ΔF508 EL4-FAP,

which likely reflect differences in the expression levels of the cell lines. Another possibility is that the correctors used may promote trafficking and functional rescue more robustly for the N-terminus CFTR ΔF508 construct.

To date, C4 is one of the most well studied correctors for CFTR ΔF508 rescue. The efficiency of rescue for C4 is very limited across multiple cell types tested[30,39,53]. C4 fails to rescue reasonable levels of mature glycosylated CFTR ΔF508 that can be detected by immunoblotting techniques[37,53]. Furthermore, the amount of protein that is rescued to the cell surface as determined by biotinylation by C4 is very limited[37]. In fact, several studies used low temperature incubation first to deliver CFTR ΔF508 to the cell surface followed by treatment with C4 to study the effects of this corrector[37,39]. This is in agreement with data obtained from both CFTR ΔF508 FAP constructs in HEK cells as well as untagged CFTR ΔF508 endogenously expressed from HBE cells where C4 correction efficiency was very poor (Table 2-2).

Molecules that bind directly to CFTR ΔF508 would represent good candidates for pharmacological therapy because they would limit off target effects. Whether or not C4 binds directly to CFTR ΔF508 is still unclear. In order to understand the corrector mechanism of action, one study showed that C4 inhibited the crosslinking of cysteine residues located TMD 6 and 7 (I340C and S877C) which suggests C4 binds directly and blocks the cross-linking reagent[96]. The channel pore blocker, benzobromone also inhibited cross-linking of these residues leading the authors to conclude that the binding site for C4 may lie near the pore region of CFTR. The concentration at which cross-linking inhibition was detected with C4 was 330uM, 33 fold higher than what is typically used for optimal correction. Moreover, concentrations within the working range for this corrector, 33uM or 3uM, were not able to inhibit cross-linking. Whether these artificially high concentrations contributed to non-specific cross-linking inhibition will require further studies. Another study showed that even high concentrations of C4 were unable to inhibit cross linking between cysteines located in TMD 6 and 12[97].

Interactions between the two halves of the CFTR molecule are thought to be important for achieving a stable folded state. To investigate this, CFTR was expressed as two separate halves, the WT form was found to have strong enough non-covalent interactions between these separated domains such that they were retained together by nickel chromatography. CFTR ΔF508 lacked the ability to form strong enough interactions between the two halves of the protein, but was restored after treatment with C4[98]. Based on these findings, Loo et al. support the idea that C4 binds to a specific interface just outside the pore region of CFTR, based on homology modeling of the structurally related P-glycoprotein, which stabilizes interaction between the two membrane spanning domains. A plausible alternative to this interpretation is that the C4 corrector acts through secondary interactions, changing the folding conformation by altering CFTR ΔF508 and chaperone interactions or modulating other CFTR ΔF508 binding proteins.

Cross-linking sensitive CFTR constructs were also used to demonstrate that C4 is capable of stabilizing CFTR ΔF508 folding in the ER. By mutating an ER exit sequence located in NBD1 (YKDAD), export of a cross-linking sensitive form of CFTR to the Golgi was blocked. In the absence of C4, no cross-linked CFTR was detected, however, after C4 treatment CFTR was efficiently cross-linked. This showed that C4 can act at the ER level to stabilize the folding defect of CFTR ΔF508. This result was further validated by consistent results obtained when ER export was blocked by the addition of the COPII dependent trafficking inhibitor, Brefeldin A.

In order to further elucidate the mechanism of C4 correction, analysis of CFTR ΔF508 stability at the PM has been examined. In CFBE41o- cells, the internalization rate for CFTR ΔF508 which has been rescued to the cell surface by low temperature, then destabilized by a shift back to the restrictive temperature is remarkably high (30% in 2.5min)[39]. Treatment with C4 reduced the internalization rate of CFTR ΔF508 from 30% to 1%, and appeared specific because CFTR WT and transferrin internalization was unchanged

by C4. Reduced endocytosis rates also corresponded to an increased surface half- life, prolonging it

from 2.5h to 4.5h. The improved cell surface stability of CFTR ΔF508 after C4 treatment did not

necessarily result in functional protein during the entire residency in the PM. CFTR ΔF508 was present

at the PM for 12 hours after C4 application but functional activity was only detectable for 6 hours after

treatment[37]. This may explain differences between the HBE functional data and PM density

measurements by FAP reporters. CFTR ΔF508 that is present in the PM but not functional will be

detected by FAP fluorescence but not by short circuit measurements in HBE cells. In HEK cells, C4

significantly augmented the amount of FAP-CFTR ΔF508 in the membrane (Figure 2-7), whereas

functional measurements in HBE cells did not show any functional improvement (Figure 2-8). A caveat

to the increased PM stability observed by Varga and Jurkuvenaite et al.[39] is that they employed a

strategy of temperature rescue to deliver CFTR ΔF508 first and then applied the corrector. When CFTR

ΔF508 was rescued by C4 without the low temperature incubation step, stabilization of the protein at

the cell surface was not detected[30]. This discrepancy may also be attributed to different cell lines used

(CFBE41o⁻ vs. polarized human airway epithelia). The endocytic rates can vary widely between different

cell types and has contributed to a lack of understanding of how C4 modulates CFTR ΔF508

trafficking[1,29,39,53].

The internalization of CFTR ΔF508 from the cell surface is a ubiquitin mediated process that is distinct

from the endocytic route of CFTR WT which does not involve ubiquitin[23,35]. Ubiquitylation of misfolded

CFTR ΔF508 at the cell surface directs the protein to the lysosome for degradation[23,99]. Inhibition of the

ubiquitin pathway is a proposed mechanism for how C4 stabilizes CFTR ΔF508 at the cell surface. A

luciferase based ubiquitin reporter was used to show that C4 partially blocks the E1-3 ubiquitin

pathway[37]. Reduction of ubiquitylation on CFTR ΔF508 conceivably would alleviate ERAD restrictions at

the ER level, increase throughput and improve surface stability by lowering the amount of protein

targeted to the lysosome.

Unlike C4, C951 displayed robust rescue in both HEK293 and HBE cells with untagged CFTR ΔF508, N-terminus, and EL4 CFTR ΔF508 FAP constructs. Because rescue by C951 is independent of cellular background, this molecule may interact directly with CFTR ΔF508 or through a common quality control pathway. Since C951 treatment alone is sufficient for rescue of CFTR ΔF508, this would suggest that C951 acts at least in part at the ER level and promotes export to the cell surface. Future studies to determine the exact mechanism of the C951 corrector will help understand the underlying defect and guide design of new correctors. Direct binding to CFTR ΔF508 could be determined by using inhibition of cross-linking assays, stabilization of purified NBD1 by differential scanning fluorimetry or by restoring the association of split halves of CFTR ΔF508 *in vitro*.

Combinations of corrector treatments, particularly C548 and C951, restored trafficking and channel function of CFTR ΔF508 more than single corrector treatments (Table 2-2). Additive or synergistic effects from co-operative corrector interactions indicate that the corrector compounds may have distinct mechanisms of action. One possibility is that each corrector is binding to a different part of the CFTR ΔF508 protein to stabilize the folding or eliminate non-productive folding intermediates. Since the folding defect of ΔF508 involves multiple domain and inter-domain interactions, multiple binding events may be necessary for complete correction of the misfolded protein. Alternatively, folding conformation changes could be effected through the modulation of chaperones that promote maturation of the protein. This also may require the activation of more than one chaperone or complex to accomplish a properly folded state. The correctors may also be acting indirectly on quality control pathways that prematurely degrade CFTR ΔF508.

Early in CFTR ΔF508 biogenesis, suppression of factors involved in the ERAD and proteasomal pathway lead to more secretion of CFTR ΔF508 from the ER to the Golgi compartment and eventually transit to the cell surface. Increasing the functional half-life of CFTR ΔF508 at the PM with correctors can also be

achieved by acting on the peripheral quality control pathway. The ESCRT (endosomal sorting complex required for transport) pathway recognizes ubiquitinated CFTR ΔF508 from the PM and triggers its removal and lysosomal degradation[23,99,100]. Correctors may increase the residency of CFTR ΔF508 in the PM by knocking down the activity of proteins such as HSC70 and CHIP. This would result in a decreased internalization and lysosomal degradation leading to an increase in steady state levels in the membrane. The PM stability of CFTR ΔF508 may also be enhanced by improving recycling efficiency by increasing the activity of sorting proteins such as Rab 4 and 11[35,101], which are responsible for returning endocytosed CFTR back to the PM[35,103]. These corrector mechanisms are not mutually exclusive as many of the quality control elements at the ER level also have a role in PM quality surveillance. This work shows additive or synergistic effects of trafficking and functional rescue with C4 and C951, C548 and C951, but not C4 and C548. C4 and C548 were applied at their maximum effective concentration and they did not augment each other, suggesting that they may have overlapping targets. In all cell types however, C548 was able to improve the efficacy of C951, indicating that the co-operative effect from this pair is independent of cell type or method of measurement. A noteworthy finding was the synergy between C548 and C951 was detected by PM density measurements in the N-terminal FAP construct. Reports of synergistic combinations of correctors have also been reported for C3 and C4, as well as correctors from distinct classes such as histone deacetylase inhibitors (SAHA)[94,102].

The co-operative rescue effect when correctors are paired is not observed when potentiators are combined. It is thought that potentiators are so effective because they bind directly to the NBDs of CFTR[103,104]. The lack of enhanced activity when potentiators are combined supports the idea that they share a common mechanism of action[94]. This is not true for correctors. Due to the complex nature of the ΔF508 mutation, a combinatorial approach of correctors may be required for sufficient rescue of functional protein.

Overall, the corrector efficacy examined by FAP fluorescence activation revealed C951 as the most potent single agent and C548 and C951 as one of the best combinations of correctors. These findings were validated by functional measurements in an endogenous cell background, polarized HBE cells. Taken together, these results demonstrate that the FAP reporter system is sensitive enough to provide detailed information about differences between correctors that correlates well with functional data obtained from a physiologically relevant cell type. As a proof of principle, the CFTR ΔF508 FAP reporter system has shown that rescue by bona fide correctors is detectable by multiple fluorescence measurement methods.

Current drug screening assays have been successful in identifying small molecules that correct CFTR ΔF508 trafficking but they are still limited. A drawback for the halide sensitive YFP screening method is the relatively small range of sensitivity. The maximum fold change observed with the YFP functional assay is ~2 fold[94]. By using FAP reporters to determine the PM density of CFTR ΔF508 the dynamic range for detecting trafficking rescue is very large. The fluorescent MG signal will continue to increase as the concentration of CFTR ΔF508 molecules in the PM increases. The fluorescent signal from the FAP reporter has a linear relationship to the number of molecules in the PM unlike the halide sensitive YFP quenching method which quickly becomes saturated from the efflux of ions[89]. Therefore, the FAP reporters are better suited to look for synergistic combinations of correctors that produce more robust rescue of CFTR ΔF508.

Ch. 2 – Materials and Methods

Iodide Efflux Assay

CFTR/FAP fusion cell lines were assessed for CFTR activity by an 6-methoxy-N-(3-sulfopropyl)

quinolinium, SPQ. Iodide solution contained NaI 130mM, Mg(NO3)2 6H2O 1mM, Ca(NO3) 4H2O 1mM,

KNO3 4mM, Glucose 10mM and HEPES Hemi-Na 20mM. Nitrate solution contained NaNO3 130mM,

Mg(NO3)2 6H2O 1mM, Ca(NO3) 4H2O 1mM, KNO3 4mM, Glucose 10mM and HEPES Hemi-Na 20mM.

Cells were plated on mattek dishes (part no p35G-1.5-14-C) 24 hours prior to iodide efflux

measurement. Correctors were added to the cells 24 hours prior to iodide efflux measurements. A

combination of 10µM C4 + 5µM C951, or DMSO (vehicle) was added. SPQ was hypotonically loaded

with Iodide and H2O 1:1 v/v and 10mM SPQ for 20min at 37°C. After loading cells with SPQ they are

imaged at 40X on an inverted epi-fluorescence microscope capturing images every 15s. Fluorescent

filter set up used to excite SPQ was 350nm and capture emission at 455nm. Cells were perfused with

buffers warmed to 37°C. For each experiment the following protocol was used: Iodide buffer was

perfused for 3 min, exchanged with Nitrate buffer for 3 min, then Nitrate buffer with 10µM Forskolin

and CFTR specific potentiator, P2 (300nM) then finally switched back to Iodide buffer for 3 min. Analysis

was performed with Image J by analyzing mean fluorescence intensity of SPQ. Data are represented by

the maximum slope of each Iodide efflux measurement.

Flow cytometry

Quantification of CFTR ΔF508 rescue to the cell surface was carried out by measurement of MG-11p

fluorescence activity using flow cytometry. HEK 293 cells stably expressing either FAP-CFTR ΔF508 or

CFTR ΔF508 EL4-FAP were plated at a cell density of $1X10^5$ cells per 35mm dish. After 12hours the

growth media was removed and replaced with 1mL of DMEM media containing various corrector

conditions: 10μM C4, 5μM C548, 5μM C951, 10μM C4 + 5μM C548, 10μM C4 + 5μM C951, 5μM C548 +

5μM C951, Vehicle (DMSO) 15μM. 24h after corrector treatment, cells were removed from the dishes

with Cellstripper™ (non-enzymatic, Cellgro). Cells were centrifuged at 500xg for 5 minutes at 4°C then

resuspended in 1mL of PBS. 50nM MG-11p fluorogen was added to all samples prior to measurement.

Sample analysis was performed by excitation with a 640nm laser and emission captured with 685/35

filter set. Each condition consisted of 10,000 recorded events. Data analysis was performed using FACS

Diva software to obtain the mean MG fluorescence ± SEM for each population. Sample size for DMSO,

C4/C951 and C548/C951 n=5. C4, C548, C951 n=3. These represent experiments performed on separate

days. Each sample was normalized to the mean of C951.

Immunoblotting

Whole cell lysates from stably expressing FAP tagged CFTR cell lines were obtained by removing cells

from 10cm dishes in RIPA buffer: 150mM NaCl, 50mM tris HCl pH7.5, 1% Triton X100, 1% sodium

deoxycholate, 0.1% SDS and 1 tablet of PIC/10mL RIPA buffer (Roche #11-836-153-011). FAP-CFTR WT

and CFTR WT EL4-FAP cell lines were grown under normal conditions, FAP-CFTR ΔF508 and CFTR ΔF508

EL4-FAP cell lines were treated with one of the following conditions for 24h prior to harvesting whole

cell lysates. (1) Vehicle control – maximum volume used for correctors of cell culture grade DMSO,

7.5μL (2) C548 5μM and C951 5μM combination (3) C4 10μM and C951 5μM combination. Cell lysates

were quantified using BCA Protein Assay Reagent (bicinchoninic acid) from Pierce. SDS PAGE separation

of whole cell lysates, transfer to immunoblotting membrane and probe with CFTR specific antibody was

performed by Kathi Peters (Frizzell Laboratory)

Ussing chamber measurements

Short circuit measurements from HBE cells using Ussing chambers was performed by Matthew Glover

(Frizzell laboratory). Corrector data for CF172p1 ΔF508/ ΔF508 homozygous background cells was

normalized by dividing each observation by the mean of all C951 observations. Corrector treatments

were applied for 24h before measurements. Conditions were as follows: Vehicle control – maximum

volume used for correctors of cell culture grade DMSO, C548 and C951 5µM each, C4 10µM.

Microscopy

Images were acquired using a Nikon confocal microscope EM CCD camera with 630nm laser excitation

and cy5 emmission filter. Cell were plated on Mattek dishes (part no p35G-1.5-14-C). For ΔF508

expressing cell lines, cells were plated at a density of $1X10^5$ cells. 12-24 hours later, cells were treated

with C4 10µM and C951 5µM or vehicle (DMSO) control. After 24 hours of treatment cells were imaged

in the growth medium at 37°C and 5% CO_2 using confocal microscopy with either cell impermeant (MG-

11p) or permeant (MG-Ester) at a concentration of 50nM.   Low temperature rescue was achieved by

incubating cells at 30°C for 24 hours.

Statistics

Statistical analysis was carried out using Graphpad Prism software. Student's t test two tailed unpaired

was performed between each corrector condition and the DMSO vehicle treated control. Statistical

significance is represented as follows: p value 0.01 to 0.05 - *, 0.001 to 0.01 - **, 0.0001 to 0.001 - ***,

<0.0001 - ****.

Reagents

Corrector compounds, C4, C548 and C951 were obtained from the Frizzell lab (Children's Hospital of

Pittsburgh. Cellstripper was purchased from Mediatech (Manassas, VA). Fluorogens, MG-11p and MG-

ester were provided by the MBIC reagent chemistry group (Carnegie Mellon University).

Chapter 3 : CFTR Trafficking

Ch. 3 – Introduction

CFTR Endocytosis

The trafficking routes of CFTR have received a great deal of attention in order to gain an understanding of the mechanisms that control where the channel is localized and how the ΔF508 itinerary differs from WT. CFTR WT experiences rapid endocytosis from the PM, around 5-10%/min, which is faster than the constitutively recycling PM protein, transferrin, or bulk membrane uptake[31,32,105]. Internalization occurs through clustering into clathrin coated pits which is controlled by the clathrin adapter complex AP-2. Endocytic motifs located in the C-terminus of CFTR, YDSI and di-leucine, are required for internalization[34,105-107]. This is followed by vesicular budding and pinching by the vesicle collar protein, dynamin. Chemical inhibition of dynamin with dynasore prevented the endocytosis of CFTR[33]. This vesicle budding reaction is mediated by the binding of SNAP-23 and Syntaxin-1, members of a t-SNARE complex (target vesicle-soluble *N*-ethylmaleimide-sensitive factor attachment protein receptors), to the first 80 amino acids of the N-terminus[105,108-110]. Over expression of SNAP-23 or Syntaxin-1 accelerates endocytosis of CFTR leading to a decrease in surface expression. Conversely, co-expression with the Syntaxin-1 binding protein, Munc-18, disrupted interactions with CFTR and stabilized CFTR at the cell surface[111,112] (Figure 3-1).

In addition to t-SNARE interactions, association with the peripheral actin cytoskeleton is necessary for regulated internalization of CFTR. CFTR is connected to the actin cytoskeleton by a multitude of dynamic scaffolding protein interactions. Filamin-A is an actin binding protein which is known to bind to CFTR and other ion channels at the membrane and tether them to the cortical actin cytoskeleton. Mutation S13F in the N-terminus of CFTR abolished binding to Filamin-A resulting in a significant reduction of chloride conductance and surface expression of CFTR[45]. At the C-terminus of CFTR, a PDZ

(PSD95, Dlg, ZO-1) domain is responsible for further interactions with the actin network. The last four

amino acids of the C-terminus of CFTR harbors a PDZ binding sequence, DTRL, which binds to a

scaffolding protein called NHERF-1 (Na^+/H^+ exchanger regulatory factor). NHERF-1 contains an ERM

domain (ezrin, radixin, moesin) that links CFTR to the actin network[113,114]. Clearly, a complex

relationship exists between the actin cytoskeleton and CFTR. Not only are there multiple interaction

domains, but they are coordinated through large scaffolding complexes. CFTR is immobilized in the PM

by the actin cytoskeleton. Single molecule tracking studies have shown that up to 50% of CFTR has

restricted movement in the PM. Removal, mutation, or masking of the PDZ domain (DTRL) increases the

mobility within the PM by up to 50%[40,115,116]. Furthermore, these interactions between the PDZ domain

of CFTR and the actin cytoskeleton are quite stable, lasting for minutes[115]. These extended interactions

may be important for maintaining the long membrane half-life of CFTR or clustering of multiple CFTR

molecules. Another finding that supports the importance of actin-CFTR interactions for PM stability

came from experiments that disrupted the actin cytoskeleton. Breakdown of the cortical F-actin

network by actin depolymerizing agents, wiskostatin and latrunculin-B, resulted in the increased PM

mobility and eventual depletion of CFTR at the cell surface[116,117]. Thus, maintenance of actin

cytoskeleton interactions is critical for the stabilization of CFTR in the membrane.

The kinetics of CFTR internalization varies depending on the cell type examined and the method of

measurement. For example, in BHK-21 cells, CFTR WT was internalized at a rate of 5% per minute as

measured by antibody labeling methods[23]. Similarly, endocytosis was rapid, 10%/min in HeLa cells,

however, in polarized epithelial cells (CFBE41o-), a rate of 2%/min was observed using biotinylation to

monitor disappearance of CFTR from the cell surface[39]. Another study that used biotinylation

techniques reported less than 1%/min in polarized CFBE41o- cells[101]. Differences in the internalization

rates may be attributed to the cellular background, method of measurement, or time intervals chosen

for analysis.

Figure 3-1: CFTR Interaction Map[114]

Regulation of CFTR in the plasma membrane involves interactions with a complex network of scaffolding proteins. At the C-terminus, CFTR binds to NHERF1 via a PDZ binding domain. NHERF1 anchors CFTR indirectly to the filamentous actin cytoskeleton through an ERM motif. Internalization of CFTR requires the binding of t-SNARE proteins, syntaxin 1 and SNAP23.

Differences in Surface Stability between CFTR WT and ΔF508

The turnover of CFTR ΔF508 at the cell membrane is much greater than CFTR WT. When CFTR ΔF508 is rescued to the cell surface with low temperature and maintained, the membrane half-life of WT and ΔF508 are similar. However, by rescuing CFTR ΔF508 to the cell surface with low temperature, then thermally destabilizing it by shifting the cells to 37°C, after 4 hours only 25% of CFTR ΔF508 remained on the surface of HeLa cells whereas 80% of CFTR WT was still present at the PM. Similarly, in polarized human airway epithelial cells over 50% of the temperature rescued CFTR ΔF508 was lost from the apical surface over the course of 4 hours at 37°C compared to only 15% for CFTR WT.

The discrepancy in PM stability between CFTR ΔF508 and WT is abundantly clear in both polarized epithelial and fibroblast cell lines. What is not as clear is the mechanism that causes this difference. Accelerated internalization of CFTR ΔF508 after thermal destabilization leads to a reduced PM density over time. Swiatecka-Urban et al. argue that CFTR ΔF508 is endocytosed more rapidly than CFTR WT, however the rate of recycling is the same which would lead to reduction in steady state levels of CFTR ΔF508 in the membrane[101]. Alternatively, Sharma et al. claim that endocytosis of CFTR ΔF508 is close to that of CFTR WT but the recycling back to the surface is severely impaired for CFTR ΔF508 causing reduced membrane expression[23].

Temperature rescued CFTR ΔF508 is ubiquitylated after thermal unfolding at the PM[23,99]. Based on trypsin susceptibility experiments, even a short incubation of 2.5h at 37°C destabilizes and partially unfolds CFTR ΔF508. Anti-ubiquitin probes revealed that destabilized CFTR ΔF508 has two fold greater amounts of ubiquitination compared to samples left at the permissive temperature. Along with this, knockdown of the E3 ubiquitin ligase, CHIP, mitigated the loss of CFTR ΔF508 from the PM after thermal

destabilization. Internalization of CFTR ΔF508 was slowed by 80% after CHIP knockdown but the endocytosis of CFTR WT or other PM proteins like transferrin was not affected[99]. The selective removal of unfolded CFTR ΔF508 from the cell surface over CFTR WT and other PM proteins is conferred by a series of chaperone interactions, Hsc70 and Hsp90, that activate the ubiquitin pathway. Prolonged chaperone interactions with CFTR ΔF508 at the PM recruits E1-3 ubiquitin enzymes which attach polyubiquitin to unfolded CFTR ΔF508 and target it for lysosomal destruction[23,62,99,100].

Regulators of recycling have been shown to have a direct impact on the amount of CFTR present at the cell surface (Figure 3-2). The Rab11 GTPase regulates the trafficking of CFTR from early endosomal compartments back to the PM[35]. Dominant negative forms of Rab11 dramatically reduced the surface expression of CFTR because without efficient recycling, endocytosed CFTR became trapped in intracellular compartments. Conversely, up-regulation of Rab11 rescued CFTR ΔF508 expression at the membrane, perhaps by addressing a recycling defect or by compensating for accelerated endocytosis. Another GTPase, Rme-1 also plays a role in regulating recycling of CFTR[118]. When internalized CFTR is routed to Rme-1 positive compartments, it is efficiently recycled back to the membrane. Functionally impaired Rme-1 mutants are defective for recycling CFTR and result in the loss of expression at the cell surface. Further investigation will be necessary to determine if over-expression or enhancement of Rme-1 function can restore CFTR ΔF508 membrane localization.

A combination of accelerated endocytosis and impaired recycling could cause the disparate membrane half-lives between CFTR ΔF508 and WT. This idea is supported by work which demonstrated both increased internalization and reduced recycling in HeLa cells measured using an ELISA (enzyme-linked immunosorbent assay) method to monitor CFTR ΔF508 movement[99]. Accelerated endocytosis and impaired recycling are not mutually exclusive possibilities to explain reduced CFTR ΔF508 PM half-life,
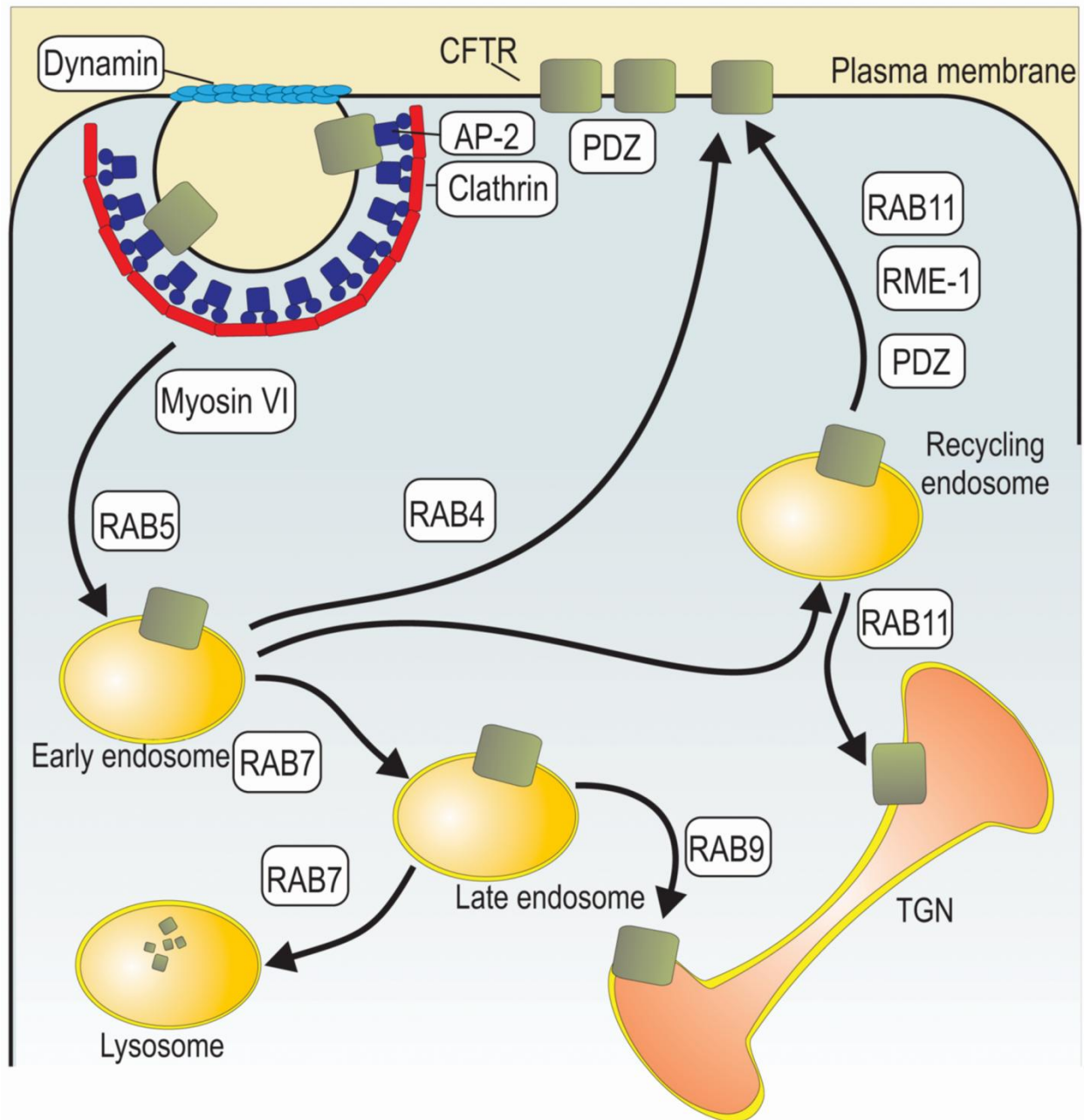
Figure 3-2: Intracellular Trafficking Pathways of CFTR[119]

Once CFTR is internalized from the cell surface by clathrin mediated endocytosis, it is directed to various cellular destinations by the endosomal sorting machinery. Rab GTPases control the trafficking fate of CFTR. Importantly, recycling of CFTR back to the membrane from the recycling endosome (ERC) is mediated by Rab11 and Rme-1. Alternatively, removal of CFTR from the trafficking pathway by lysosomal degradation is handled by Rab7.

however the extent to which each process influences the steady-state levels of CFTR at the cell surface may differ across different cell types.

Thus far, methods to study CFTR trafficking have relied largely on biochemical techniques such as biotinylation, ELISA and immunofluorescence. All of these detection systems severely limit the temporal resolution of the assay. Due to the multiple binding and wash steps required by these biochemical methods, it is impossible to study the movement of CFTR from the cell surface in living cells with fine temporal resolution. In distinction, FAP based detection is genetically encoded and does not require any wash steps, enabling one to closely examine the exact trafficking route of CFTR from the cell surface to intracellular compartments and recycling back to the membrane in real time. Investigating CFTR trafficking from the cell surface with live cell fluorescence imaging will enable direct visualization of CFTR molecules and particle tracking instead of monitoring changes in the steady-state levels. Furthermore, using organelle specific fluorescent labels like lysotracker which localizes to intracellular structures like the lysosome, we can directly monitor CFTR at critical sorting steps. The results presented herein demonstrate that the FAP reporter platform can accurately monitor the trafficking routes of CFTR. This work provides the basis for elucidating key differences in the between CFTR WT and ΔF508 such as rates of internalization and lysosomal degradation.

Ch. 3 – Results

Internalization of CFTR

To investigate the trafficking of CFTR in living cells, we studied internalization from the cell surface by confocal fluorescence microscopy. Stable HEK293 cell lines expressing the FAP-CFTR WT construct were used to measure the rate of internalization. In order to quantify the amount of signal that is accumulated in intracellular compartments over time, a cytoplasmic volume marker, cell-tracker green (Invitrogen C7025), was chosen because this dye is cell permeant and activated by cellular esterases. After esterification, cell-tracker green is trapped inside the cell and provides a fluorescent indicator of the intracellular volume. Furthermore, the spectrum of cell-tracker green does not interfere with the long wavelength emission of MG. To assess the rate of internalization from the surface, we first labeled FAP-CFTR WT at the membrane with the impermeant fluorogen, MG-11p. Immediately after the addition of MG-11p, fluorescent signal was only observed at the membrane. Time lapse imaging was performed over the course of one hour to monitor internalization of CFTR WT from the cell surface. Since the cells were maintained at 37°C and 5% CO2 without any pre-incubation on ice, we expected the trafficking reflect the normal behavior of CFTR. Over time, we observed an accumulation of signal inside the cell which we concluded must arise from CFTR that has undergone endocytosis from the PM. The fluorogen binding to the FAP has a low nanomolar dissociation constant and therefore after binding at the cell surface, it will remain bound to the FAP even after endocytosis into intracellular compartments. The coincidence of MG fluorescence signal with the cell-tracker green signal was used to determine the fraction of signal that was present in intracellular compartments. In order to quantify the amount of fluorescent signal present in intracellular compartments over time, we used image analysis software (NIH ImageJ) to segment the MG channel from the cell-tracker green channel. Cell-tracker green defines the cytoplasmic volume and therefore, to look for intracellular signal we measured the MG signal that

98

was coincident with cell-tracker green signal. Typically, this type of analysis is performed by manually defining the cell cytoplasm, however due to the number of images generated during this muti-color, z-stack, time-lapse experiment, manual determination of the cell-tracker green volume was not feasible. To solve this, the cell-tracker green channel was used to create a mask that would define the cytoplasmic area, and then the MG fluorescence within this mask was summed. In this way, we could quickly integrate the total MG fluorescence signal that is contained within the cell-tracker volume (See Ch.3. Materials and Methods).

Consistent with reports from the literature, we found that endocytosis was rapid, as we detected intracellular signal as early as 5min after fluorogen addition[31,32,105] (Figure 3-3 and Figure 3-4). FAP-CFTR WT signal continued to accumulate inside of the cell until 25 minutes when the intracellular signal reached near maximum and began to plateau. Because recycling of CFTR will redistribute signal back to the cell surface, we are unable to distinguish CFTR that has remained at the PM from that which has internalized and reemerged at the cell surface. Instead, what we can determine is the steady-state distribution of CFTR WT. This steady state distribution reflects the rates of internalization, recycling, delivery of new CFTR and protein degradation. From this data we can conclude that an equilibrium is established by 25 minutes. More specifically, we determined that the steady-state ratio of surface labeled FAP-CFTR WT inside the cell was 30% of the total MG signal from the cell (Figure 3-4). This may represent two pools of CFTR, a highly dynamic mobile fraction and a static membrane bound pool. During the early, linear phase of internalization, 5 minutes, the rate of internalization of FAP-CFTR WT from the surface was calculated to be ~3%/min of the total surface labeled pool (Figure 3-4). This finding is in general agreement with previously published internalization results[101,120].
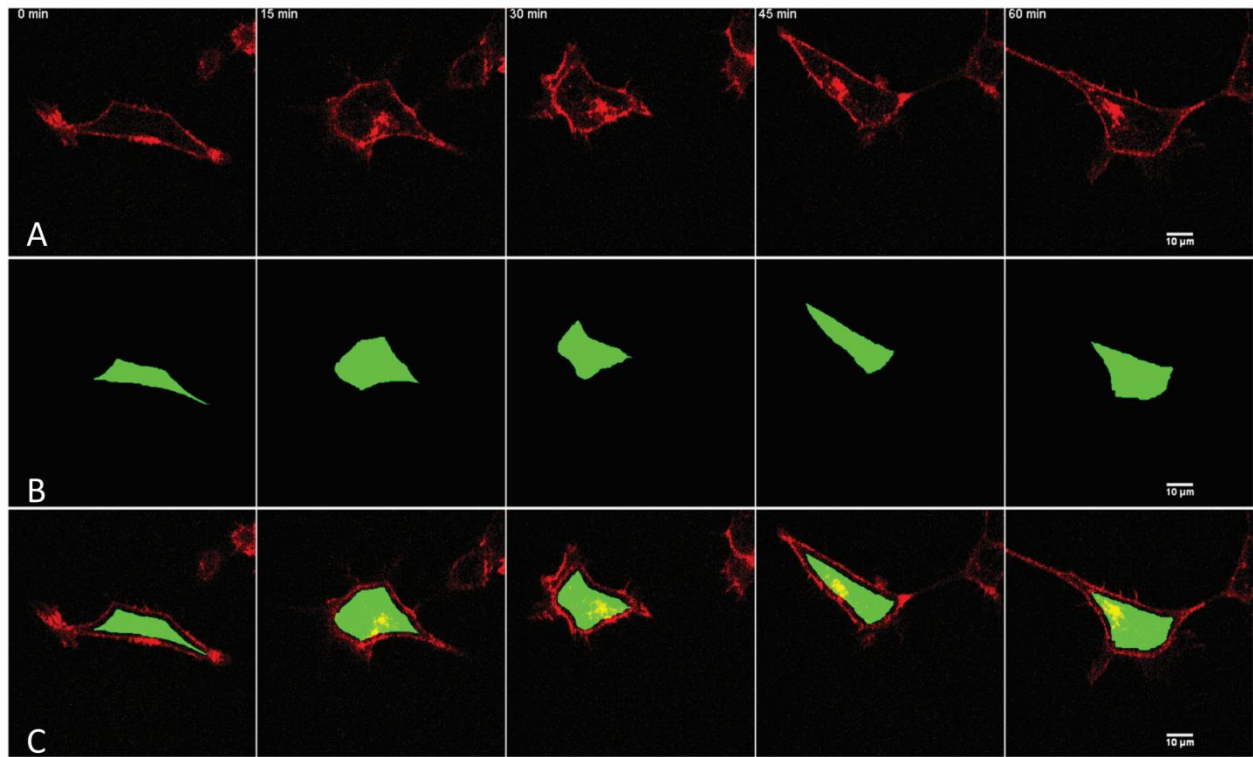
Figure 3-3: Visualization of CFTR Internalization

Time-lapse confocal fluorescence microscopy was used to observe endocytosis of FAP-CFTR WT in living cells. (A) Cell impermeant fluorogen, 50nM MG-11p, was added to cells at t=0 min and remained present throughout the experiment. (B) The cytoplasm was labeled using cell-tracker green dye. (C) Merge of the MG and cell-tracker green channels. Confocal Z-stacks capturing the MG and cell-tracker signals were taken every 5 minutes for 1 hour. Data are presented as an image montage with a single confocal section from every 15 minutes. In the beginning, CFTR WT is labeled exclusively at the cell surface, however, endocytosis results in the accumulation of MG signal in concentrated intracellular compartments over time. Scale bars are 10µM.
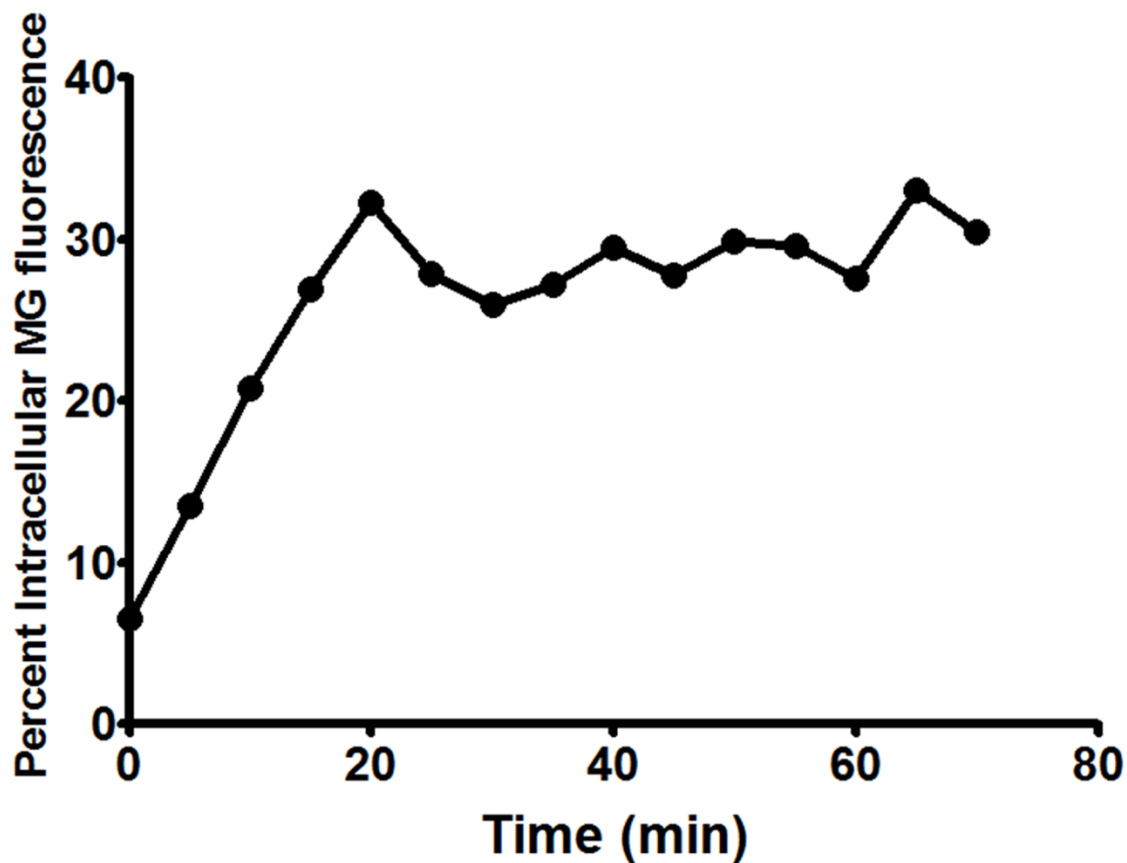
Figure 3-4: Quantification of FAP-CFTR WT Internalization

The amount of CFTR WT internalized over time was determined by image analysis from Figure 3-3. Internalized CFTR WT was calculated by integrating the MG fluorescence which coincident with the cytoplasmic marker. A ratio of internalized to the total MG fluorescence signal over time was plotted to determine the rate and dynamics of CFTR WT internalization. (See Ch. 3 Materials and Methods for detailed description of image analysis)

Co-Localization of CFTR WT with Lysosomes

Next, we asked whether CFTR WT is transported to the lysosome after internalization from the cell

surface. Even though wild-type CFTR does not dramatically translocate to lysosomal compartments like

CFTR ΔF508 after thermal destabilization, we reasoned that normal turnover of the PM proteins would

direct a small population of CFTR WT to the lysosomal compartment. To test this, we labeled lysosomes

with a cell permeant low pH indicator using a commercially available dye, lysotracker green (Invitrogen

L-7526). We used confocal time-lapse fluorescence microscopy to monitor the movement of CFTR WT

from the PM to lysosomal compartments. Cell impermeant fluorogen was added to cells expressing

FAP-CFTR WT and was present throughout the duration of the experiment. Confocal Z-stacks were

taken at 5 minute intervals over 1 hour acquiring fluorescence images from both the MG emission and

the lysotracker green emission channel. As expected, initially the MG fluorescence was restricted to the

PM and did not coincide with intracellular lysosomal compartments. Over time however, CFTR WT

underwent endocytosis and a small fraction of the total MG signal did colocalize with lysosomal

compartments (Figure 3-5). Colocalization was detected using the "colocalization highlighter" plugin for

NIH ImageJ which implements Pearson's correlation method to determine which pixels have overlapping

MG and lysotracker signal. The total amount of colocalized MG and lysotracker signal increased during

the first 25 minutes then reached a plateau (Figure 3-6). There was a slight drop in colocalization of

CFTR WT and lysotracker green between 40 and 60 minutes. This inconsistency may be attributed to

loss of MG signal upon entrance into acidic compartments or photobleaching of lysotracker green.
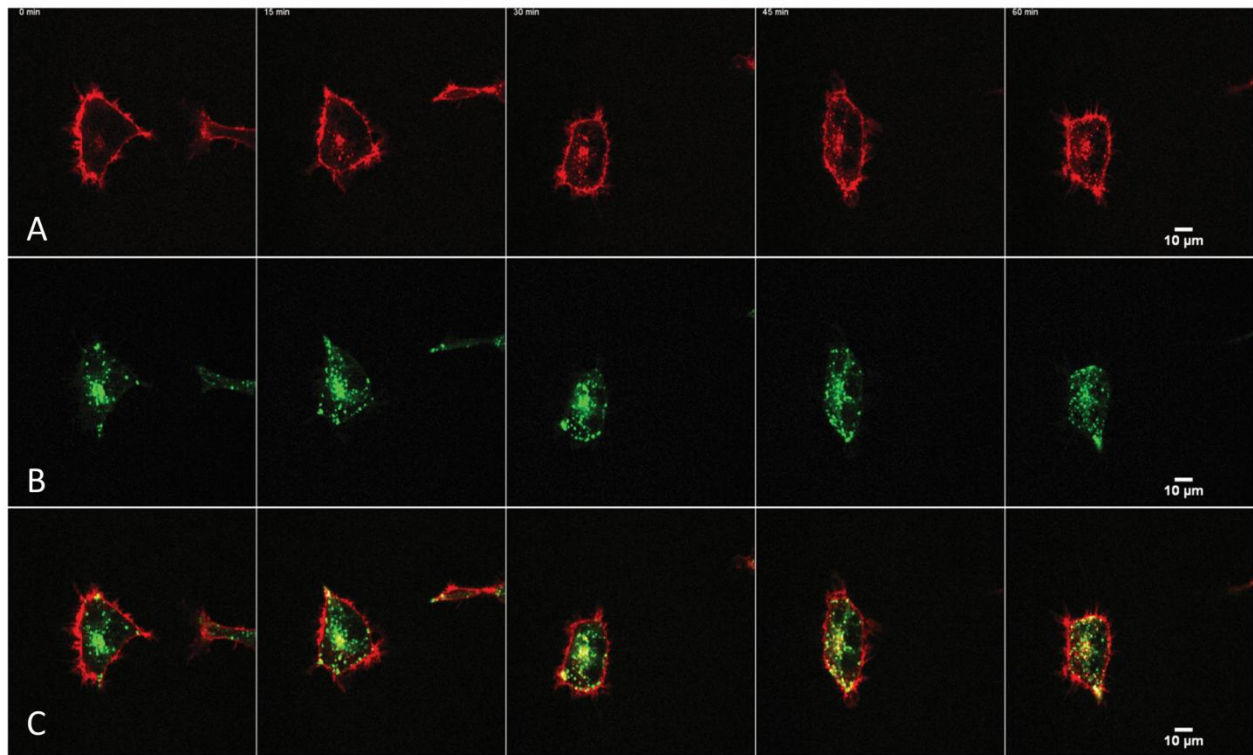
Figure 3-5: Endocytosed FAP-CFTR WT Co-localizes with Lysosomal Compartments

Time-lapse confocal fluorescence microscopy was used to visualize co-localization of FAP-CFTR WT with lysosomes in living cells. (A) Cell impermeant fluorogen, 50nM MG-11p, was added to cells at t=0 min and remained present throughout the experiment. (B) Lysosomes were stained using lysotracker green (C) Merge of the MG and lysotracker green channels, co-localized pixels indicated in white. Confocal Z-stacks capturing the MG and lysotracker green signal were taken every 5 minutes for 1 hour. Data are presented as an image montage with a single confocal section from every 15 minutes. Co-localization of FAP-CFTR WT and lysosomes was detected using NIH ImageJ. Scale bars are 10µM.
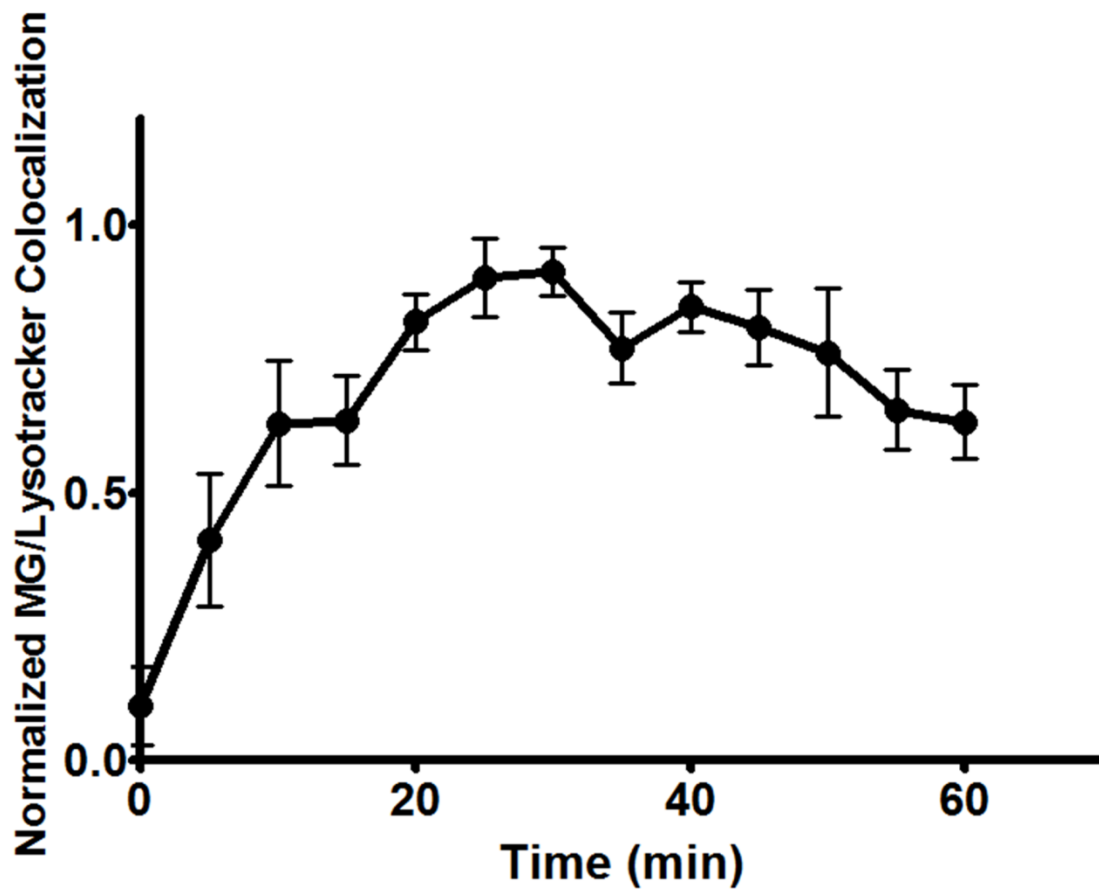
Figure 3-6: Quantification of Lysosomal Co-Localization with FAP-CFTR WT

Co-localization of internalized FAP-CFTR WT with lysosomes was calculated from time lapse microscopy data in Figure 3-5. The amount of co-localization was normalized to the maximum and was plotted as a function of time. A steady increase is observed until a plateau is reached at 25 minutes. Data are represented as the mean, error bars indicate ± SEM, n=3.

Ch. 3 – Discussion

This work demonstrates direct visualization of CFTR trafficking from the cell surface in living cells using FAP detection. By using the FAP-CFTR reporter system we have eliminated the need for incubation or wash steps. In contrast, immunofluorescence approaches that label extracellular epitopes engineered into CFTR require long incubations on ice, multiple blocking and wash steps plus fixation[15,30,35]. Similarly, biotinilyation necessitates ice cold oxidation of the surface groups of PM proteins followed by biotin conjugation. Moreover, biotinylation assays typically involve immunoprecipitation and protein gel electrophoresis rather than live cell imaging to assess rates of CFTR internalization[39]. Our FAP visualization method offers a rapid detection platform without performing long incubations on ice and fixing cells, and enables live cell imaging with high temporal resolution. The results presented in this study serve as a proof of principle to demonstrate the feasibility of detecting CFTR trafficking using the FAP platform. The time interval of every 5 minutes was chosen to reduce the effects of photobleaching and to accommodate 9 confocal sections at 10 separate stage positions. Based on the marginal amount of photobleaching of the MG fluorogen even after 2 hours of imaging we are confident that the time scale resolution can be dramatically improved by reducing the number of stage positions and confocal sections.

The rates of internalization observed for FAP-CFTR WT fall within the expected range. Previous reports vary widely depending on the cell type examined and method of measurement. Some studies claim internalization of surface CFTR around 2%/min, whereas other estimates range between 5-10%/min[30,34,39,100,101,105]. Over time, internalized fluorescence signal from PM labeled FAP-CFTR WT reached a steady-state distribution between the cell surface and a perinuclear compartment. CFTR and other PM proteins such as transferrin that undergo recycling are known to accumulate in the endosomal recycling compartment (ERC) which resides near the nucleus[35,118,121-123] The accumulation of intracellular

MG signal near the nucleus may represent FAP-CFTR WT in the ERC or another endosomal sorting compartment. Counter-staining with specific endosomal markers will be necessary to confirm this.

By defining the cytoplasm of cells with a fluorescent label using cell-tracker green dye we were able to quantify the amount of internalized MG signal. Through optimization of the imaging protocol to improve the cytoplasmic volume marker signal and by using more advanced image analysis software such as Imaris™, the quantification accuracy of internalized signal should improve substantially. Imaris software is a powerful image analysis software package that specializes in tracking fluorescent marker in 3d volumes. Imaris has particle tracking capabilities that are not possible with NIH ImageJ [124,125]. By plotting the trajectories of fluorescent signals (particles) from the cell surface into the cell, we can more precisely elucidate the dynamics of internalization and recycling by focusing on individual particles instead of the steady state distribution of the fluorescent signal. Therefore, future experiments to measure internalization will use Imaris to ensure robust quantification.

Although determination of CFTR WT internalization by fluorescence microscopy has produced results that are in agreement with other studies, this method has certain limitations. The spatial resolution of a confocal fluorescence microscope even with a 60X high numerical aperature objective is limited to ~200nm in the XY plane[126]. For this reason we are unable to distinguish molecules that are near the cell surface. As such, we cannot account for CFTR that has been internalized, however, remains close to the PM. Further experiments involving enzymatic removal of surface proteins by trypsin for example would enable precise quantification of internalized fluorescent signal without any ambiguity of spatial resolution. In this method, cells expressing the FAP-CFTR constructs would be exposed to impermeant fluorogen for various time intervals, then either treated with trypsin to remove signal at the cell surface or removed with a non-enzymatic method to preserve the total fluorescence, both surface and intracellular. By dividing the fluorescent signal from trypsin treated cells by signal from non-

enzymatically suspended cells, a ratio of intracellular to total fluorescence could be established. This intracellular to total fluorescence ratio could be measured by non-imaging based fluorescence detection methods such as flow cytometry or multi-well fluorimetry. Taking this approach does not provide the same information rich data sets or temporal resolution that time-lapse fluorescence microscopy generates. Therefore, a combination of both time-lapse microscopy and enzymatic surface protein removal methods will complement each other to elucidate the trafficking behavior of CFTR.

We observed that a small yet detectable fraction of FAP-CFTR WT was internalized from the cell surface and colocalized with lysosomal compartments. The rate of colocalization between MG signal and lysotracker green closely reflected the rates obtained for the overall internalization of FAP-CFTR WT. Under normal conditions, a small amount of CFTR WT is expected to be degraded, however the prediction for CFTR ΔF508 is much faster turnover and therefore greater colocalization with lysosomal compartments.

This study serves as a proof of principle to demonstrate the live cell imaging using FAP reporters can sensitively detect internalization of CFTR or colocalization with lysososmes. We would like to extend this method to study the properties of CFTR ΔF508. For example, studies have shown that after temperature rescue to the cell surface, CFTR ΔF508 can be thermally destabilized resulting in accelerated removal from the PM. Using the FAP platform, we can examine the whether or not corrector compounds stabilize CFTR ΔF508 at the cell surface. Furthermore, by looking at lysosome colocalization we would like to study how correctors influence the endocytic fate of CFTR ΔF508 after removal from the cell surface.

Ch. 3 – Materials and Methods

Microscopy

HEK 293 cells expressing FAP-CFTR WT were plated on Mattek dishes (part no p35G-1.5-14-C) and imaged using a Nikon confocal microscope at 60X magnification with an EM CCD camera. 488nm excitation and TRITC emission was used to capture signal from the cell-tracker dye, 630nm excitation and cy5 emission filter was used for MG signal. Cell tracker green dye (Invitrogen C7025) was added at 1μM and incubated with cells at 37°C for 15m prior to imaging. Cells were imaged at 37°C and 5% CO_2. At t=0 minutes, cell impermeant fluorogen (100nM MG-11p) was added to the cells. Time lapse, Z-stack images were acquired every 5 minutes for 1 hour.

Internalization Assay

Image data-sets were imported into NIH ImageJ software using the LOCI bio-formats import plugin (http://www.loci.wisc.edu/software/bio-formats). The cell-tracker channel was used as a marker for the cytoplasm. To do this, the cell-tracker images were converted to binary images and an appropriate threshold was chosen to capture the cytoplasmic volume faithfully. The binary cell-tracker masks were then processed using the erode function to shrink the area in order to avoid overlap with signal from MG at the cell surface. Images from the top and bottom of the Z-stack were excluded from analysis because they contained too much overlapping signal from the MG and cell-tracker channels. Quantification of internalized MG signal coincident with cell-tracker mask was determined by using the integrated density measurement from the MG channel that was confined within the cell-tracker mask and averaged across the Z-stack. Total MG signal was obtained from defining a region of interest which contained the entire cell and using the integrated density measurement function and averaged across the Z-stack. A ratio of the intracellular MG signal and total cell signal over time was plotted to

determine the rate of internalization. The rate per minute was calculated using the 5 minute time point because this was in the linear range of internalization and this time point was used in previously published studies[101].

Lysotracker Co-localization

Lysotracker green (Invitrogen L-7526) was added to the cells at a final concentration of 75nM and incubated at 37°C for 15m prior to imaging. The amount of co-localization between the MG channel and Lysotracker green channel over time was determined by using the co-localization highlighter plugin for NIH ImageJ. The number of co-localized pixels was normalized to the maximum for each trial. Data presented are the mean ± standard error of the mean (SEM), n=3 trials.

Conclusions and Future Directions

The development of a unique fluorescent detection platform has addressed an unmet need in the cystic fibrosis research field. Considerable progress has been made towards understanding the biology and physiology of CFTR; however, technological restrictions have hampered breakthroughs in drug development for cystic fibrosis. The key to successful drug development is a good assay. High throughput drug screening for CF is an emerging field that is gaining momentum, but is still restricted by the underlying assays. Our fluorescence based approach would streamline the current drug development pipeline by eliminating the multiple wash and labeling steps required for established assays. Furthermore, instead of indirect measurement of CFTR rescue, the FAP detection platform directly measures the density of CFTR molecules in the PM with very high dynamic range. Compared to the limited detection range of halide sensitive YFP screening approaches, FAP based methods would facilitate combinatorial screening to look for synergistic effects that may be missed due to saturated signals obtained in functional assays. Translation from low-throughput to HTS formats will undoubtedly require optimization. The most straightforward and popular HTS approach would entail multi-well fluorimetry screening. Due to the reduced sensitivity relative to confocal microscopy and flow cytometry, the signal to noise ratio will need improvement to provide a robust assay. Alternatively, this FAP-CFTR detection system could be adapted for flow cytometry based drug screening. For this application, the FAP reporter system would best be expressed in a non-adherent cell line such as U937. Since our lab already has successful collaborations established with a flow cytometry HTS center, University of New Mexico Center for Molecular Discovery, this route is an attractive option.

A logical progression for advancing the FAP based CFTR reporter platform is a transition to specialized cell types. Polarized epithelial cells are an excellent model for studying the natural behavior of CFTR as they contain the all of the same folding and trafficking machinery found in cells lining the respiratory

tract. Currently, the retroviral constructs used to transduce fibroblast cell lines with FAP-CFTR

constructs are not amenable for transduction of epithelial cells. Instead, new retroviral delivery systems

will be required for efficient transduction. Molecular cloning of CFTR WT and ΔF508 FAP tagged genes

into a robust adenoviral vector system could be carried out in order to establish stable epithelial cell

lines for studying CFTR in a native cell background.

We are now in a position to answer the question of whether stimulation of CFTR by PKA induces

insertion into the PM. The regulated trafficking of CFTR from intracellular compartments to the cell

surface in response to PKA activation appears to occur only in certain cell types, but whether this is due

to the cellular background, expression levels or method of measurement is unclear[119,127-130]. Intestinal

cells seem to exhibit more dramatic translocation of CFTR upon PKA phosphorylation than polarized

epithelial cells. There remain questions about the exact mechanisms of this process. Is this due to

accelerated exocytosis or reduced endocytosis? By using our cell impermeant fluorogen labeling

platform, we are capable of answering these questions. PKA stimulated insertion of CFTR into the PM

can be directly measured by an increase in FAP cell-impermeant fluorogen activation. Alternatively, if

endocytosis is modulated by PKA activity, CFTR internalization could be monitored through coincident

labeling of MG-11p over time with a cytoplasmic volume marker, i.e. cell-tracker. We will test different

cell types looking for Fsk induced FAP-CFTR insertion by increases in activation of cell impermeant

fluorogen to address whether cellular machinery require for regulated insertion of CFTR is specific to cell

background.

Recent advances in fluorogen synthesis have produced more sophisticated reporters of environmental

conditions. For example, fusion of a pH sensitive dye to the MG fluorogen, CypHer3-MG, uses FRET to

detect the location and acidity of intracellular compartments. This reagent would be extremely useful

for determining the trafficking routes of CFTR from the cell surface. When bound to FAP-CFTR fusion

proteins, the CypHer3-MG fluorogen would be carried along during the normal trafficking itinerary and reports in living cells, the local pH which is unique to specific compartments. As CFTR is internalized and sorted throughout the endosomal or lysosomal pathway, changes in the acidity between these compartments could be monitored by the FRET based pH fluorogen sensor. In addition to acidic compartment detection, pH sensitive fluorogen probes may also provide insight into the bicarbonate secretion behavior of CFTR. Not only does CFTR transport chloride across the apical surface of epithelial cells, but $HCO3^-$ balance is also regulated by this channel. Compared to the chloride transport activity of CFTR, very little is known about the secretion of $HCO3^-$. This is due in part to the technical difficulty of measuring concentrations of bicarbonate in cell culture growth conditions. Electrophysiology methods like patch clamp or complicated growth chamber rigs such as the pH stat have been used to determine the amount of bicarbonate secretion by CFTR, however they require specialized equipment and expertise. There are also fluorescent indictors of intracellular pH, BCECF, for example, which are useful for determining CFTR activity dependent changes in compartmental pH, but are not specific to CFTR localized compartments[131]. Fluorogens with pH sensing capabilities are only active when bound to FAP tagged CFTR and therefore would provide a site specific readout of CFTR bicarbonate secretion.

The scarcity of tools available to detect CFTR at the cell surface in living cells has impeded advancement in the understanding of CFTR trafficking. Thus far, cellular imaging has relied on immunofluorescence to detect subcellular localization; however, this method requires long incubations, wash steps and fixation. Fusions of CFTR with GFP have provided meaningful insight into total cellular distribution but does not discriminate protein that is at the cell surface.

By tagging CFTR with FAP reporters using two strategies, the N-terminus and the fourth extracellular loop, we have joined the advantages of fluorescent proteins with the selectivity of antibody labeling. We have shown that trafficking of CFTR can be precisely monitored by FAP detection using time-lapse

confocal fluorescence microscopy. Internalization of CFTR from the cell surface to intracellular compartments was investigated by co-labeling cells with impermeant fluorogen and a cytoplasmic marker. Transit to degradation pathways was evaluated by examining the co-localization of FAP-CFTR with a lysosomal marker. These experiments establish the basis for future trafficking studies to investigate differences between CFTR WT and ΔF508 and characterize the effects of correctors.

Importantly, we have demonstrated that the FAP reporter system reflects the behavior of untagged CFTR. This was accomplished through a battery of validation methods. Proper membrane localization and topology were verified by fluorescence microscopy with cell impermeant and permeant fluorogens. Biochemical properties, including folding and maturation were assessed by immunoblotting with CFTR specific antibodies. Physiological activity was confirmed by functional assays which measured iodide efflux. Finally, a key finding was the detection of trafficking rescue of CFTR ΔF508 with low temperature or small molecule correctors. Taken together, we conclude that the FAP tagged CFTR reporter constructs faithfully recapitulate the most important aspects of CFTR biology. Therefore, they should serve as a meaningful technology for studying the properties of CFTR, and for seeking and developing new therapeutic drugs.

References

1   Pedemonte, N. *et al.* Small-molecule correctors of defective DeltaF508-CFTR cellular processing identified by high-throughput screening. *J Clin Invest* **115**, 2564-2571, doi:10.1172/JCI24898 (2005).

2   Bobadilla, J. L., Macek, M., Jr., Fine, J. P. & Farrell, P. M. Cystic fibrosis: a worldwide analysis of CFTR mutations--correlation with incidence data and application to screening. *Hum Mutat* **19**, 575-606, doi:10.1002/humu.10041 (2002).

3   Riordan, J. R. *et al.* Identification of the cystic fibrosis gene: cloning and characterization of complementary DNA. *Science* **245**, 1066-1073 (1989).

4   Sheppard, D. N. & Welsh, M. J. Structure and function of the CFTR chloride channel. *Physiol Rev* **79**, S23-45 (1999).

5   Cohn, J. A. *et al.* Increased risk of idiopathic chronic pancreatitis in cystic fibrosis carriers. *Hum Mutat* **26**, 303-307, doi:10.1002/humu.20232 (2005).

6   Davis, P. B. Cystic fibrosis since 1938. *Am J Respir Crit Care Med* **173**, 475-482, doi:10.1164/rccm.200505-840OE (2006).

7   Rommens, J. M. *Cystic Fibrosis Mutation Database*, <http://www.genet.sickkids.on.ca/StatisticsPage.html> (2011).

8   Boucher, R. C. Regulation of airway surface liquid volume by human airway epithelia. *Pflugers Arch* **445**, 495-498, doi:10.1007/s00424-002-0955-1 (2003).

9   Matsui, H. *et al.* Evidence for periciliary liquid layer depletion, not abnormal ion composition, in the pathogenesis of cystic fibrosis airways disease. *Cell* **95**, 1005-1015 (1998).

10   Mall, M., Grubb, B. R., Harkema, J. R., O'Neal, W. K. & Boucher, R. C. Increased airway epithelial Na+ absorption produces cystic fibrosis-like lung disease in mice. *Nat Med* **10**, 487-493, doi:10.1038/nm1028 (2004).

11   Tarran, R., Button, B. & Boucher, R. C. Regulation of normal and cystic fibrosis airway surface liquid volume by phasic shear stress. *Annu Rev Physiol* **68**, 543-561, doi:10.1146/annurev.physiol.68.072304.112754 (2006).

12   Knowles, M. R. & Boucher, R. C. Mucus clearance as a primary innate defense mechanism for mammalian airways. *J Clin Invest* **109**, 571-577, doi:10.1172/JCI15217 (2002).

13   Saiman, L. Microbiology of early CF lung disease. *Paediatr Respir Rev* **5 Suppl A**, S367-369 (2004).

14   Foundation, C. F. Patient Registry Annual Report. (2009).

15   Kreda, S. M. & Gentzsch, M. Imaging CFTR protein localization in cultured cells and tissues. *Methods Mol Biol* **742**, 15-33, doi:10.1007/978-1-61779-120-8_2 (2011).

16   Riordan, J. R. CFTR function and prospects for therapy. *Annu Rev Biochem* **77**, 701-726, doi:10.1146/annurev.biochem.75.103004.142532 (2008).

17   Proesmans, M., Vermeulen, F. & De Boeck, K. What's new in cystic fibrosis? From treating symptoms to correction of the basic defect. *Eur J Pediatr* **167**, 839-849, doi:10.1007/s00431-008-0693-2 (2008).

18   Elkins, M. R. *et al.* A controlled trial of long-term inhaled hypertonic saline in patients with cystic fibrosis. *N Engl J Med* **354**, 229-240, doi:10.1056/NEJMoa043900 (2006).

19   Tarran, R., Donaldson, S. & Boucher, R. C. Rationale for hypertonic saline therapy for cystic fibrosis lung disease. *Semin Respir Crit Care Med* **28**, 295-302, doi:10.1055/s-2007-981650 (2007).

20   Rommens, J. M. *et al.* Identification of the cystic fibrosis gene: chromosome walking and jumping. *Science* **245**, 1059-1065 (1989).

21   Chang, X. B. *et al.* Role of N-linked oligosaccharides in the biosynthetic processing of the cystic fibrosis membrane conductance regulator. *J Cell Sci* **121**, 2814-2823, doi:10.1242/jcs.028951 (2008).

22   Glozman, R. *et al.* N-glycans are direct determinants of CFTR folding and stability in secretory and endocytic membrane traffic. *J Cell Biol* **184**, 847-862, doi:10.1083/jcb.200808124 (2009).

23   Sharma, M. *et al.* Misfolding diverts CFTR from recycling to degradation: quality control at early endosomes. *J Cell Biol* **164**, 923-933, doi:10.1083/jcb.200312018 (2004).

24   Okiyoneda, T. *et al.* Role of calnexin in the ER quality control and productive folding of CFTR; differential effect of calnexin knockout on wild-type and DeltaF508 CFTR. *Biochim Biophys Acta* **1783**, 1585-1594, doi:10.1016/j.bbamcr.2008.04.002 (2008).

25   Cheng, S. H. *et al.* Defective intracellular transport and processing of CFTR is the molecular basis of most cystic fibrosis. *Cell* **63**, 827-834 (1990).

26   Ward, C. L. & Kopito, R. R. Intracellular turnover of cystic fibrosis transmembrane conductance regulator. Inefficient processing and rapid degradation of wild-type and mutant proteins. *J Biol Chem* **269**, 25710-25718 (1994).

27   Ward, C. L., Omura, S. & Kopito, R. R. Degradation of CFTR by the ubiquitin-proteasome pathway. *Cell* **83**, 121-127 (1995).

28   Tector, M. & Hartl, F. U. An unstable transmembrane segment in the cystic fibrosis transmembrane conductance regulator. *Embo J* **18**, 6290-6298, doi:10.1093/emboj/18.22.6290 (1999).

29   Varga, K. *et al.* Efficient intracellular processing of the endogenous cystic fibrosis transmembrane conductance regulator in epithelial cell lines. *J Biol Chem* **279**, 22578-22584, doi:10.1074/jbc.M401522200 (2004).

30   Cholon, D. M., O'Neal, W. K., Randell, S. H., Riordan, J. R. & Gentzsch, M. Modulation of endocytic trafficking and apical stability of CFTR in primary human airway epithelial cultures. *Am J Physiol Lung Cell Mol Physiol* **298**, L304-314, doi:10.1152/ajplung.00016.2009 (2010).

31   Prince, L. S., Workman, R. B., Jr. & Marchase, R. B. Rapid endocytosis of the cystic fibrosis transmembrane conductance regulator chloride channel. *Proc Natl Acad Sci U S A* **91**, 5192-5196 (1994).

32   Swiatecka-Urban, A. *et al.* PDZ domain interaction controls the endocytic recycling of the cystic fibrosis transmembrane conductance regulator. *J Biol Chem* **277**, 40099-40105, doi:10.1074/jbc.M206964200 (2002).

33   Young, A. *et al.* Dynasore inhibits removal of wild-type and DeltaF508 cystic fibrosis transmembrane conductance regulator (CFTR) from the plasma membrane. *Biochem J* **421**, 377-385, doi:10.1042/BJ20090389 (2009).

34   Lukacs, G. L., Segal, G., Kartner, N., Grinstein, S. & Zhang, F. Constitutive internalization of cystic fibrosis transmembrane conductance regulator occurs via clathrin-dependent endocytosis and is regulated by protein phosphorylation. *Biochem J* **328 (Pt 2)**, 353-361 (1997).

35   Gentzsch, M. *et al.* Endocytic trafficking routes of wild type and DeltaF508 cystic fibrosis transmembrane conductance regulator. *Mol Biol Cell* **15**, 2684-2696, doi:10.1091/mbc.E04-03-0176 (2004).

36   Okiyoneda, T. & Lukacs, G. L. Cell surface dynamics of CFTR: the ins and outs. *Biochim Biophys Acta* **1773**, 476-479, doi:10.1016/j.bbamcr.2007.01.004 (2007).

37   Jurkuvenaite, A. *et al.* Functional stability of rescued delta F508 cystic fibrosis transmembrane conductance regulator in airway epithelial cells. *Am J Respir Cell Mol Biol* **42**, 363-372, doi:10.1165/rcmb.2008-0434OC (2010).

38   Luo, Y., McDonald, K. & Hanrahan, J. W. Trafficking of immature DeltaF508-CFTR to the plasma membrane and its detection by biotinylation. *Biochem J* **419**, 211-219, 212 p following 219, doi:10.1042/BJ20081869 (2009).

39   Varga, K. *et al.* Enhanced cell-surface stability of rescued DeltaF508 cystic fibrosis transmembrane conductance regulator (CFTR) by pharmacological chaperones. *Biochem J* **410**, 555-564, doi:10.1042/BJ20071420 (2008).

40   Haggie, P. M. & Verkman, A. S. Monomeric CFTR in plasma membranes in live cells revealed by single molecule fluorescence imaging. *J Biol Chem* **283**, 23510-23513, doi:10.1074/jbc.C800100200 (2008).

41   Mattheyses, A. L., Simon, S. M. & Rappoport, J. Z. Imaging with total internal reflection fluorescence microscopy for the cell biologist. *J Cell Sci* **123**, 3621-3628, doi:10.1242/jcs.056218 (2010).

42   Peters, K. W. *et al.* CFTR Folding Consortium: methods available for studies of CFTR folding and correction. *Methods Mol Biol* **742**, 335-353, doi:10.1007/978-1-61779-120-8_20 (2011).

43   Howard, M. *et al.* Epitope tagging permits cell surface detection of functional CFTR. *Am J Physiol* **269**, C1565-1576 (1995).

44   Barriere, H. *et al.* Revisiting the role of cystic fibrosis transmembrane conductance regulator and counterion permeability in the pH regulation of endocytic organelles. *Mol Biol Cell* **20**, 3125-3141, doi:10.1091/mbc.E09-01-0061 (2009).

45   Thelin, W. R. *et al.* Direct interaction with filamins modulates the stability and plasma membrane expression of CFTR. *J Clin Invest* **117**, 364-374, doi:10.1172/JCI30376 (2007).

46   Szent-Gyorgyi, C. *et al.* Fluorogen-activating single-chain antibodies for imaging cell surface proteins. *Nat Biotechnol* **26**, 235-240, doi:10.1038/nbt1368 (2008).

47   Babendure, J. R., Adams, S. R. & Tsien, R. Y. Aptamers switch on fluorescence of triphenylmethane dyes. *J Am Chem Soc* **125**, 14716-14717, doi:10.1021/ja037994o (2003).

48   Nygren, J., Svanvik, N. & Kubista, M. The interactions between the fluorescent dye thiazole orange and DNA. *Biopolymers* **46**, 39-51, doi:10.1002/(SICI)1097-0282(199807)46:1<39::AID-BIP4>3.0.CO;2-Z (1998).

49   Boder, E. T. & Wittrup, K. D. Yeast surface display for screening combinatorial polypeptide libraries. *Nat Biotechnol* **15**, 553-557, doi:10.1038/nbt0697-553 (1997).

50   Boder, E. T. & Wittrup, K. D. Optimal screening of surface-displayed polypeptide libraries. *Biotechnol Prog* **14**, 55-62, doi:10.1021/bp970144q (1998).

51   Feldhaus, M. J. *et al.* Flow-cytometric isolation of human antibodies from a nonimmune Saccharomyces cerevisiae surface display library. *Nat Biotechnol* **21**, 163-170, doi:10.1038/nbt785 (2003).

52   Ahner, A., Nakatsukasa, K., Zhang, H., Frizzell, R. A. & Brodsky, J. L. Small heat-shock proteins select deltaF508-CFTR for endoplasmic reticulum-associated degradation. *Mol Biol Cell* **18**, 806-814, doi:10.1091/mbc.E06-05-0458 (2007).

53   Pedemonte, N., Tomati, V., Sondo, E. & Galietta, L. J. Influence of cell background on pharmacological rescue of mutant CFTR. *Am J Physiol Cell Physiol* **298**, C866-874, doi:10.1152/ajpcell.00404.2009 (2010).

54   Coloma, M. J., Hastings, A., Wims, L. A. & Morrison, S. L. Novel vectors for the expression of antibody molecules using variable regions generated by polymerase chain reaction. *J Immunol Methods* **152**, 89-104 (1992).

55   Gronwald, R. G. *et al.* Cloning and expression of a cDNA coding for the human platelet-derived growth factor receptor: evidence for more than one receptor class. *Proc Natl Acad Sci U S A* **85**, 3435-3439 (1988).

56   Chesnut, J. D. *et al.* Selective isolation of transiently transfected cells from a mammalian cell population with vectors expressing a membrane anchored single-chain antibody. *J Immunol Methods* **193**, 17-27 (1996).

57   Invitrogen. pDisplay manual. (2011). <http://tools.invitrogen.com/content/sfs/manuals/pdisplay_man.pdf>.

58   Holleran, J. *et al.* Fluorogen-activating proteins as biosensors of cell-surface proteins in living cells. *Cytometry A* **77**, 776-782, doi:10.1002/cyto.a.20925 (2010).

59   Nolan, G. (2011). <http://www.stanford.edu/group/nolan/retroviral_systems/phx.html>.

60   Verkman, A. S. & Jayaraman, S. Fluorescent indicator methods to assay functional CFTR expression in cells. *Methods Mol Med* **70**, 187-196, doi:10.1385/1-59259-187-6:187 (2002).

61   Apaja, P. M., Xu, H. & Lukacs, G. L. Quality control for unfolded proteins at the plasma membrane. *J Cell Biol* **191**, 553-570, doi:10.1083/jcb.201006012 (2010).

62   Barriere, H. *et al.* Molecular basis of oligoubiquitin-dependent internalization of membrane proteins in Mammalian cells. *Traffic* **7**, 282-297, doi:10.1111/j.1600-0854.2006.00384.x (2006).

63   Helenius, A. & Aebi, M. Roles of N-linked glycans in the endoplasmic reticulum. *Annu Rev Biochem* **73**, 1019-1049, doi:10.1146/annurev.biochem.73.011303.073752 (2004).

64   Lewis, H. A. *et al.* Structure of nucleotide-binding domain 1 of the cystic fibrosis transmembrane conductance regulator. *Embo J* **23**, 282-293, doi:10.1038/sj.emboj.7600040 (2004).

65   Thibodeau, P. H., Brautigam, C. A., Machius, M. & Thomas, P. J. Side chain and backbone contributions of Phe508 to CFTR folding. *Nat Struct Mol Biol* **12**, 10-16, doi:10.1038/nsmb881 (2005).

66   Thibodeau, P. H. *et al.* The cystic fibrosis-causing mutation deltaF508 affects multiple steps in cystic fibrosis transmembrane conductance regulator biogenesis. *J Biol Chem* **285**, 35825-35835, doi:10.1074/jbc.M110.131623 (2010).

67   DeCarvalho, A. C., Gansheroff, L. J. & Teem, J. L. Mutations in the nucleotide binding domain 1 signature motif region rescue processing and functional defects of cystic fibrosis transmembrane conductance regulator delta f508. *J Biol Chem* **277**, 35896-35905, doi:10.1074/jbc.M205644200 (2002).

68   Hoelen, H. *et al.* The primary folding defect and rescue of DeltaF508 CFTR emerge during translation of the mutant domain. *PLoS One* **5**, e15458, doi:10.1371/journal.pone.0015458 (2010).

69   Mornon, J. P., Lehn, P. & Callebaut, I. Atomic model of human cystic fibrosis transmembrane conductance regulator: membrane-spanning domains and coupling interfaces. *Cell Mol Life Sci* **65**, 2594-2612, doi:10.1007/s00018-008-8249-1 (2008).

70   Mornon, J. P., Lehn, P. & Callebaut, I. Molecular models of the open and closed states of the whole human CFTR protein. *Cell Mol Life Sci* **66**, 3469-3486, doi:10.1007/s00018-009-0133-0 (2009).

71   Serohijos, A. W. *et al.* Phenylalanine-508 mediates a cytoplasmic-membrane domain contact in the CFTR 3D structure crucial to assembly and channel function. *Proc Natl Acad Sci U S A* **105**, 3256-3261, doi:10.1073/pnas.0800254105 (2008).

72   Denning, G. M. *et al.* Processing of mutant cystic fibrosis transmembrane conductance regulator is temperature-sensitive. *Nature* **358**, 761-764, doi:10.1038/358761a0 (1992).

73   Wang, X., Koulov, A. V., Kellner, W. A., Riordan, J. R. & Balch, W. E. Chemical and biological folding contribute to temperature-sensitive DeltaF508 CFTR trafficking. *Traffic* **9**, 1878-1893, doi:10.1111/j.1600-0854.2008.00806.x (2008).

74   Pind, S., Riordan, J. R. & Williams, D. B. Participation of the endoplasmic reticulum chaperone calnexin (p88, IP90) in the biogenesis of the cystic fibrosis transmembrane conductance regulator. *J Biol Chem* **269**, 12784-12788 (1994).

75   Gnann, A., Riordan, J. R. & Wolf, D. H. Cystic fibrosis transmembrane conductance regulator degradation depends on the lectins Htm1p/EDEM and the Cdc48 protein complex in yeast. *Mol Biol Cell* **15**, 4125-4135, doi:10.1091/mbc.E04-01-0024 (2004).

76   Egan, M. E. *et al.* Calcium-pump inhibitors induce functional surface expression of Delta F508-CFTR protein in cystic fibrosis epithelial cells. *Nat Med* **8**, 485-492, doi:10.1038/nm0502-485 (2002).

77   Farinha, C. M. & Amaral, M. D. Most F508del-CFTR is targeted to degradation at an early folding checkpoint and independently of calnexin. *Mol Cell Biol* **25**, 5242-5252, doi:10.1128/MCB.25.12.5242-5252.2005 (2005).

78   Loo, T. W., Bartlett, M. C. & Clarke, D. M. Thapsigargin or curcumin does not promote maturation of processing mutants of the ABC transporters, CFTR, and P-glycoprotein. *Biochem Biophys Res Commun* **325**, 580-585, doi:10.1016/j.bbrc.2004.10.070 (2004).

79   Meacham, G. C., Patterson, C., Zhang, W., Younger, J. M. & Cyr, D. M. The Hsc70 co-chaperone CHIP targets immature CFTR for proteasomal degradation. *Nat Cell Biol* **3**, 100-105, doi:10.1038/35050509 (2001).

80   Younger, J. M. *et al.* Sequential quality-control checkpoints triage misfolded cystic fibrosis transmembrane conductance regulator. *Cell* **126**, 571-582, doi:10.1016/j.cell.2006.06.041 (2006).

81   Sun, F. *et al.* Derlin-1 promotes the efficient degradation of the cystic fibrosis transmembrane conductance regulator (CFTR) and CFTR folding mutants. *J Biol Chem* **281**, 36856-36863, doi:10.1074/jbc.M607085200 (2006).

82   Dalemans, W. *et al.* Altered chloride ion channel kinetics associated with the delta F508 cystic fibrosis mutation. *Nature* **354**, 526-528, doi:10.1038/354526a0 (1991).

83   Galietta, L. J. *et al.* Novel CFTR chloride channel activators identified by screening of combinatorial libraries based on flavone and benzoquinolizinium lead compounds. *J Biol Chem* **276**, 19723-19728, doi:10.1074/jbc.M101892200 (2001).

84   Pedemonte, N. *et al.* Phenylglycine and sulfonamide correctors of defective delta F508 and G551D cystic fibrosis transmembrane conductance regulator chloride-channel gating. *Mol Pharmacol* **67**, 1797-1807, doi:10.1124/mol.105.010959 (2005).

85   Van Goor, F. *et al.* Rescue of CF airway epithelial cell function in vitro by a CFTR potentiator, VX-770. *Proc Natl Acad Sci U S A* **106**, 18825-18830, doi:10.1073/pnas.0904709106 (2009).

86   Yang, H. *et al.* Nanomolar affinity small molecule correctors of defective Delta F508-CFTR chloride channel gating. *J Biol Chem* **278**, 35079-35085, doi:10.1074/jbc.M303098200 (2003).

87   Hwang, T. C., Wang, F., Yang, I. C. & Reenstra, W. W. Genistein potentiates wild-type and delta F508-CFTR channel activity. *Am J Physiol* **273**, C988-998 (1997).

88   Jayaraman, S., Haggie, P., Wachter, R. M., Remington, S. J. & Verkman, A. S. Mechanism and cellular applications of a green fluorescent protein-based halide sensor. *J Biol Chem* **275**, 6047-6050 (2000).

89   Galietta, L. J., Haggie, P. M. & Verkman, A. S. Green fluorescent protein-based halide indicators with improved chloride and iodide affinities. *FEBS Lett* **499**, 220-224 (2001).

90   Van Goor, F. *et al.* Rescue of DeltaF508-CFTR trafficking and gating in human cystic fibrosis airway primary cultures by small molecules. *Am J Physiol Lung Cell Mol Physiol* **290**, L1117-1130, doi:10.1152/ajplung.00169.2005 (2006).

91   Carlile, G. W. *et al.* Correctors of protein trafficking defects identified by a novel high-throughput screening assay. *Chembiochem* **8**, 1012-1020, doi:10.1002/cbic.200700027 (2007).

92   Sampson, H. M. *et al.* Identification of a NBD1-binding pharmacological chaperone that corrects the trafficking defect of F508del-CFTR. *Chem Biol* **18**, 231-242, doi:10.1016/j.chembiol.2010.11.016 (2011).

93   Trzcinska-Daneluti, A. M. *et al.* High-content functional screen to identify proteins that correct F508del-CFTR function. *Mol Cell Proteomics* **8**, 780-790, doi:10.1074/mcp.M800268-MCP200 (2009).

94   Lin, S. *et al.* Identification of synergistic combinations of F508del cystic fibrosis transmembrane conductance regulator (CFTR) modulators. *Assay Drug Dev Technol* **8**, 669-684, doi:10.1089/adt.2010.0313 (2010).

95   Wang, Y., Loo, T. W., Bartlett, M. C. & Clarke, D. M. Additive effect of multiple pharmacological chaperones on maturation of CFTR processing mutants. *Biochem J* **406**, 257-263, doi:10.1042/BJ20070478 (2007).

96   Wang, Y., Loo, T. W., Bartlett, M. C. & Clarke, D. M. Correctors promote maturation of cystic fibrosis transmembrane conductance regulator (CFTR)-processing mutants by binding to the protein. *J Biol Chem* **282**, 33247-33251, doi:10.1074/jbc.C700175200 (2007).

97   Loo, T. W., Bartlett, M. C. & Clarke, D. M. Correctors promote folding of the CFTR in the endoplasmic reticulum. *Biochem J* **413**, 29-36, doi:10.1042/BJ20071690 (2008).

98   Loo, T. W., Bartlett, M. C. & Clarke, D. M. Correctors enhance maturation of DeltaF508 CFTR by promoting interactions between the two halves of the molecule. *Biochemistry* **48**, 9882-9890, doi:10.1021/bi9004842 (2009).

99   Okiyoneda, T. *et al.* Peripheral protein quality control removes unfolded CFTR from the plasma membrane. *Science* **329**, 805-810, doi:10.1126/science.1191542 (2010).

100   Okiyoneda, T., Apaja, P. M. & Lukacs, G. L. Protein quality control at the plasma membrane. *Curr Opin Cell Biol* **23**, 483-491, doi:10.1016/j.ceb.2011.04.012 (2011).

101   Swiatecka-Urban, A. *et al.* The short apical membrane half-life of rescued {Delta}F508-cystic fibrosis transmembrane conductance regulator (CFTR) results from accelerated endocytosis of {Delta}F508-CFTR in polarized human airway epithelial cells. *J Biol Chem* **280**, 36762-36772, doi:10.1074/jbc.M508944200 (2005).

102   Hutt, D. M. *et al.* Reduced histone deacetylase 7 activity restores function to misfolded CFTR in cystic fibrosis. *Nat Chem Biol* **6**, 25-33, doi:10.1038/nchembio.275 (2010).

103   Kim Chiaw, P., Wellhauser, L., Huan, L. J., Ramjeesingh, M. & Bear, C. E. A chemical corrector modifies the channel function of F508del-CFTR. *Mol Pharmacol* **78**, 411-418, doi:10.1124/mol.110.065862 (2010).

104   Moran, O., Galietta, L. J. & Zegarra-Moran, O. Binding site of activators of the cystic fibrosis transmembrane conductance regulator in the nucleotide binding domains. *Cell Mol Life Sci* **62**, 446-460, doi:10.1007/s00018-004-4422-3 (2005).

105   Prince, L. S. *et al.* Efficient endocytosis of the cystic fibrosis transmembrane conductance regulator requires a tyrosine-based signal. *J Biol Chem* **274**, 3602-3609 (1999).

106   Weixel, K. M. & Bradbury, N. A. The carboxyl terminus of the cystic fibrosis transmembrane conductance regulator binds to AP-2 clathrin adaptors. *J Biol Chem* **275**, 3655-3660 (2000).

107   Weixel, K. M. & Bradbury, N. A. Mu 2 binding directs the cystic fibrosis transmembrane conductance regulator to the clathrin-mediated endocytic pathway. *J Biol Chem* **276**, 46251-46259, doi:10.1074/jbc.M104545200 (2001).

108   Cormet-Boyaka, E. *et al.* CFTR chloride channels are regulated by a SNAP-23/syntaxin 1A complex. *Proc Natl Acad Sci U S A* **99**, 12477-12482, doi:10.1073/pnas.192203899 (2002).

109   Naren, A. P., Quick, M. W., Collawn, J. F., Nelson, D. J. & Kirk, K. L. Syntaxin 1A inhibits CFTR chloride channels by means of domain-specific protein-protein interactions. *Proc Natl Acad Sci U S A* **95**, 10972-10977 (1998).

110   Peters, K. W., Qi, J., Watkins, S. C. & Frizzell, R. A. Syntaxin 1A inhibits regulated CFTR trafficking in xenopus oocytes. *Am J Physiol* **277**, C174-180 (1999).

111   Ganeshan, R., Di, A., Nelson, D. J., Quick, M. W. & Kirk, K. L. The interaction between syntaxin 1A and cystic fibrosis transmembrane conductance regulator Cl- channels is mechanistically distinct from syntaxin 1A-SNARE interactions. *J Biol Chem* **278**, 2876-2885, doi:10.1074/jbc.M211790200 (2003).

112   Naren, A. P. *et al.* Regulation of CFTR chloride channels by syntaxin and Munc18 isoforms. *Nature* **390**, 302-305, doi:10.1038/36882 (1997).

113   Guggino, W. B. The cystic fibrosis transmembrane regulator forms macromolecular complexes with PDZ domain scaffold proteins. *Proc Am Thorac Soc* **1**, 28-32, doi:10.1513/pats.2306011 (2004).

114   Guggino, W. B. & Stanton, B. A. New insights into cystic fibrosis: molecular switches that regulate CFTR. *Nat Rev Mol Cell Biol* **7**, 426-436, doi:10.1038/nrm1949 (2006).

115   Bates, I. R. *et al.* Membrane lateral diffusion and capture of CFTR within transient confinement zones. *Biophys J* **91**, 1046-1058, doi:10.1529/biophysj.106.084830 (2006).

116   Haggie, P. M., Kim, J. K., Lukacs, G. L. & Verkman, A. S. Tracking of quantum dot-labeled CFTR shows near immobilization by C-terminal PDZ interactions. *Mol Biol Cell* **17**, 4937-4945, doi:10.1091/mbc.E06-08-0670 (2006).

117   Ganeshan, R., Nowotarski, K., Di, A., Nelson, D. J. & Kirk, K. L. CFTR surface expression and chloride currents are decreased by inhibitors of N-WASP and actin polymerization. *Biochim Biophys Acta* **1773**, 192-200, doi:10.1016/j.bbamcr.2006.09.031 (2007).

118   Picciano, J. A., Ameen, N., Grant, B. D. & Bradbury, N. A. Rme-1 regulates the recycling of the cystic fibrosis transmembrane conductance regulator. *Am J Physiol Cell Physiol* **285**, C1009-1018, doi:10.1152/ajpcell.00140.2003 (2003).

119   Ameen, N., Silvis, M. & Bradbury, N. A. Endocytic trafficking of CFTR in health and disease. *J Cyst Fibros* **6**, 1-14, doi:10.1016/j.jcf.2006.09.002 (2007).

120   Swiatecka-Urban, A. *et al.* Myosin VI regulates endocytosis of the cystic fibrosis transmembrane conductance regulator. *J Biol Chem* **279**, 38025-38031, doi:10.1074/jbc.M403141200 (2004).

121   Ghosh, R. N., Mallet, W. G., Soe, T. T., McGraw, T. E. & Maxfield, F. R. An endocytosed TGN38 chimeric protein is delivered to the TGN after trafficking through the endocytic recycling compartment in CHO cells. *J Cell Biol* **142**, 923-936 (1998).

122   Ghosh, R. N. & Maxfield, F. R. Evidence for nonvectorial, retrograde transferrin trafficking in the early endosomes of HEp2 cells. *J Cell Biol* **128**, 549-561 (1995).

123   Jakab, R. L., Collaco, A. M. & Ameen, N. A. Physiological relevance of cell-specific distribution patterns of CFTR, NKCC1, NBCe1, and NHE3 along the crypt-villus axis in the intestine. *Am J Physiol Gastrointest Liver Physiol* **300**, G82-98, doi:10.1152/ajpgi.00245.2010 (2011).

124   Braun, A. *et al.* Afferent lymph-derived T cells and DCs use different chemokine receptor CCR7-dependent routes for entry into the lymph node and intranodal migration. *Nat Immunol* **12**, 879-887, doi:10.1038/ni.2085 (2011).

125   Rueden, C. T. & Eliceiri, K. W. Visualization approaches for multidimensional biological image data. *Biotechniques* **43**, 31, 33-36 (2007).

126   Schermelleh, L., Heintzmann, R. & Leonhardt, H. A guide to super-resolution fluorescence microscopy. *J Cell Biol* **190**, 165-175, doi:10.1083/jcb.201002018 (2010).

127   Bertrand, C. A. & Frizzell, R. A. The role of regulated CFTR trafficking in epithelial secretion. *Am J Physiol Cell Physiol* **285**, C1-18, doi:10.1152/ajpcell.00554.2002 (2003).

128   Bradbury, N. A. *et al.* Regulation of plasma membrane recycling by CFTR. *Science* **256**, 530-532 (1992).

129   Denning, G. M., Ostedgaard, L. S., Cheng, S. H., Smith, A. E. & Welsh, M. J. Localization of cystic fibrosis transmembrane conductance regulator in chloride secretory epithelia. *J Clin Invest* **89**, 339-349, doi:10.1172/JCI115582 (1992).

130   Loffing, J., Moyer, B. D., McCoy, D. & Stanton, B. A. Exocytosis is not involved in activation of Cl-secretion via CFTR in Calu-3 airway epithelial cells. *Am J Physiol* **275**, C913-920 (1998).

131   Hug, M. J., Clarke, L. L. & Gray, M. A. How to measure CFTR-dependent bicarbonate transport: from single channels to the intact epithelium. *Methods Mol Biol* **741**, 489-509, doi:10.1007/978-1-61779-117-8_30 (2011).

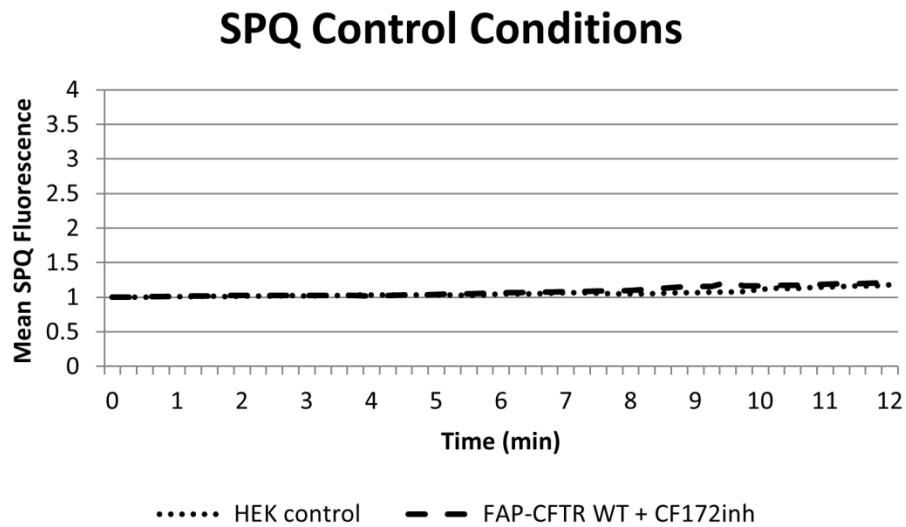# Supplemental Figures

SPQ Control Conditions

Figure S-1: SPQ Control

SPQ fluorescence measurements with control conditions. Naïve HEK293 cells do not exhibit a Fsk responsive iodide efflux. Cells stably expressing FAP-CFTR WT normally have a robust iodide efflux capability (Figure 1-9), however in the presence of the CFTR specific inhibitor, CF172inh, no change iodide transport is detected.
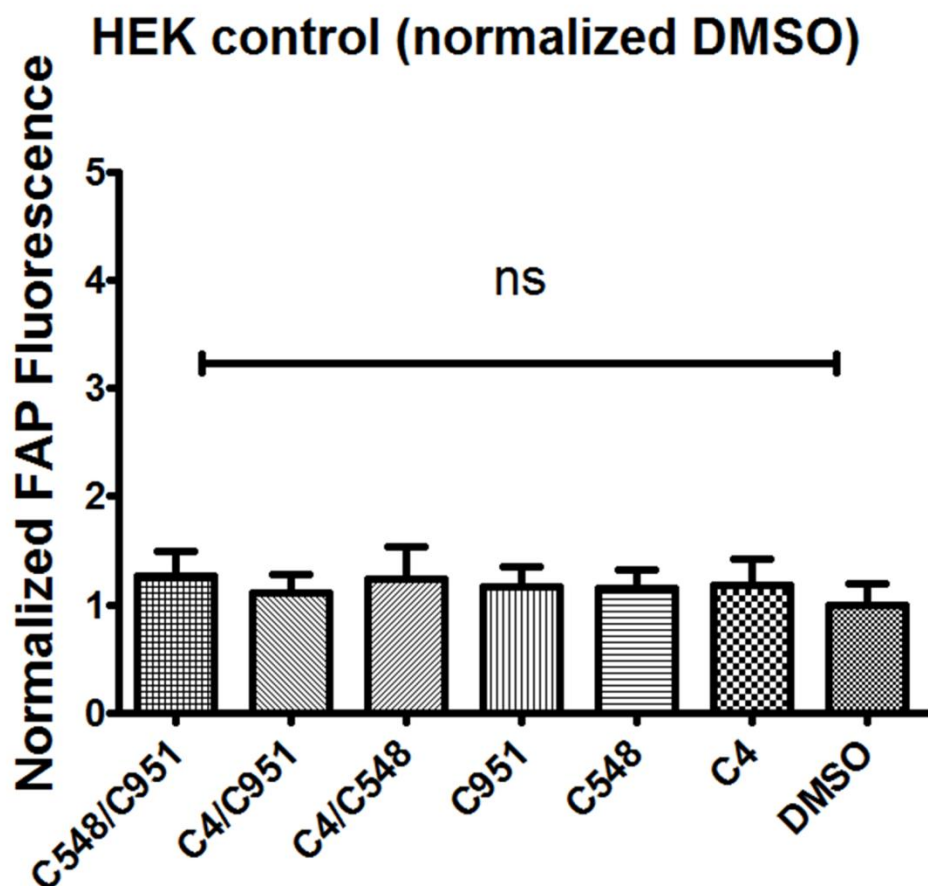
Figure S-2: Corrector Treatment Does Not Produce Non-Specific Fluorogen Labeling

Naïve HEK293 cells were treated with each corrector condition indicated for 24 hours. Cells were exposed to 50nM MG-11p and the fluorescence activity was measured by flow cytometry. The mean fluorescence for each condition was normalized to DMSO. There was no statistical difference found between corrector treatment and DMSO.